PhD course in Biochemistry

XXXIII Cycle (Academic year 2017-2020)

Aberrant protein O-GlcNAcylation promotes Alzheimer-like neuropathology

PhD Student

Ilaria Zuliani

Tutor

Prof. Fabio Di Domenico

PhD Coordinator

Prof. Stefano Gianni

1. INTRODUCTION

1. Protein O-GlcNAcylation

Protein post-translational modification (PTM) enables cells to promptly adapt to different stimuli trough the direct and dynamic control of protein functions. Considering their importance, a great deal of effort has been put over the years into understanding the role of most common PTMs such as phosphorylation, ubiquitylation and acetylation in cell physiology. However, beyond these well-characterized modifications, there are few others PTMs whose role is far from being understood. Among these, protein O-GlcNAcylation is the most recently discovered and has emerged as very abundant in cells with a prominent role in a wide range of cellular processes.

Protein O-GlcNAcylation was first discovered in the early 1980s by Hart *et al*. when bovine milk galactosyltransferase, in conjunction with UDP-[^{3}H] galactose, was used to probe for accessible N-acetylglucosamine (GlcNAc) moieties on glycoconjugates of living cells. This study revealed the presence of O-glycosidically linked GlcNAc on lymphocyte cell-surface proteins[1]. Subsequent analysis clarified that O-linked GlcNAc monosaccharide residues are present in most intracellular compartments and are particularly abundant in cytoplasmic, nuclear and mitochondrial proteins[2,3].

O-GlcNAcylation differs in many aspects from other forms of canonical protein glycosylation: (I) O-GlcNAc is not elongated to form more complex glycan structures; (II) unlike other O-glycosylation the addiction of O-GlcNAc does not typically occur in the Golgi apparatus; (III) O-GlcNAc is almost exclusively found in nuclear, cytoplasmic and mitochondrial proteins rather than membrane and secretory proteins; (IV) O-GlcNAcylation occurs through

a highly dynamic process that involves the rapid addiction and removal of the sugar from serine and threonine residues[4,5]. This dynamic process seems to be unique to this glycosylation motif and gives to O-GlcNAc the ability to modulate protein functions, cellular signalling and transcription regulatory pathways in response to nutrients and stress[3,6,7]. After decades of study, more than one thousand O-GlcNAcylated proteins have been identified in viruses, bacteria, plants and animals and this number continues to rapidly grow as the technology for the detection of O-GlcNAc improves. O-GlcNAc-proteome, although not yet complete, has revealed a diverse set of proteins engaged in numerous cellular functions. Indeed, protein involved in functions ranging from carbohydrate metabolism, signalling, transcription and stress response are well represented in the O-GlcNAc-proteome. In this sense, O-GlcNAcylation has a great similarity with protein phosphorylation and shares with this PTM the ability to transiently modulate protein function according to cellular state[7].

1.1 The hexosamine biosynthetic pathway

The sugar substrate for O-GlcNAcylation is provided by a specific metabolic pathway named the hexosamine biosynthetic pathway (HBP), which integrates extracellular physiological inputs, including nutrient availability, with the metabolism of carbohydrate, amino acid, nucleotide and fatty acid components to produce UDP-GlcNAc[8]. Upon entering the cell by glucose transporting proteins (GLUT), glucose is converted to glucose-6-phosphate. Glucose-6-phosphate can undertake glycogen synthesis or, after conversion to fructose-6-phosphate, enter the glycolytic pathway. Whereas most of the glucose is consumed in these metabolic pathways, approximately 2-5% of intracellular glucose is channelled into the HBP to form UDP-GlcNAc.

Glutamine-fructose-6-phosphate amidotrasferase 1 (GFAT1) catalyses the first and rate-limiting step of the HBP, which converts fructuse-6-phosphate and glutamine into glucosamine-6-phosphate. GFAT1 activity is regulated by feedback inhibition by UDP-GlcNAc[9,10] but also by other key sensors of cellular nutrient state. In this context, adenosine 3'-5'-monophosphate (cycling AMP)-dependent kinase (AMPK) is known to inhibit GFAT1 activity under nutrient depletion or stress conditions, in order to reduce the amount of nutrients entering the HBP flux[11,12]. In the subsequent step, the enzyme glucosamine-phosphate N-acetyltransferase (GNPNAT) catalyzes the acetylation of glucosamine-6-phosphate to generate N-acetylglucosamine-6-phosphate (GlcNAc-6P). This is followed by GlcNAc phosphomutase-mediated isomerization into GlcNAc-1-phosphate (GlcNAc-1-P). Finally, UTP from nucleotide metabolism and GlcNAc-1P produce UDP-GlcNAc through UDP-N-acetylglucosamine pyrophosphorylase enzyme. Moreover, free GlcNAc can be recycled via the GlcNAc savage pathway, which converts GlcNAc to GlcNA-6-phosphate that can be utilized by the HBP[13,14]. Since the HBP utilizes major metabolites to produce UDP-GlcNAc, cells use it as a sensor of energy/nutrients availability. As a result, O-GlcNAc signalling is highly sensitive to metabolic state and cellular stress (i.e. heat shock, hypoxia, nutrient deprivation), although the mechanisms mediating this response are only partially elucidated[15].

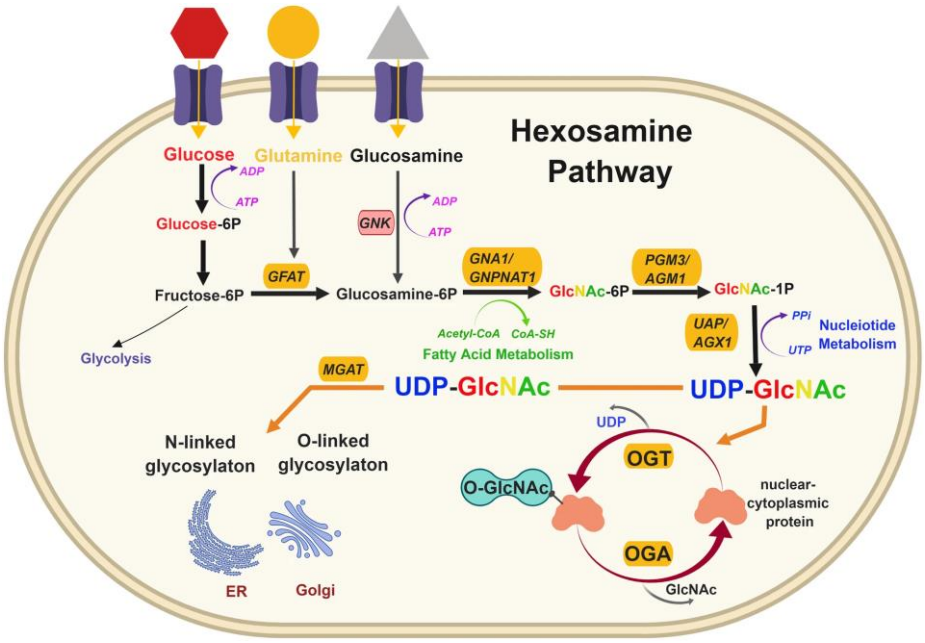

Figure 1: The hexosamine biosynthetic pathway. The hexosamine biosynthetic pathway (HBP) is a minor branch of the glycolitic pathway that results in the production of UDP-GlcNAc, the activated substrate for protein O-GlcNAcylation. As the HBP flux integrates molecules from carbohydrate (fructose-6-phosphate), amino acid (glutamine/glucosamine), neucleotide (UTP) and lipid (Acetyl-CoA) metabolism, the production of UDP-GlcNAc is considered a valuable intracellular sensor of cell metabolic status. UDP-GlcNAc is the substrate for O-GlcNAc transferase (OGT), which catalyzes the post-translational modification of serine/threonine protein residues by O-linked β-N-acetylglucosamine (O-GlcNAc). Differing from most protein post-translational modifications, O-GlcNAcylation is regulated by a single enzyme for attachment (OGT) and a single enzyme for removal (OGA). This PTM is a dynamic and ubiquitous process that occurs predominantly in the cytosol and nucleus, affecting a diverse array of protein functions and transcriptional events.

1.2 Enzymes regulating O-GlcNAc cycling

Unlike other PTMs which are under the control of multiple writers and erasers, only two highly evolutionarily conserved enzymes are responsible for the cycling of O-GlcNAc on Ser/Thr residues of targeted proteins. The enzyme O-GlcNAc transferase (OGT) catalyses the addiction of the activated sugar UDP-GlcNAc produced by the HBP, whereas the enzyme O-GlcNAcase (OGA) is responsible for its rapid removal. Unlike protein phosphorylation, O-GlcNAcylation is not associated with a clear consensus motif and different mechanisms are responsible for target specificity of O-GlcNAc cycling enzymes. These mechanisms appear to be built into the cellular machinery at multiple levels and include differences in structure and localization among OGT and OGA isoforms, post-translational modification of O-GlcNAc cycling enzymes and interactions with multiple accessory proteins, which address their actions toward specific substrate groups[16]. This complex regulation of O-GlcNAc cycling enzymes activity ensure the maintenance of O-GlcNAcylation homeostasis under different cellular conditions.

1.2.1 O-GlcNAc transferase (OGT)

Structure. OGT is ubiquitously expressed in all mammalian tissues but is most abundant in pancreas, brain, heart and skeletal muscle[17,18]. The human Ogt gene is located at the Xq13.1 genomic locus and is alternatively spliced to generate nucleocytoplasmic (nc), mitochondrial (m) and short (s) isoforms. These isoforms are distinguished by their N-terminal domains which contain diverse number of tetratricopeptide repeats (TPRs)[19]. Despite differences in their N-terminal domains, all OGT isoforms share a common C-terminal

domain which contains two catalytic regions responsible for their glycosyltransferase activity[20]. The OGT TPR-domain participates in substrate recognition and is necessary for the glycosylation of numerous substrates such as nucleoporin 62 and the RNA pol II C-domain[21,22]. Furthermore, growing evidences suggest that the TPR-domain may also influence OGT selectivity by mediating its oligomerization and the transient interaction with accessory proteins. As a matter of fact, heterotrimeric OGT complexes have been reported in tissues such as kidney, spleen, liver and pancreas[23–25] and multimerization of OGT into homo-oligomers has also been observed[26]. Mutations of TPR-domain prevent the formation of OGT multimers and attenuate O-GlcNAcylation of selected substrates, suggesting that OGT-OGT association may favour interactions with certain targets[27].

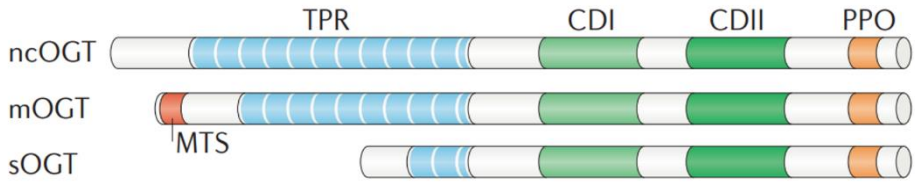

Figure 2: Schematic representation of O-GlcNAc transferase (OGT) isoforms. The nucleocytoplasmic (ncOGT), mitochondrial (mOGT) and short (sOGT) isoforms of OGT differ in length owing to variable numbers of amino-terminal tetratricopeptide repeats (TPRs) but share common carboxy-terminal catalytic (CDI and II) and phosphoinositide-binding (PPO) domains. mOGT contains a unique N-terminal mitochondrial targeting sequence (MTS).

***Regulation*.** Considering the importance of maintaining O-GlcNAc homeostasis, the regulation of OGT takes place at different levels ranging from post-translation modifications, subcellular partitioning of different isoforms and fluctuations of protein expression levels under certain stimuli. OGT itself

is both O-GlcNAcylated and phosphorylated at multiple Ser, Thr and Tyr residues[26,28]. Although the effect of OGT O-GlcNAcylation has still to be clarified, its phosphorylation on specific residues seems to be linked to its enzymatic activity. In this context, acute insulin stimulation is known to enhance insulin-receptor mediated OGT tyrosine phosphorylation and activity[29]. An interplay between OGT and the insulin-regulated mitotic protein glycogen synthase kinase (GSK3) has also been hypothesized. Indeed, GSK3β-mediated phosphorylation of OGT on Ser3 and 4 enhances OGT activity as well[30]. Interestingly, both Ser3 and 4 are also sites of O-GlcNAcylation[30], supporting the idea of a cross-talk between O-GlcNAc and phosphorylation that may regulate the function of OGT itself. In addition, OGT can be phosphorylated by the nutrient-sensitive AMP-activated protein kinase (AMPK) on Thr444, regulating both OGT selectivity and nuclear localization[31]. Interestingly, both AMPK and GSK3β are OGT substrates and their activities are sensitive to global O-GlcNAc perturbation[21,31,32], providing a perfect example of the dynamic regulation between O-GlcNAc cycling enzymes and kinase/phosphatase which is necessary for the coordination of protein signalling.

Although mechanisms controlling OGT intracellular trafficking are not well understood, different stimuli may influence OGT subcellular localization thus affecting OGT interaction with subsets of cellular proteome. In line with its nutrient-sensing role, insulin stimulation is known to promote OGT transfer from the nuclear compartment to the cytosol and plasma membrane in adipocytes and fibroblasts[29,33]. On the contrary, glucose-deprivation has proved to favour OGT cytosolic localization upon AMPK activation[31]. In this context, several AMPK subunits have shown to be dynamically modified by

O-GlcNAc and AMPK activation itself seems to be influenced by its O-GlcNAcylation state, defining a complex interplay between these enzymes[31]. These evidences suggest that the cellular metabolic state may not only influence OGT activity but also its subcellular localization and therefore its targets. Finally, OGT transcript and protein levels are known to fluctuate in response to various stimuli such as oxidative or nutrient stress[34–36], consistent with the role of this enzyme as a sensor of cellular metabolic state. Growing evidence also suggests that tissue-specific regulation of OGT is impacted during physiological aging, thus contributing to the imbalance of O-GlcNAc cycling that characterize many age-related disorders[37–39].

1.2.2. O-GlcNAcase (OGA)

Structure. The O-GlcNAcase (OGA) enzyme is a monomeric hexosaminidase (~130kDa) ubiquitously expressed with a prevalent distribution in the brain, skeletal muscle and pancreas[40–42]. OGA is known to exert its optimal O-β-linked GlcNAc cleaving activity at near neutral pH[41,43]. This characteristic, together with its prevalent distribution into the nucleus and the cytosol, clearly distinguish this O-GlcNAc cycling enzyme from the acidic hexosaminidases located into the lysosomes[40]. Two different isoforms of OGA have been identified, a full-length protein (OGA) and a short isoform (sOGA), both arising from the alterative splicing of the human Mgea5 gene on chromosome 10[40,44]. Both OGA isoforms contain an N-terminal domain with glycosidase activity, while just the full-length OGA is characterized by a C-terminal domain sharing homology with acetyl-transferase (AT) enzymes[40]. The functional role of the AT-like domain of OGA is still a matter of discussion. If on one hand a study by Toleman *et al.* reported an intrinsic histone

acetyltransferase activity of OGA *in vitro*[45], a more recent study reported the lack of detectable binding between acetyl-CoA and the recombinant AT-like domain of human OGA[46], possibly excluding its assumed AT activity.

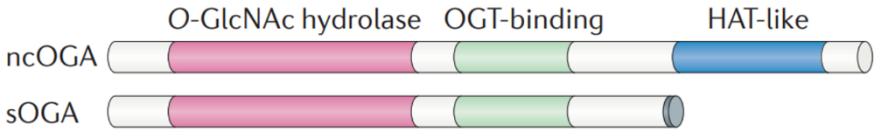

Figure 3: Schematic representation of O-GlcNAcase (OGA) isoforms. The nucleocytoplasmic (ncOGA) and short (sOGA) isoforms of OGA possess identical N-terminal O-GlcNAc hydrolase domains and central OGT-binding regions; however, sOGA lacks the C-terminal histone acetyltransferase-like (HAT-like) domain that is present in ncOGA.

Regulation. Although O-GlcNAc cycling enzymes share common regulation strategies, some mechanisms are still not fully elucidated. Even though the catalytic mechanism of OGA and its function in cellular homeostasis have been intensively studied, the regulation of this enzyme activity is poorly understood. A specific site of O-GlcNAcylation at Ser405 has been described for OGA, within the region that mediates its interaction with OGT[47,48]. Moreover, OGA has been shown to be an OGT substrate[49], suggesting a reciprocal regulation between these two enzymes that has no further been clarified. Like OGT, also OGA levels change according to certain stimuli. For example, OGA protein levels are reduced upon OGT silencing thus implicating the involvement of OGT in the regulation of OGA expression and stability[32]. A possible account for OGA regulation by OGT is that the gene encoding for OGA is located in a region targeted by the PcG repressor complex of which OGT is a component[50,51]. Furthermore, OGA protein levels seem to fluctuate according to the relative abundance of O-GlcNAcylated proteins. Pharmacological

elevation of global O-GlcNAc levels indeed induces OGA transcription, suggesting a possible feedback loop aimed at upholding O-GlcNAc homeostasis[52].

1.3 Crosstalk between protein O-GlcNAcylation and phosphorylation

O-GlcNAcylation is in many ways similar to protein phosphorylation. Both modifications occur on serine and threonine residues, cycling on their protein substrates with a variable rate that depends upon the protein, the modification site and cellular state. They are also highly responsive to nutrients, as their donor substrates (UDP-GlcNAc and ATP) are high-energy products from cellular metabolism. Taking all these factors into consideration, a reciprocal crosstalk between these two PTMs is easily conceivable. A large-scale study by Wang *et al.* first described the consistent changes in phospho-proteome dynamics in response to the global increase of protein O-GlcNAcylation. Indeed, elevated O-GlcNAc levels resulted in lower phosphorylation at 280 sites and increased phosphorylation at 148 sites. Also, changes in the O-GlcNAcylation profile were observed upon inhibition of serine/threonine phosphatases, giving proof of the extensive interplay between these two PTMs[53]. Subsequent studies clarified that O-GlcNAcylation/phosphorylation crosstalk takes place at different levels: if on one hand the two PTMs compete for the occupancy of the same or proximal sites (reciprocal crosstalk) on to the other side also the mutual modification of each other writers and erasers has a role in their regulation[54–56]. In this context, a study on the proteome of murine synaptosomes revealed that 52% of the identified protein phosphatases were

phosphorylated and 8% were O-GlcNAc-modified. In addition, 66% of the identified kinases were phosphorylated, whereas 16% were O-GlcNAcylated, confirming that most of kinases and phosphatases undergoes these two PTMs as a mechanism of regulation[57]. In the last decade, growing knowledge on this topic confirmed the importance of a correct balance between these two PTMs to regulate cellular signalling, transcription and correct response to nutrients and stress conditions. Indeed, abnormal interplay between O-GlcNAcylation and phosphorylation has proved to underly dysregulation in cancer, diabetes and neurodegenerative diseases[58,59].

2. Down syndrome

Down syndrome (DS) is the most common chromosomal disorder and the most frequent genetic cause of intellectual disability affecting about 6 million people worldwide[60,61]. Although the primary cause of this condition is the abnormal triplication of chromosome 21, DS may be considered as a multifactorial disease, where an abnormal expression of trisomic genes arises not only from genetic, but also environmental factors. Thus, trisomy leads to a deregulated scenario that also affects disomic genes and that ultimately results in largely different phenotypes. The increased dosage of the gene encoded on chromosome 21 is known to affect diverse pathways, including those involved with brain development, metabolism, and neuronal networks[62,63] . The genetic alterations indeed are responsible of the major clinical features of the disease such as craniofacial abnormalities, small brain size, accelerated aging, and cognitive defects. Individuals with DS are also more likely to develop certain health conditions, including hypothyroidism, autoimmune diseases, epilepsy, haematological disorders, and Alzheimer-like dementia[64]. Because of recent advance in health care and management of co-occurring illnesses, life expectancy of people with DS has largely improved[65,66]. As a matter of fact, the average lifespan of DS individuals has approximately doubled over the past 30 years to 55-60 years of age[67–69]. Consequently, up to 35 years old, mortality rate of adults with DS is comparable to that of adults affected by other intellectual disabilities. However, after age 35, mortality rates double every 6.4 years in DS as compared to every 9.6 years for people without DS[67]. Despite the consistent increase in life expectancy, one of the reasons that strongly compromise adult

DS subjects' quality of life has to be found in the development of a form of dementia similar to Alzheimer's disease[69–71].

2.1 Aging in Down syndrome and the development of Alzheimer-like dementia

The aging process in DS population lead to increased risk of developing Alzheimer's disease (AD) since adult age. Recent findings suggest that 75% of adults with DS survive to 50 years old and 25% reach the age of 60[72]. The portion of these surviving individuals that develop clinical signs of dementia can fluctuate considerably. In the range of age of 20-29, virtually no individual show symptoms of dementia[73,74]. Between the ages of 30-39 years, reports of prevalence range between 0 to 33% of individuals being clinically demented. From 40-49 years of age, 5,7-55% may be demented and between 50-59 years prevalence ranges from 4-55%. In the end, the range of individuals affected by dementia over the age of 60 years is between 15-77%[68]. For DS people older than 40 years old, dementia follows a similar course to that seen in Alzheimer's disease[75,76], with declines in recall and explicit memory[77] and in language function[78] usually preceding dementia. However, early-onset dementia in younger DS individuals (aged 30-40 years) often manifests as changes in behaviour and personality[75,76], with symptoms including apathy, increasing impulsivity and executive dysfunction. Understanding the factors that underlie the variation in symptom presentation and age of clinical onset of dementia in people with DS may provide insights into the pathophysiological mechanisms of both sporadic and DS-associated AD (DS-AD)[79,80]. Thus, DS offers a unique

model to investigate the early molecular changes that precede the appearance of the manifest clinical signs of AD-related dementia.

Alzheimer's disease (AD) is a chronic neurodegenerative disease with well-defined pathophysiological mechanisms, mostly affecting medial temporal lobe and associative neocortical structures. Neuritic plaques and neurofibrillary tangles represent the pathological hallmarks of AD, and are respectively related to the accumulation of the amyloid-beta peptide (Aβ) in brain tissues, and to cytoskeletal changes that arise from the hyperphosphorylation of microtubule-associated Tau protein in neurons. According to the amyloid hypothesis of AD, the overproduction of Aβ is a consequence of the disruption of homeostatic processes that regulate the proteolytic cleavage of the amyloid precursor protein (APP)[81]. Several studies on this topic revealed that from a molecular point of view, DS neuropathology and AD have many common features, counting the deposition of senile plaques and neurofibrillary tangles, together with cellular dysfunction such as mitochondrial defects, increased oxidative stress, and metabolic alterations[63,71,82,83]. One of the main links between AD and DS is related to the triplication of the amyloid precursor protein gene (APP), which is encoded on chromosome 21. As a matter of fact, a small percentage of DS individuals having only a partial trisomy for APP gene do not have the same elevated risk to develop AD, even still more consistent than the rest of the population[84,85]. Likewise, high expression of APP in fibroblasts of individuals with DS is necessary and enough to cause morphological and functional anomalies in early endosomes, which participate in neuron growth, homeostasis, and synaptic functions[86]. Taken together these findings support the conclusion that an extra dose of the APP gene is sufficient to cause AD in DS subjects.

Moreover, trisomy of chromosome 21 results in increased gene dosage for all genes on this chromosome, including several genes in addition to APP that may also be involved in related mechanisms. Among triplicated genes, both dual specificity tyrosine phosphorylation regulated kinase 1A (DYRK1A) and the regulator of calcineurin 1 (RCAN1) have a well-established role in the aberrant phosphorylation of tau protein, which is one of the main mechanisms underlying the formation of toxic neurofibrillary tangles in AD[87–90]. Furthermore, trisomy 21 is characterized by mitochondrial dysfunction and enhanced production of reactive oxygen species (ROS)[87,91] that may contribute to accelerated aging reported in DS people[92]. Indeed, oxidative damage is increased in prenatal DS brain compared to non-DS controls[93,94]and is also higher in adult DS brain compared to age-matched controls[82,95]. Interestingly, superoxide dismutase 1 (SOD1), which has a pivotal role in ROS processing, is encoded on chromosome 21. Consistent with this, increased SOD1 activity has been suggested to cause accelerated cell senescence by the abnormal accumulation of toxic hydrogen peroxide[96]. According these evidences, several genes can modulate the course of AD neuropathology in DS population and further work is required to determinate their role and relative importance.

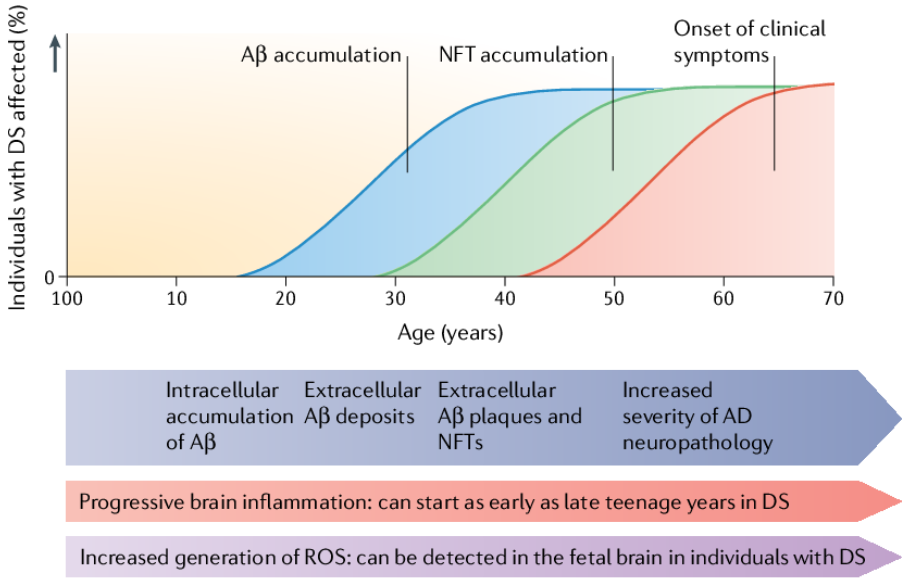

Figure 4: Hypothetical progression of Alzheimer-like neuropathology in Down syndrome. A proposed timeline from birth to over 60 years of age of Alzheimer's disease (AD) pathology in individuals with Down syndrome (DS). Mitochondrial dysfunction and increased generation of reactive oxygen species (ROS) occur as early as in the foetal brain. Brain inflammation can begin as early as in the late teens with the presence of activated microglial cells. By the age of 40 years, both extracellular Aβ and neurofibrillary tangles (NFTs) are present in sufficient quantities for a neuropathological diagnosis of AD. As individuals with DS As individuals with DS age to over 50 years, AD neuropathology increases in severity and clinical signs of dementia become frequent.

2.1.1. Down syndrome and APP processing

Among the aberrantly over-expressed genes in DS individuals, the gene encoding the amyloid precursor protein (APP) is thought to have the key role in the pathology of AD. The additional copy of APP may drive the development of AD in DS population by increasing the levels of amyloid-β (Aβ), a cleavage product of APP that misfold and accumulates in the brain forming toxic plaques. APP is a type I transmembrane protein essential for normal brain development and possibly also for adult brain plasticity[97]. This

protein can undergo two major proteolytic pathways by different sets of enzymes: a canonical via (non-amyloidogenic) and an amyloidogenic one that leads to the formation of amyloid plaques. In the non-amyloidogenic pathway APP is initially cleaved by an α-secretase in the middle of the Aβ sequence, thus precluding the formation of Aβ. This activity generates a soluble APP fragment (sAPPα) and a membrane-bound C-terminal fragment of APP (α-CTF). α-CTF can be further cleaved by γ-secretase generating the so-called p3 fragment and the amyloid intracellular domain (AICD). On to the other hand, the potentially amyloidogenic pathway consists of a β-secretase-mediated cleavage of APP that results in the secretion of sAPPβ, and a second membrane-bound C-terminal fragment of APP (β-CTF). Further cleavage of β-CTF by γ-secretase generates several aggregation-prone Aβ peptides that results in the progressive formation of senile plaques in the brain parenchyma[98].

The additional copy of APP in DS does not typically result in substantial Aβ accumulation until the second or third decade of life. This lack of early Aβ accumulation may be due to APP not becoming dosage sensitive until adulthood, as it's suggested by both animal and human studies[99–101]. Despite this, increased levels of soluble Aβ are found in one out of two DS foetal brain[102], suggesting that APP processing may not be sufficient to cause extensive Aβ accumulation in the developing brain but is still present even decades before the overt presence of clinical symptoms. In line with these findings, increased Aβ levels have been reported in human cell models like pluripotent stem cells derived from children and young adults affected by DS[86,103,104]. One of the possible explanations for the lack of early Aβ accumulation in DS is the initial efficiency of cellular clearance system.

Indeed, the progressive dysfunction of intracellular degradative systems that characterize DS neuropathology may contribute to the later accumulation of toxic aggregates[105,106].

2.1.2 Down syndrome and tau protein

Tau is the major microtubule associated protein in neurons and interacts with tubulin to promote and stabilize its assembly into microtubules[107], allowing axonal transport of vesicles[108]. In AD, tau can no longer associate with microtubules because of its hyperphosphorylated state, thus resulting in the formation of toxic neurofibrillary tangles (NFTs). Pathological brain changes of aged subjects affected by DS are nearly identical to those of patients with AD consisting of both amyloid plaques and NFTs. Studies on *post-mortem* samples have shown that progression of NFTs in DS adults follows a similar staging as in AD, starting in the cortex region, and then spreading in the hippocampus, inferior temporal cortex and neocortex[109]. As observe di AD patients without DS, NFTs expansion beyond these areas appears to be preceded by Aβ accumulation[110]. A potential contributing factor for tau hyperphosphorylation in DS brain may be the overexpression of the dual specificity tyrosine phosphorylation regulated kinase 1A (DYRK1A), a ubiquitously expressed protein kinases which is strongly expressed in heart and brain tissues[111,112]. DYRK1A is encoded on chromosome 21 and its mRNA has been found overexpressed in DS foetal brains[113]. DYRK1A was proved to phosphorylate tau at Thr212 *in vitro*, a residue that is found hyperphosphorylated in AD brains[114]. Furthermore, mice overexpressing human DYRK1A shows high levels of phosphorylated tau both on Thr212 and Ser202-204, sites proved to be involved in NFTs formation[115]. In addition,

DYRK1A also downregulates the levels of neural restrictive silencing factor (NRSF), a neuroprotective protein, which is reduced people with AD[116]. According to these evidences, the extra copy of DYRK1A seems to contribute at different levels to the early onset of AD in DS subjects.

Another potential factor contributing to DS tau hyperphosphorylation is the overexpression of the regulator of calcineurin 1 (RCAN1), also encoded on chromosome 21. RCAN1 inhibits calcineurin and may enhance tau phosphorylation by lowering calcineurin phosphatase activity and increasing GSK3β levels, one of the main kinases driving tau phosphorylation[117]. In addition, high levels of RCAN1 is observed in the hippocampus and cortex region from AD individuals, supporting its possible role in the neurodegenerative mechanisms[118]. Furthermore, APP may also play a role in tau phosphorylation in DS brain since Aβ-42 peptide seems to upregulate both DYRK1A[119] and RCAN1[120]. Thus, the overexpression of chromosome 21-encoded genes appears to cooperate driving both precocious Aβ accumulation and aberrant tau phosphorylation and consistently favouring the neurodegenerative process in DS.

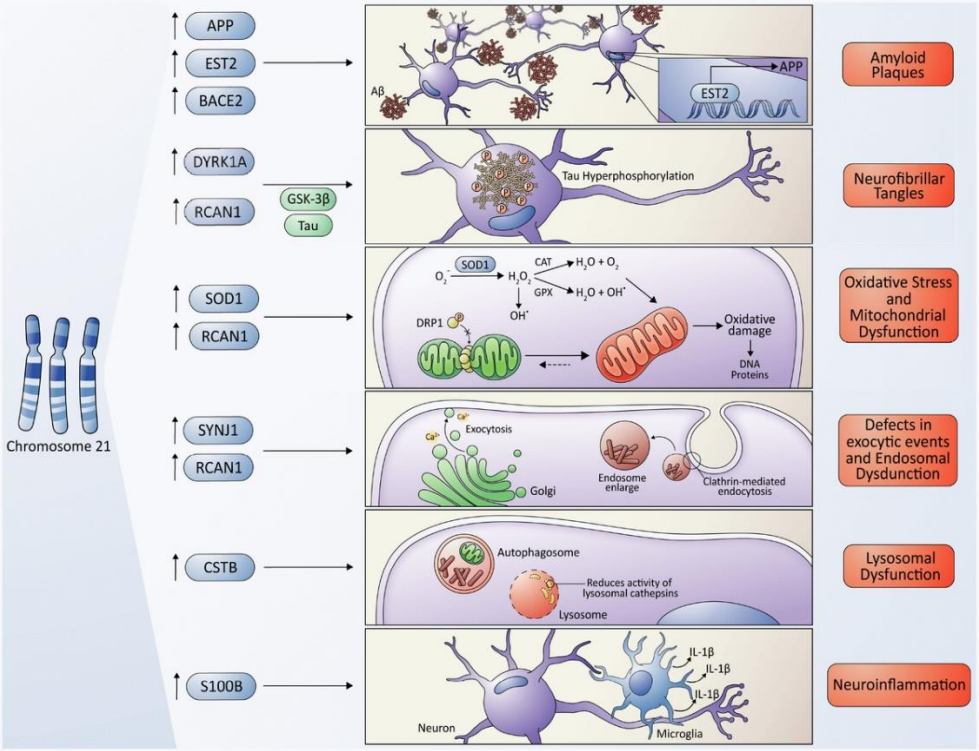

Figure 5: Molecular cross-talking between Down syndrome and Alzheimer's disease. Overexpression of some genes located on chromosome 21 have been linked to the development of neuropathological characteristics of AD in DS. Among them, the APP gene encodes the amyloid precursor protein, and the EST2 gene encodes a transcription factor that promotes the expression of APP, giving rise to the Aβ toxic peptides, which form the amyloid plaques. Also, the overexpression of RCAN1 and its activity as an inhibitor of the phosphatase Calcineurin contributes to the hyperphosphorylation of tau driven by some kinases, among them, the kinase encoded by the DIRK1A gene, that contributes to the formation of neurofibrillary tangles. In addition, SOD1 leads to an increase in ROS levels and oxidative stress due to an imbalance in the ratio of SOD1 and other antioxidant enzymes, resulting in H2O2 accumulation and mitochondrial dysfunctions. Defects in endosomal trafficking and lysosomal proteolysis linked to DS-related genes further contribute to DS neuropathological phenotype. In the end, the astrocyte-derived cytokine S100B has been associated with the activation of glial cells, following by an increase in IL-1β in the nervous system, influencing the neuropathology of AD and DS.

2.1.3 Metabolic alterations in Down syndrome

Among the previously described alterations, trisomy is known to contribute to altered energy metabolism that appears to be a strong determinant in the development of pathological phenotypes associated with DS. Alterations include, among others, mitochondrial defects, increased oxidative stress levels, impaired glucose, and lipid metabolism, finally resulting in reduced energy production and cellular dysfunctions. These molecular defects seem to account for a high incidence of metabolic disorders in DS individuals, i.e., diabetes and/or obesity, as well as a higher risk of developing AD.

Amino acids. Among metabolic defects, alterations of several amino acid concentrations have been observed in the blood of DS individuals compared with age-matched control subjects[121]. Specifically, plasma from DS subjects showed: (I) reduced levels of histidine, lysine, tyrosine, phenylalanine, leucine, isoleucine, and tryptophan; (II) increased levels of phenylalanine and tyrosine; (III) higher levels of leucine, isoleucine, cysteine, and phenylalanine at an age vulnerable to Alzheimer's changes; (IV) decreased concentration of serine at any age; and (V) increased lysine concentration in patients above 10 years old, possibly associated to accelerated aging[121]. A recent study also evidenced changes in the levels of metabolites involved in the methylation cycle, including cysteine, cystathionine, choline, and dimethylglycine. Indeed, mass spectrometry analysis reported a significant increase of the concentrations of these amino acids in DS plasma as well as the levels of S-adenosylhomocysteine and S-adenosylmethionine[122]. Higher levels of these metabolites in DS seem to be strongly associated with the triplication of cystathionine β-synthase (CBS), an enzyme catalysing the synthesis of cystathionine from homocysteine which is encoded on chromosome 21[123].

Indeed, DS-related CBS overexpression seems to be linked with reduced homocysteine levels together with impaired mitochondrial function, as indicated by accumulation of Krebs cycle intermediaries in DS human dermal fibroblasts. Furthermore, the study by Szabo *et al.* showed that consequent increased production of H2S is responsible for mitochondrial deficits, in particular though the inhibition of complex IV[124]. In line with these results, DS cells showed a significant impairment of mitochondrial complexes activities, oxygen consumption and ATP generation, showing how alterations in amino acids metabolism may drive mitochondrial defects that characterized DS pathology.

***Lipid metabolism*.** DS individuals are characterized by an altered lipid metabolism. Growing number of studies demonstrated that DS children show higher levels of circulating cholesterol, low-density lipoproteins (LDL), and triglycerides with respect to age-matched controls[125–127]. Altered lipid profile in DS seems to lead an increased risk of cerebrovascular events[128] and overweight/obesity[126]. In this context, defects in lipid metabolism seems to be extended also to the brain since altered lipid profile was also reported in prefrontal cortex samples from DS individuals with respect to matched controls[129]. Indeed, a lipidomic study by Yu *et al.* showed reduced glycerophospholipid metabolism in DS together with reduced ratio of cholesterol to phospholipid concentration, phosphatidylcholine, and phosphatidylethanolamine levels[129]. In addition, in a very recent study, Hwang *et al.* observed that DS fibroblast are characterized by reduced levels of sphingosine derivatives called long chain bases (LCBs), which seem to be responsible for nuclear membrane alterations associated with accelerated aging process in DS[130].

Glucose metabolism. People affected by DS have a significantly lower glucose metabolic rate in the parietal and temporal cortical areas, which are the first typically affected in AD[131]. In addition, the cerebral glucose metabolic rate measured with the aid of positron emission tomography (PET) and [^{13}F]2-fluoro-2-deoxy-D-glucose undergoes to a significant reduction in older DS patients compared to younger DS[132]. Subsequent analysis also demonstrated that DS individuals are characterized by less efficient glycolytic flux. Hexokinase-II protein levels are significantly reduced in the frontal cortex of DS individuals[133], confirming an altered glycolytic pathway. In addition, phosphoglucose isomerase (PGI) is down regulated in foetal brain with DS and phosphofructokinase (PFK) activity, the rate limiting enzyme of glucose metabolism, is markedly impaired in frontal and temporal lobe and cerebellum from DS individuals while it is increased in the occipital lobe [134]. Interestingly, the human liver-type subunit of PFK (PFKL) is encoded by a gene residing on chromosome 21 and is triplicated in DS. In line with this, increased PFK activity is commonly found in fibroblasts and erythrocytes from DS patients, as a result of increased gene dosage[135]. Transgenic mice that overexpress PFK liver type (Tg- PFKL) showed alteration in glucose metabolism as indexed by increased metabolic flux in brain and reduced clearance from blood[136]. Although controversial results have been observed in different areas of DS adult brain, PFK specific activity is almost doubled in brains of embryonic Tg-PFKL mice, suggesting that the gene-dosage effects may change during aging[137]. These age-dependent changes of gene expression further complicate the "gene-dosage effects" hypothesis of trisomy 21, contributing to the multifaceted aberrant metabolism observed at different ages[138].

Glucose is the major source of energy for mammalian brain. Since brain neurons cannot synthesize or store glucose, they are fully dependent on glucose import to ensure their functionality. Glucose enters the brain via glucose transporters (GLUTs) primarily present at the BBB. Among the most important GLUTs in mammalian brain, GLUT1 is expressed in micro vessels and glia, but not in neurons. GLUT3, together with GLUT1, is the predominant GLUT responsible for glucose transport and its mainly neuron specific. On to the other hand, GLUT2 seems to be only expressed in astrocytes. GLUT4 instead seems to be the mediator of insulin effects on the brain[139]. *Post-mortem* investigations of AD brains showed decreased protein levels of GLUT1 and GLUT3[140], especially in the cerebral cortex[141]. On the other hand, in these patients, the level of GLUT2 is significantly increased; whereas, there is no significant difference in GLUT4 level in the brain of AD patients compared to healthy controls[142]. According to the required role of GLUTs in delivering glucose to the brain, altered GLUTs levels detected in DS brain[133] could further contribute to disrupted glucose metabolism. While glucose uptake and metabolism are finely regulated by insulin in peripheral tissues/organs, the brain was thought to be not affected by insulin in terms of glucose uptake[143]. Recent advances in the comprehension of brain functions highlighted that the actions of insulin are more pronounced in the central nervous system than previously thought. Indeed, insulin plays a major role in the regulation of gene expression and cellular metabolism, both events that sustain neuronal activity and synaptic plasticity mechanisms[143]. In this scenario, dysfunctions of insulin signalling in the brain of DS patients are of interest in order to better understand DS neurodegeneration. Although insulin or proteins belonging to the insulin signalling pathway are not encoded by genes located on chromosome 21, insulin signalling is at the crossroad among intracellular events driving cell

metabolism in terms of glucose, fatty acids, and proteins synthesis/utilization[144]. Recent advances in the comprehension of brain functions highlighted that the actions of insulin are more pronounced in the central nervous system than previously thought. Furthermore, alterations of brain insulin signalling have been associated with a higher risk of developing age-related cognitive decline and neurodegenerative diseases[145]. In this context, brain insulin resistance (defined as an insufficient response to insulin by target cells; Figure 6) represents a pivotal event driving AD neurodegeneration[143] and has been associated with increased Aβ production[146], increased inflammatory processes[147], and high oxidative stress levels[148]. Moreover, insulin resistance may even precede other neuropathological alterations by several decades, indicating an active role of impaired glucose metabolism in driving AD neurodegenerative processes[149]. Interestingly, among the common neuropathological features with AD, also DS brains seems to be early characterized by brain insulin resistance[133]. Indeed, markers of brain insulin resistance are evident in DS brains even before the appearance of clinical signs of AD neuropathology[133], suggesting a role for insulin signalling alterations in the early onset of AD in people with DS[79].

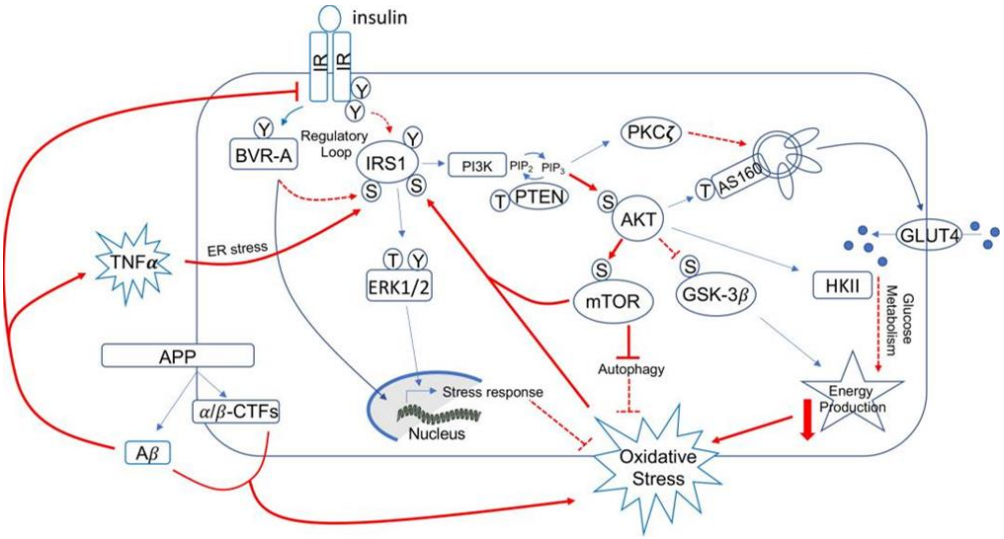

Figure 6: Schematic representation of the insulin signalling: Under physiological conditions, the activation of insulin signalling requires the binding of insulin to the insulin receptor (IR), which auto-phosphorylates on Tyr residues (e.g., Tyr1158/1162/1163) and promotes the receptor tyrosine kinase-mediated phosphorylation of its substrate (IRS1) on specific Tyr residues (e.g., 632). Once activated, IRS1 works as a scaffold protein, driving the activation of the two main harms of the insulin signalling: (I) the MAPK pathway, mainly involved in gene transcription and (II) the PI3K/Akt axis that is critical for activating downstream proteins that mediates insulin neurotrophic outcomes. Indeed, Akt promotes the phosphorylation of several targets, among which are: (I) GSK3β which has a role energy production and tau phosphorylation; (II) mTOR, which regulates protein synthesis and autophagy; and (III) AS160. This latter is responsible for the translocation of GLUT4-containing vesicles to the plasma membrane to mediate glucose uptake. During the development of brain insulin resistance, a dysregulation of a number of these proteins was observed. From a molecular point of view, brain insulin resistance phenomenon is characterized by key events such as reduced IR protein levels and/or increased IRS1 inhibitory phosphorylation levels (e.g., Ser307, Ser636), that are responsible for the uncoupling between IR and IRS1.

Energetic metabolism. The pathological metabolic phenotype of DS may result in reduced catabolic processes and impaired energy production. Within this scenario, defects of mitochondrial function are known to contribute to a

general loss of cellular functions, most of which strictly depend on ATP availability[150–152]. Indeed, growing evidence demonstrated that loss of mitochondrial structure and function, together with increased ROS production, strongly contribute to DS pathological phenotypes[152]. As a matter of fact, defects in mitochondrial functionality have been observed in basically all DS cells. Fibroblasts and lymphoblastoid cells from DS subjects show deficits in the oxidative phosphorylation (OXPHOS) system such as the complex I activity, the ATP synthase, the ADP/ATP translocator, and the adenylate kinase enzyme, ultimately leading to significant energy deficit and increased ROS production in mitochondria[153,154]. Reduced OXPHOS rate was also found in neural progenitor cells (NPCs) isolated from the hippocampus of Ts65Dn mice (murine model of DS)[155] and skin fibroblasts form DS subjects[156]. Thus, mitochondrial dysfunction is considered an inherent feature of DS, associated with increased oxidative stress[157].

2.2 Role of altered O-GlcNAcylation in Alzheimer's Disease progression.

An increasing number of studies have recently highlighted the importance of altered glucose metabolism in the progression of AD[158]. Among the molecular mechanisms that may clarify the contribution of glucose hypometabolism in the neurodegenerative process, the alteration of O-GlcNAc homeostasis seems an appealing theory. This hypothesis suggests that impaired glucose uptake/metabolism in the brain could lead to decreased protein O-GlcNAcylation levels. Such decrease in O-GlcNAc levels reflects a failure of the protective mechanism of O-GlcNAc in the brain and thereby favours the

progression of AD. In this context, several studies have recently correlated brain hypoglycaemia with decreased O-GlcNAcylation, supporting their convergence to AD neurodegeneration[159–161]. Most importantly, altered O-GlcNAcylation of brain's key proteins, such as APP and tau has proved to affect their phosphorylation and to trigger the formation of amyloid plaques and neurofibrillary tangles[162]. Indeed, although reduced glucose metabolism may be a downstream consequence of Aβ toxicity[163], many studies also confirmed that impaired O-GlcNAcylation in the brain could, in principle, contribute to Aβ accumulation. Although APP was proved to be O-GlcNAcylated almost 20 years ago by Griffith *et al.*[164], only recently this PTM has proved to affect its processing and thus Aβ formation. In this context, a recent work by Jacobsen and Iverfeldt demonstrated that increasing overall protein O-GlcNAcylation in SHSY cells though the use of OGA inhibitors or OGA siRNAs results in an increase in sAPPα, a product of the non-amyloidogenic pathway, and a decrease in Aβ secretion, suggesting that O-GlcNAcylation could have protective effects in AD progression[165]. Furthermore, the reduction of APP amyloidogenic cleavage induced by the boost of O-GlcNAcylation seems to be related to the inhibition of APP endocytosis that prevents its amyloidogenic processing by BACE1. As a matter of fact, O-GlcNAcylation on Thr576 residue of APP is known to prevent its endocytosis, eventually reducing Aβ production[166]. In this context, it has recently been proved that long-term OGA inhibition leads to the reduction of toxic Aβ-40 and Aβ-42 peptides in the brain, decreased Aβ plaques formation and neuroinflammation, finally resulting in improved cognition in 5xFAD-AD mice[167]. In line with the putative role of O-GlcNAcylation in regulating APP processing, OGA inhibitor treatment proved to reduce Aβ production also by lowering γ-secretase activity both *in vitro* and *in vivo*[167].

Unlike APP, the role of protein O-GlcNAcylation for tau protein has been more extensively studied during the last decades. O-GlcNAcylation on tau proteins, when first discovered in samples of bovine tissues, indicated a stoichiometry of about 4 moles of O-GlcNAc per mole of tau proteins[168]. Since then, many O-GlcNAcylation sites were identified on human tau protein (e.g. Thr123, Ser208, Ser400, Ser409, Ser412), most of which are found to be phosphorylated in brains from AD patients[169,170]. Most interestingly, O-GlcNAcylation seems to inhibit tau intracellular aggregation by reducing its abnormal phosphorylation, thus restoring cognitive functions[171]. In line with these reciprocal relationship between O-GlcNAcylation and phosphorylation, O-GlcNAcylated levels of tau have proved to be inversely related to phosphorylated tau levels[172]. In this contest, the reduction in glucose levels in fasting animals have proved to reduced O-GlcNAcylation and increase tau phosphorylation[173]. Furthermore, O-GlcNAcylated tau levels are reduced upon the use of okadaic acid (Ser/Thr phosphatase inhibitor)[174], confirming the cross-talk between this two PTMs. Conversely, when AD mice were treated with the selective OGA inhibitor, Thiamet-G, which increased the level of O-GlcNAcylation, the decrease in tau phosphorylation was proportional to the increase in O-GlcNAc level in the brain[175]. On the contrary, when tau phosphorylation was increased using an OGT inhibitor, the opposite effect was observed[176]. Chronic OGA inhibition also reduced tau levels in the CSF of AD mice[177]. Moreover, a recent study using bigenic TAPP mice, which manifest both amyloid and tau pathologies, reported the effects of long-term OGA inhibition using Thiamet-G. OGA inhibition blocked cognitive decline in these mice in parallel to decreases in Aβ levels and amyloid plaques in the brain and showed a clear trend toward decreased insoluble tau[171], thus confirming the

modulation of protein O-GlcNAcylation as a promising approach to counteract AD progression.

3. Metabolic diseases and neurodegeneration

Metabolic syndrome is a cluster of conditions (insulin resistance, obesity, hyperglycaemia, hypertension, and dyslipidaemia) that underlie the onset and progression of a number of pathologies including Type-2 diabetes mellitus (T2DM), non-alcoholic steatohepatitis, coronary heart disease, obesity, stroke and cognitive decline. Growing body of epidemiological evidence suggest that metabolic syndrome may be important in the development of age-related cognitive decline, mild cognitive impairment, vascular dementia and Alzheimer's disease[178]. In line with the relationship between altered metabolic phenotype and dementia, it is suggested that T2DM and defect in glucose metabolism might predispose to poorer cognitive performances and more rapid cognitive decline during ageing. Clinical and experimental evidence has indicated that glucose intolerance and diabetes induce dementia through various mechanisms such as atherosclerosis, microvascular disease, glucose toxicity, and impaired insulin metabolism[179]. Several large longitudinal population-based studies on this topic in fact confirmed a complex relationship between diabetes mellitus and dementia[180]. In this scenario, a prospective study by Ohara identified diabetes as a risk factor for all-cause dementia, especially AD. In addition, higher levels of 2-hour post-load glucose, fasting insulin and homeostasis model assessment of insulin resistance were significantly associated with increased risk of neuritic plaques[181]. Furthermore, a recent study by Janson *et al.* observed that T2DM or impaired fasting glucose might be present in up to 80% of patients with AD[182]. Aside from AD, T2DM is also

liked to other forms of cognitive disfunctions, such as mild cognitive impairment (MCI) or diabetes-associated cognitive decrements[183]. Interestingly, in 2015, a large cohort study from Canada indicated that the risk of dementia is already increased in patients with newly diagnosed diabetes[184]. Moreover, elevated plasma concentrations of glucose in individuals without diabetes have also been linked to an increased risk of dementia[185], confirming the relevance of altered metabolic profile in driving cognitive decline. In this context obesity has also been related with increased risk of developing dementia. Indeed, overweight and increased body mass index (BMI) in midlife has revealed to be a risk factor for dementia in later life[186]. In addition, the link between obesity in mid-life and the future risk of developing dementia has been confirmed by several studies[187–189]. Most interestingly, obesity has been shown to increase the risk of dementia independently from T2DM. A longitudinal study by Withmer *et al*. proved that individuals with the largest sagittal abdominal diameter have a nearly 3-fold risk of developing dementia compared to the smallest diameter[190]. Another study on this topic observed that larger waist-hip ratio is associated with decreased hippocampal volume[191], confirming the link between the accumulation of abdominal fat and cognitive dysfunctions. According to these data, metabolic alterations such as those occurring in diabetes and obesity seems to drive cognitive alterations, probably based on overlapping neurodegenerative mechanism, including oxidative stress, mitochondrial dysfunction, and inflammation.

3.1 High-Fat-Diet in mice: a model of metabolic-induced cognitive decline

The associations between consumption of a high-fat or 'standard' diet and metabolic disorders such as obesity, diabetes, and cardiovascular disease have long been recognized and a great deal of evidence now suggests that diets high in fat can also have a profound impact on the brain, behaviour, and cognition. As the brain cannot synthesise or store energy reserves, food provides its immediate source of energy and thereby may influence structure and function[192]. Indeed, the brain is particularly vulnerable to the effects of obesogenic diets, especially during early life comprising periods of rapid growth, maturation, and development[193]. Growing evidence have proved the detrimental impact of diets rich in saturated fatty acids, and extensive research has shown that diet-induced obesity potentially results in memory impairment in rodents[194]. In this context, animal models have proven to be very precious in acquiring basic knowledge about metabolic alterations driving cognitive decline. One of the most well-characterized experimental models used to study the role of metabolic syndrome in driving obesity, T2DM and consequent cognitive decline is obtained by feeding mice with the so called "high-fat diet". This model of diet-induced obesity and insulin resistance closely mimic molecular changes occurring in metabolic syndrome that precede obesity, diabetes and dementia, such as hyperglycaemia, hyperinsulinemia, insulin resistance, decreased autophagy and dyslipidaemia[195]. In this scenario, mice fed with a high-fat diet (HFD) for only one day show a rapid drop in the performance of episodic memory task, that can be rapidly reversed switching to a low-fat diet[196]. Furthermore, mice fed with a HFD for a long period of time show poor learning and memory performance[197], as well as depressive and

anxiety-like behaviours[198,199]. Several interactive processes have been proposed to underlie cognitive decline related to poor diet including oxidative stress and inflammation[200], increased blood brain barrier permeability[201], reduced neurotrophic factors[202], altered mitochondrial functionality[203] and insulin insensitivity[204,205]. In a study by Woodie and Blythe, by focusing on hypercaloric diet (high in fat and fructose) and its effects on cognitive performances, the authors demonstrated that hypercaloric diet promotes insulin dysregulation, hyperlipidaemia, and poor cognitive performance. These observations indicate that the combination of a high-fructose and high-fat diet may altered lipid and energy metabolism similar to clinical diabetes, with elevation of fasting glucose and increased cholesterol levels[206]. These changes were also found in rats fed with a HFD, suggesting that insulin resistance is a probable mediator to HFD-induced cognitive deficits[207]. In support of this, also mice fed with HFD exhibit a significant increase in obesity, lower glucose and insulin tolerance as compared to animals fed with standard diet. These changes are accompanied by consistent alterations of the insulin signalling in the brain, with reduced insulin receptor activation together with increase inhibitory phosphorylation of the insulin receptor substrate (IRS)[208]. In addition, HFD mouse brain exhibits biochemical changes related to increase Aβ deposition, neurofibrillary tangle formation and decreased synaptic plasticity, suggesting that changes in insulin sensitivity might contribute to cognitive impairment and the onset of AD-related hallmarks in HFD mice[208]. In line with these findings, human epidemiological studies indicate that long-term hyperinsulinemia and obesity caused by dietary fat intake are risk factor for dementia, whereas insulin administered to AD patients, by regulating glucose transport, energy metabolism, neuronal growth and synaptic plasticity, improves memory formation[209], thus confirming the role of insulin-resistance in AD progression.

Together with reduced insulin sensitivity, mice fed with high fat diet also show reduced brain cortex bioenergetic, altered mitochondrial function and oxidative stress. Indeed, mitochondria from brain cortex of HFD mice showed reduced respiratory capacity, decreased oxygen consumption and reduced ATP production[210]. In addition, HFD animals also showed a decrease in SOD enzyme activity, the first line of defence against oxidative stress, contributing to the increased oxidative stress of these animals. Accordingly, HFD induces an imbalance of ratio GSH/GSSG, a clear sign of altered redox state[210]. In line with these findings, another work by Miotto *et al.* indicates that HFD consumption is responsible for impaired mitochondrial bioenergetic together with an increased mitochondrial H_2O_2 emission as a result of impaired ADP sensitivity[203]. Furthermore, mice fed with HFD show increased levels of catalase and superoxide dismutase (enzymes involved in the antioxidant response) and high levels of 4-hydroxynonenal-adducts (marker of oxidative damage), supporting an increase in oxidative stress/damage and the stimulation of an antioxidant response[203]. All together this data supports the idea of common molecular mechanisms that could underlie both neurodegenerative disease and cognitive decline in HFD animals.

3.2 Role of O-GlcNAcylation in metabolic diseases

Nutrients-responsive protein O-GlcNAcylation has emerged as an important key actor in many of the major diseases associated with metabolic dysfunctions. O-GlcNAc signalling has been proved to have a role in regulating adipose tissue dynamics in metabolic adaptation to nutrient availability. In details, a recent study by Yang *et al.* proved that loss of adipose OGT specifically promotes lipolysis in visceral fat by decreasing O-

GlcNAcylation, while overexpression of adipose OGT inhibits adipose tissue lipolysis and promotes diet-induced obesity and whole-body insulin resistance. This study provided extensive evidences for the role of increased adipose O-GlcNAcylation as a molecular signature for obesity and diabetes and further confirmed the essential role for OGT in lipolysis regulation[211]. In line with these recent findings, an aberrant increase of protein O-GlcNAcylation has been directly linked to insulin resistance and to hyperglycaemia-induced glucose toxicity, two hallmarks of diabetes and diabetic complications. Indeed, hyperglycaemia induces elevated O-GlcNAcylation of some key transcription factors and cofactors (e.g. FoxO1, PCG-1α), promoting gluconeogenesis and lipogenesis. This, in turn, further increases glucose level, forming a vicious cycle that worsens the glucose toxicity effects and thus aggravates the progression of diabetes and diabetic complications[212]. In this context, biochemical analysis of erythrocyte proteins (from patients diagnosed as normal, prediabetic or diabetic) reveals that the levels of both protein O-GlcNAcylation and OGA are elevated in diabetic compared to that of the control group[213]. And more importantly, protein O-GlcNAcylation and OGA levels are significantly elevated in prediabetic samples as well, suggesting that O-GlcNAcylation could be used as a potential tool for the early screening of pre-diabetic conditions.

Together with its role in the regulation of gluconeogenesis and lipid metabolism, O-GlcNAcylation has been proved to play a pivotal role in controlling insulin signalling. Indeed, many effector molecules of insulin signalling pathway are also O-GlcNAcylated, often in a reciprocal manner to phosphorylation on specific serine residues[7,212,214]. Interestingly, it has been reported that almost all major player of insulin signalling pathway (e.g. IRS1,

PI3K, AKT) are regulated through a reciprocal crosstalk between O-GlcNAcylation and phosphorylation that regulates insulin signalling through positive/negative feedbacks. In this context, chronic elevation of O-GlcNAc has been hypothesized as a possible contributor to the onset of insulin resistance, at least in part though the persistent O-GlcNAcylation of PI3K and Akt on stimulatory serine sites[212,215]. *In vitro* and *in vivo* studies have proved that rising total protein O-GlcNAcylation levels, by either genetic manipulation or OGA inhibition, results in the development of insulin resistance and diabetes[216–218]. However, OGA inhibition in 3T3-L1 adipocytes did not induce insulin resistance[219], suggesting a more complex relationship between phosphorylation and O-GlcNAcylation rather than just a yin-yang mechanism. Interestingly, inhibitory serine residues of IRS1 can also be O-GlcNAcylated[220], leading to the possibility of hypoglycaemia-mediated reduced O-GlcNAcylation on inhibitory serine residues of IRS1 that may result in its increased phosphorylation and development of impaired insulin signalling in AD brain. This evidence seems to suggest that the disruption of the harmonious balance between O-GlcNAcylation and phosphorylation may contribute to the unproper functioning of the insulin pathway and be responsible for the onset of the insulin resistance[4]. As extensively discussed before, hypoglycaemia and reduced protein O-GlcNAcylation are well-demonstrated feature of AD progression[160,172,221]. Since altered glucose metabolism, impaired O-GlcNAcylation and defective insulin signalling seems to cooperate in the progression of the neurodegenerative process, the comprehension of the complex interplay between them could highlight new insights into the pathological mechanisms.

2. AIM OF THE WORK

Growing evidences have recently pointed out disturbances of protein O-GlcNAcylation as a possible link between altered brain metabolism and the progression of neurodegenerative processes. As observed in Alzheimer's disease (AD) brain, flaws of the cerebral glucose uptake translate into reduced HBP flux thus leading to impaired protein O-GlcNAcylation. Notably, the nutrient-related reduction of O-GlcNAcylated proteins triggers an aberrant increase of tau and APP phosphorylation in AD brain, favouring the formation of toxic neurofibrillary tangles and β-amyloid plaques therefore contributing to disease pathogenesis.

Given that Down syndrome (DS) and AD share similar metabolic alterations and common pathological markers within the brain, it is conceivable to suppose a role for aberrant O-GlcNAcylation in driving DS neurodegeneration. In this scenario, the present work discloses, for the first time, the possible role of protein O-GlcNAcylation in DS-related dementia. To achieve this goal, we exploited a well-established murine model of DS (Ts2Cje) to investigate changes in global protein O-GlcNAcylation, focusing on the hippocampal region, which has a high impact on cognitive functions. We also evaluated possible alterations occurring in the O-GlcNAc enzymatic machinery, by analysing OGT/OGA cycle and GFAT1 activation state. Supporting the notion that impaired protein O-GlcNAcylation can affect commonly recognized AD hallmarks, we further investigated APP and tau post-translational modifications in Ts2Cje mice to assess the role of impaired O-GlcNAcylation in mediating the progression of AD-like dementia in DS. Since defective O-GlcNAcylation has been proved to play a key role in AD progression, current research is focused on small molecules that can possibly

modulate protein O-GlcNAcylation as a novel therapeutic target to counteract neurodegeneration[222]. Considering the promising results obtained on various AD models[170,175,177,223], we also tested putative neuroprotective effects of a brain-targeting strategy in our DS model, shading a light on the possible mechanisms through which the intranasal administration of Thiamet-G (selective OGA inhibitor) could exert benefits in Ts2Cje mice.

The common motif that has emerged from these studies strongly suggests that altered metabolism, defective HBP and impaired O-GlcNAcylation are important hallmarks associated with neurodegeneration. As extensively discussed before, an altered O-GlcNAcylation profile is a well-demonstrated feature of both AD[160,172,221] and metabolic disorders like T2DM and obesity[211,213]. In order to discern the contribution of metabolic-induced changes in the neurodegenerative process, the second part of this work has focused on the study of O-GlcNAcylation homeostasis in wild type mice fed with a diet high in fat content. In details, we aimed to confirm the role of altered O-GlcNAcylation as a driving event that favours the development of AD signatures in the brain identifying the contribute of nutrients overload by using high fat diet (HFD) mice. Furthermore, we explored the impact of nutrients overload on mitochondrial functionality, thus suggesting another possible link between dysfunctional O-GlcNAcylation and cognitive decline in the HFD model.

3. MATERIALS AND METHODS

3.1 Animal models

Down Syndrome model. Experiments were conducted on Ts2Cje mice (Rb(12.Ts171665Dn)2Cje) and euploids animals (B6EiC3SnF1). Ts2Cje are a well-established murine model of DS characterized by a triple copy of a Robertsonian fusion chromosome carrying the distal end of Chr16 and Chr12. Parental generations were purchased from Jackson Laboratories (Bar Harbour, ME, USA). Mouse colony was raised by repeated crossbreed of Ts2Cje (Ts2) trisomic females with euploid (Eu) males. Since these breeding pairs produce litters containing both trisomic and euploid offspring, resultant progeny was genotyped to determine the presence of the trisomic segment using Quantitative-PCR, as previously described by Reinoldth *et al.*[224]. Mice were housed in clear Plexiglas cages (20 x 22 x 20 cm) under standard laboratory conditions with a temperature of 22 ± 2 °C and 70% humidity, a 12-h light/dark cycle and free access to food and water. For the initial longitudinal study, both Ts2 and Eu mice were sacrificed by cervical dislocation at different time-points (3, 6, 9, 12 and 18 months of age) and brain areas were collected for preliminary western blot analysis. For the 6-months-focused analysis, Ts2 and Eu mice at the selected age (n=6/group) were perfused with saline solution through intracardiac injection. Brain was dissected in halves: one hemisphere was fixed for immunofluorescence analysis while the other section was used for remaining biochemical evaluations. All samples were flash-frozen and stored at − 80 °C until utilization. All the experiments were performed in strict compliance with the Italian National Laws (DL 116/92), the European Communities Council Directives (86/609/EEC). Experimental protocol was approved by Italian Ministry of Health (#1183/2016-PR).

Table 1: Samples characteristics of animals used for aging study, 6-months-old-focused analysis and TMG intranasal treatment reporting respective group of treatment, gender, age, experimental use and average weight before and after TMG treatment.

Group		Genotype	n.	Gender	Age months	Experimental Use				Initial Weight	Final Weight
				(m/f)	(avg ± SD)					g (avg ± SD)	
Aging	3 m	Euploid	6	1/5	3.2±0.5	WB n=6/group				\	
		Ts2Cje	6	1/5	3.3±0.4						
	6 m	Euploid	6	4/2	6.2±0.4						
		Ts2Cje	6	2/4	6.4±0.5						
	9 m	Euploid	6	1/5	9.4±0.5						
		Ts2Cje	6	3/3	9.1±0.9						
	12 m	Euploid	6	5/1	11.4±0.2						
		Ts2Cje	6	4/2	11.6±0.4						
6-months-old		Euploid	6	4/2	6.2±0.4	WB n=6/group	qRT-PCR n=5/group	IP n=4/group		\	
		Ts2Cje	6	2/4	6.4±0.5						
		Euploid	3	2/1	5.3±1.1	Immunofluorescence n=3/group					
		Ts2Cje	3	2/1	5.6±0.8						
		Euploid	5	3/2	5.5±0.6	OGA and GFAT1 Assays n=5/group					
		Ts2Cje	5	2/3	5.3±0.6						
Treatment	Veh	Euploid	6	3/3	6.7±0.8	WB SB ELISA n=6/group	qRT-PCR n=5/group	OGA Assay n=5/group	IP n=4/group	38.6±9.8	37.9±9.4
		Ts2Cje	6	3/3	6.7±0.8					33.3±6.0	32.5±5.0
	TMG	Euploid	6	3/3	6.8±0.4					34.4±8.8	33.9±8.1
		Ts2Cje	6	4/2	6.6±0.5					31.7±4.7	30.0±5.6

High Fat Diet model. Male C57BL/6 mice (30–35 days old), derived from Animal Facility of Catholic University, were used and randomly assigned to two feeding regimens: (I) standard diet (SD, control) and (II) high fat diet (HFD). Mice were housed in clear Plexiglas cages (20 x 22 x 20 cm) under standard laboratory conditions with a temperature of 22 ± 2 °C and 70% humidity, a 12-h light/dark cycle. Animals were fed with their respective diet and water ad libitum and body weight was weekly monitored (Table 2). At the end of the diet period, animals were sacrificed trough cervical dislocation and brain areas were collected for subsequent biochemical analysis. All samples were flash-frozen and stored at − 80 °C until utilization. All animal procedures were approved by the Ethics Committee of the Catholic University and were fully compliant with Italian (Ministry of Health guidelines, Legislative Decree No. 116/1992) and European Union (Directive No. 86/609/EEC) legislations on animal research. The methods were carried out in strict accordance with the approved guidelines.

3.2 High Fat Diet

Male C57BL/6 mice from same litter were randomly assigned to different experimental groups. Animals were fed with SD or HFD (whose caloric intake was composed by 60% of saturated fatty acids) for 6 weeks. The diets were purchased from Mucedola Srl (Italy).

Group	n.	Initial Weight	Final Weight	Experimental Use		
		g (avg ± SD)				
Standard Diet	6	12.6±2.3	28.7±4.0	**WB** n=6/group	**IP** n=3/group	**OGA and GFAT1 Assay** n=6/group
High Fat Diet	6	12.3±2.3	37.5±5.0			
Standard Diet	8	12.7±2.0	28.5±3.2	**Mitochondrial Complexes Activity and ATP** n=8/group		
High Fat Diet	8	12.2±2.2	37.4±5.5			

Table 2: Samples characteristics of animals used for HFD study reporting respective group of treatment, experimental use, and average weight before and after diet differentiation.

3.3 Thiamet-G intranasal treatment

A pilot study was performed to identify the effective Thiamet-G dose to use for the intranasal treatment. This preliminary dose-response study was performed on a restricted number of Eu animals (n=3/group; Eu=3m) which were respectively administered with Vehicle solution (Veh; PBS 1X solution) or 1 μg, 5 μg, 10 μg, 25 μg and 50 μg of Thiamet-G solution (TMG; HY-12588, MedChemExpress). Animals were treated with a single intranasal delivery of 10 μL to each nostril and sacrificed 8-hours later though cervical dislocation. Brain areas were collected, and western blot analysis was performed to evaluate treatment efficacy. Our data demonstrated that the intranasal administration of 25 μg of TMG was able to significantly increase the global levels of O-GlcNAcylated proteins. Once identified the effective dose, 6-months old Ts2Cje and Euploid mice were divided in four experimental groups (n=6/group) according to genotype and intranasal treatment received. Based on previously published data on Thiamet G treatment in rodents, which demonstrated that the administration of the drug achieved the peak of increased O-GlcNAc levels after 8-10 hours[225], we opted to treat our animals twice a day

with the effective dose of 25 µg for 5 days, with the aim of achieving a stable elevation of O-GlcNAcylated proteins for a short period of time. Treatment was well tolerated although a physiological loss of weight was noticed due to prolonged animal manipulation. Indeed, an equal weight loss was observed in TMG-treated mice as well as animal treated with vehicle solution (Table 1). No change in food intake or drinking water consumption was observed. At the end of treatment animals were euthanized and perfused with sterile PBS through an intracardiac puncture. After sacrifice, brains were collected and saved for subsequent analysis.

3.4 Immunofluorescence

Entire brains from 6-months old Ts2Cje mice and corresponding euploids were fixed in a 4% formaldehyde aqueous solution for 24-hours at 4 °C. Fixed brains were then cryoprotected for the next 48-hours at 4 °C with a solution containing 20% of sucrose and 0.02% of NaN3. Brains were frozen on a temperature-controlled freezing stage, coronal sectioned (20 µm) on a sliding cryostat (Leica Biosystems, Wetzlar, Germany), and stored in a solution of PBS containing 0.02% NaN3 at 4 °C until utilization. Brain sections were mounted on glass slide. Once dried, brain sections underwent to a heat-induced antigen retrieval step in a 10 mM EDTA solution, pH=6.0, for 20 minutes at 55 °C[226]. After 4 washes with filtered PBS, sections were blocked with a solution containing 10% normal goat serum and 0.2% Triton X-100 in filtered PBS. Slides were then incubated 24h at 4 °C with following antibodies: GFAP (1:500; anti-rabbit; 840001, BioLegend), IBA1 (1:250; anti-rabbit; GTX100042, GeneTex), NeuN-1 (1:500; anti-rabbit, 702022, Invitrogen TermoFisher Scientific), O-GlcNAc CTD110.6 (1:100; anti-mouse, SC-

59623, Santa Cruz Biotechnology), O-GlcNAc RL2 (1:50; anti-mouse, #MABS157, Sigma-Aldrich). Slides were then washed with filtered PBS and incubated with Alexa Fluor -488 nm and -594 nm secondary antibodies (1:1500; A11029, A11034, Invitrogen TermoFisher Scientific) for 1-hour and a half at room temperature. Tissues were then stained with Sudan black (0.1% Sudan Black B in 70% ethanol; 199664, Sigma-Aldrich) to block auto fluorescence inherent to the sample. Slides were then washed, incubated with DAPI (10 mg/mL; IS-7712, Immunological Sciences) for 1 minute and washed again. One slide per group was stained without primary antibodies to establish nonspecific background signal. At the end cover slip glasses were placed using a drop of Fluoromount aqueous mounting medium (F4680, Sigma-Aldrich) and glasses were kept at room temperature to dry. All slides were imaged using Zeiss AXio (Carl Zeiss, Oberkochen, Germany). All immunolabeling acquisition intensities, field sizes, and microscopy settings were kept consistent across images. Images were analyzed using ImageJ. Image montages for figures were collated in Illustrator and Photoshop Cs6 (Adobe System) software programs and were based upon brain images that most closely approximated the group means.

3.5 Western blot

All brain samples used for Ts2Cje longitudinal study, 6-months focused analysis, TMG treatment and HFD analysis were homogenized following the same procedure. The hippocampus region was thawed in RIPA buffer (pH 7.4) containing 50 mM Tris-HCl (pH 7.4), 150 mM NaCl, 1% NP-40, 0.25% sodium deoxycholate,1 mM EDTA, 0,1% SDS, protease inhibitor cocktail

(1:100; 539132, Millipore), phosphatase inhibitor cocktail (1:100; P5726, Sigma-Aldrich), PUGNAc (OGA inhibitor, 100 μM; A7229, Sigma-Aldrich), Benzyl-2-Acetamido-2-Galactopyranose (OGT inhibitor, 2 mM; B4894, Sigma-Aldrich). Brains were homogenized by 20 strokes of a Wheaton tissue homogenizer, sonicated, and centrifuged at 14 000 rpm for 40 minutes at 4 °C to remove debris. Supernatant was collected and total protein concentration was determined by the BCA method (Pierce™ BCA Protein Assay Kit, 23227, ThermoFisher Scientific) according to manufacturer instructions. For western blot analysis, 15 μg of proteins were separated via SDS-PAGE using Criterion™ TGX Stain-Free™ precast gel (Bio-Rad) and transferred to a nitrocellulose membrane by Trans-Blot Turbo Transfer System (Bio-Rad). The blot was imaged by ChemiDoc MP imaging system (Bio-Rad) using the Stain-Free Blot settings. Protein total load captured by Stain-Free technology was later used for total protein normalization. Following, nitrocellulose membrane was blocked using 3% BSA (bovine serum albumin; 9048-46-8, SERVA) or Milk 5% (skim milk powder; 42590, SERVA) in 1X Tris Buffer Saline (TBS; #1706435, Bio-Rad) containing 0.01% Tween20 and incubated overnight at 4 °C with the following primary antibodies: α-CTF and β-CTF (1:5000; SAB5200113, Sigma-Aldrich), pThr172AMPK (1:1000; GTX52341, GeneTex), AMPKα1/2 (1:500; SC-74461, Santa Cruz Biotechnology), APP (1:5000; SAB5200113, Sigma-Aldrich), pThr642AS160 (1:1000; GTX55118, GeneTex), AS160 (1:500; MA514840, Invitrogen TermoFisher Scientific), AT8 (1:1000; MN1020, Invitrogen TermoFisher Scientific), Atg7 (1:1000; SC-376212, Santa Cruz Biotechnology;), Atg5-12 (1:1000; SC-133158, Santa Cruz Biotechnology;), Beclin-1 (1:1000; 3738, Cell Signaling Technology), pSer243GFAT1 (1:1000; S343C, MRC-PPU), GFAT1 (1:1000; 28121, IBL), GLUT1 (1:500; ab40084, Abcam), GLUT3 (1:500; SC-74497, Santa Cruz

Biotechnology), GLUT4 (1:500; SC-53566, Santa Cruz Biotechnology), pTyr1146/1150/1151IR (1:1000; GTX25681, GeneTex), IR (1:1000; 3020, Cell Signaling), pTyr612IRS1 (1:1000; GTX24868, GeneTex), pSer636IRS1 (1:1000; GTX32400, GeneTex), LC3 I-II (1:1000; NB1002220, Novus Biologicals), mTOR (1:1000; 2983, Cell Signaling Technology), pSer2448mTOR (1:1000; 5536, Cell Signaling Technology), OGA (1:1000; SAB-4200267, Sigma-Aldrich), O-GlcNAc CTD110.6 (1:500; SC-59623, Santa Cruz Biotechnology), O-GlcNAc RL2 (1:1000; MABS157, Sigma-Aldrich), OGT (1:500; SC-74546 Santa Cruz Biotechnology), PSD95 (1:1000; 3450, Cell Signaling Technology), pSer/Thr (1:5000; ab17464, Abcam), Syntaxin 1A (1:1000; Ab1453, Abcam), SQSTM1 (1:1000; SC-28359, Santa Cruz Biotechnology), pSer404tau (1:1000; ab92676, Abcam), tau (1:1000; orb46243, Biorybt), Total OXPHOS cocktail (1:5000; Ab1104113, Abcam). Next day, all membranes were washed with 1X TBS containing 0.01% Tween20 and incubated at room temperature for 1-hour with respective horseradish peroxidase-conjugated secondary antibodies: anti-rabbit (1:10000; L005661, Bio-Rad Laboratories), anti-mouse (1:10000; L005662, Bio-Rad Laboratories), anti-sheep, (1:3000; A3415, Sigma-Aldrich). As necessary, enhanced sensitivity was obtained using secondary antibodies able to detect only native IgG (1:200; TidyBlot, #STAR209, Bio-Rad Laboratories. 1:1000; TrueBlot, 18-8817-30, Rockland Immunochemicals). Blots were then imaged via the ChemiDoc MP imaging system using Chemiluminescence settings. Subsequent determination of relative abundance via total protein normalization was calculated using Image Lab 6.1 software (Bio-Rad Laboratories).

3.6 Slot Blot

For the analysis of total protein-bound 4-hydroxy-2-nonenals (HNE-adducts) and 3-nitrotyrosine (3-NT) levels, 3 µl of hippocampus homogenate from Ts2Cje and Eu both treated with TMG and Vehicle (n=6/group) were incubated with 6 µl of Laemmli Buffer (0.125 M Tris base pH=6.8, 4% (v/v) SDS, and 20% (v/v) glycerol). The resulting samples (250 ng/well) were loaded under vacuum onto a nitrocellulose membrane using a slot blot apparatus. Membranes were blocked for 1 h at room temperature with 3% of bovine serum albumin in TBS solution containing 0.01% Tween 20 and incubated at room temperature for 2 hours with the corresponding primary antibodies: 3-NT (1:1000; N5538, Sigma-Aldrich) and HNE polyclonal antibody (1:2000; NB100-63093, Novus Biologicals). Membranes were then washed three times with TBS solution containing 0.01% Tween 20 and incubated for 1 h at room temperature with respective alkaline phosphatase secondary antibodies from Sigma-Aldrich: anti-mouse (A1293; 1:3000) and anti-goat (A4187; 1:3000). Membranes were later washed three times in TBS solution containing 0.01% Tween 20 and developed with Sigma Fast BCIP/NBT (5-Bromo-4-chloro-3-indolyl phosphate/Nitro blue tetrazolium substrate). Blots were dried, acquired with Chemi-Doc MP imaging system and analysed using Image Lab 6.1 software (Bio-Rad Laboratories).

3.7 Immunoprecipitation

For OGT: Sepharose beads were used to immunoprecipitate OGT (EZView Red Protein G Beads, Sigma-Aldrich) according to manufacturer instructions. Briefly, different sample-sets (100 µg of proteins) were incubated overnight at

4 °C with the primary antibody for OGT (1:100; SC-74546 Santa Cruz Biotechnology) in IP buffer containing 10 mM Tris (pH=7.6), 140 mM NaCl, 0.5% NP40, phosphatase inhibitor cocktail (1:100; P5726, Sigma-Aldrich), PUGNAc (OGA inhibitor, 100 μM; A7229, Sigma-Aldrich), Benzyl-2-Acetamido-2-Galactopyranose (OGT inhibitor, 2 mM; B4894, Sigma-Aldrich). Next day, all samples were incubated with 20 μL of Protein G beads (EZView Red Protein G Beads, E3403, Sigma-Aldrich) for 2-hours at room temperature and then washed three times with RIA buffer containing 10 mM Tris (pH=7.6), 140 mM NaCl, 1% NP40. Afterwards, standard western blot procedure was performed. Resulting blots were incubated overnight at 4 °C with the following primary antibodies: O-GlcNAc CTD110.6 (1:500; SC-59623, Santa Cruz Biotechnology), O-GlcNAc RL2 (1:1000; MABS157, Sigma-Aldrich), OGT (1:500; SC-74546, Santa Cruz Biotechnology), pSer/Thr (1:5000; ab17464, Abcam) and detected by the horseradish peroxidase-conjugated secondary antibodies: anti-mouse (1:10000; L005662, Bio-Rad Laboratories) and anti-rabbit (1:10000; L005661, Bio-Rad Laboratories). IP results were normalized on the total amount of OGT and analysed following the same procedures used for western blot.

For APP, Tau and NDUFB8 (Complex I): Magnetic beads were used to immunoprecipitate APP and tau (SureBeads™ Protein G Magnetic Beads; 1614023, Bio-Rad Laboratories) according to manufacturer instructions. Briefly, 100 µL of magnetic beads were magnetized using specific tube-magnetic rack and washed three times with 1X PBS containing 0.1% Tween20. Primary antibody for APP (1:100; SAB5200113, Sigma-Aldrich), tau (1:50; orb46243, Biorybt) and NDUFB8-Complex I (1:100; NBP2-75586) was incubated with Magnetic Beads for 30 minutes at room temperature. After

three washes, 100 μg of proteins for each sample were incubated for 1-hour and 30 minutes at room temperature. After additional three washes, standard western blot procedure was performed for APP and tau IP. Resulting blots were incubated overnight at 4 °C with the following primary antibodies: APP (1:5000; SAB5200113, Sigma-Aldrich), tau (1:1000; orb46243, Biorybt), O-GlcNAc CTD110.6 (1:500; SC-59623, Santa Cruz Biotechnology), O-GlcNAc RL2 (1:1000; MABS157, Sigma-Aldrich), pSer/Thr (1:5000; ab17464, Abcam) and detected by the horseradish peroxidase-conjugated secondary antibodies: anti-mouse (1:10000; L005662, Bio-Rad Laboratories), anti-rabbit (1:10000; L005661, Bio-Rad Laboratories), and by horseradish peroxidase-conjugated secondary antibodies able to detect only native IgG (1:200; TidyBlot, #STAR209, Bio-Rad Laboratories; 1:1000; TrueBlot, 18-8817-30, Rockland Immunochemicals). IP results were normalized on the total amount of APP or tau and analysed following the same procedures used for western blot.

3.8 OGA assay

OGA enzymatic activity was measured using the synthetic substrate p-nitrophenyl N-acetyl-β-D-glucosaminide (pNP-GlcNAc) as described by Zachara and colleagues[227]. All samples used for Ts2 6-months-focused analysis, intranasal TMG treatment and HFD analysis were processed using the same procedure. Briefly, 15 mg of hippocampus were thawed in RIPA buffer (pH=7.4) containing 50 mM Tris (pH=7.4), 50 mM NaCl, 1% NP-40, 0.25% sodium deoxycholate,1 mM EDTA, 0,1% SDS, protease inhibitor cocktail (1:100; 539132, Millipore), phosphatase inhibitor cocktail (1:100; P5726, Sigma-Aldrich). Brains were homogenized by 20 strokes of a Wheaton

tissue homogenizer, sonicated, and centrifuged at 14 000 rpm for 40 minutes at 4 °C to remove debris. Supernatant was collected, desalted using Zeba™ Spin Desalting Columns (89882; ThermoFisher Scientific) and protein concentration was determined by the BCA method (Pierce™ BCA Protein Assay Kit, 23227, ThermoFisher Scientific) according to manufacturer instructions. Samples (150 μg of proteins) were incubated with activity assay buffer containing 2 mM pNP-GlcNAc, 50 mM sodium cacodylate (pH=6.4), 50 mM N-acetylgalactosamine and 0.3% BSA at 37 °C for 2-hours. Reaction was stopped by the addition of 500 mM Na2CO3 and absorbance was measured at 405 nm (Multiskan EX, Thermo Labsystems). OGA activity is reported as enzyme activity units where 1U catalyzes the release of 1 μmol pNP/min from pNP-GlcNAc. OGA activity for each group was normalized on corresponding protein expression levels.

3.9 GFAT1 assay

GFAT1 enzymatic activity was performed adapting a procedure developed by McClain and colleagues[228]. GFAT1 activity for Ts2 6-months-focused analysis and HFD analysis was assessed though the measuring of its enzymatic product glucosamine 6-phosphate (GlcN6P). Briefly, 15 mg of hippocampus were thawed in 80 μL Lysis buffer (pH=7.5) containing 100 mM KCl, 1 mM EDTA, 50 mM Na3PO4, protease inhibitor cocktail (1:100; 539132, Millipore), phosphatase inhibitor cocktail (1:100; P5726, Sigma-Aldrich). Brains were homogenized by 20 strokes of a Wheaton tissue homogenizer, sonicated and centrifuged at 14 000 rpm for 40 minutes at 4 °C to remove debris. Supernatant was collected and total protein concentration was determined by the BCA method (Pierce™ BCA Protein Assay Kit, 23227, Thermo Fisher Scientific)

according to manufacturer instructions. Samples (240 µg of proteins) were incubated with activity assay buffer containing 1 mM EDTA, 1 mM DTT, 40 mM NaHPO4 (pH=7.4), 12 mM fructose 6-phosphate and 12 mM L-glutamine at 37 °C for 45 minutes. Reaction was stopped by the addition of PCA 1 M (1:2) to induce protein precipitation. Samples were then incubated 10 minutes on ice and centrifuged at 16 000g 4 °C for 10 minutes. Supernatant was extracted with chloroform (1:2) and 100 µL of the aqueous phase were collected for HPLC analysis. GlcN6P generated during the reaction was detected by derivatization of the sample with 2-volumes of o-phthalaldehyde (OPA) reagent (100 µL of 10 mg/mL OPA in EtOH, 900 µL sodium borate 100 mM pH=9.7 and 2 µL 3-mercaptopropionic acid). Reaction was incubated for 10 minutes at room temperature protected from light and sample was diluted 1:1000 in the mobile phase for HPLC detection. Chromatographic separation was performed using an isocratic elution, the mobile phase was composed by Na3PO4 15 mM, pH=7.2 (phase A) and Acetonitrile (phase B) (90:10). A Symmetry C18 column (300 Å, 5µm, 4.6 mm X 250 mm, 1/pk, Waters Corporation) was used for separation. Fluorescence of the sample eluent (λ=340/450) was analysed using a fluorescent detector (RF-551, Shimadzu) and the peak area was integrated using a dedicated software (Empower 2, Waters Corporation). OPA-derivatized GlcN6P standards (G5509, Sigma-Aldrich) were run separately to determine the retention time (1.8 s) and to generate a standard curve to correlate area to activity. The correlation coefficient between the concentration of GlcN6P standards and the area under the GlcN6P peak was 0.999. Activity is expressed as U/mg protein where 1 U represents the generation of 1 pmol of GlcN6P/min. GFAT1 activity for each group was normalized on corresponding protein expression levels.

3.10 RNA extraction and quantitative real-time RT PCR

RNA was extracted from the hippocampus of Ts2Cje and Eu treated both with TMG and Vehicle using Tissue Total RNA Kit according to manufacturer's instructions (Abcam). RNA was quantified using the Biospec Nano spectrophotometer (Shimadzu, Columbia, MD, USA), and RNA was reverse transcribed using the cDNA High Capacity kit (Applied Biosystems, Foster City, CA, USA), including reverse transcriptase, random primers and buffer according to manufacturer's instructions. The cDNA was produced through a series of heating and annealing cycles in the MultiGene OPTIMAX 96-well Thermocycler (LabNet International, Edison, NJ, USA). Real time PCR (Q-PCR) was carried out using the following cycling conditions: 35 cycles of denaturation at 95 °C for 20 s; annealing and extension at 60 °C for 20 s, using the SensiFAST™ SYBR® No-ROX Kit (Bioline, London, UK). PCR reactions were carried out in a 20 μl reaction volume in a CFX Connect Real Time PCR machine (Bio-Rad Laboratories). Primers used for the evaluation of gene expression were designed as follow: GADPH (Fw: ACAGTCCATGCCATCACTGCC; Rv: GCCTGCTTCACCACCTTCTTG), OGA (Fw: TGGAAGACCTTGGGTTATGG; Rv: TGCTCAGCTTCTTCCACTGA), OGT (Fw: CTGTCACCCTTGACCCAAAT; Rv: ACGAAGATAAGCTGCCACAG). Relative mRNA concentrations were calculated from the take-off point of reactions (threshold cycle, Ct) using the comparative quantification method performed by Bio-Rad software and based upon the ΔΔCt method. Ct values for GAPDH expression served as a normalizing signal[229].

3.11 Aβ 1-42 ELISA

Mouse Aβ 1-42 ELISA Kit (KMB3441; Invitrogen TermoFisher Scientific) was used to determine the levels of amyloid β 1-42 peptide in Ts2 and Eu mice treated with Veh or TMG. Briefly, ~10 mg of hippocampus was thawed in ice-cold DEA buffer (10 µL/mg tissue; 0.2% Diethanolamine in 50 mM NaCl) with protease inhibitor cocktail (1:100; 539132, Millipore). After centrifugation (15 000 rpm 1 h 30 min 4°C), supernatant was retained as Aβ soluble fraction. Aβ1-42 was then measured according to manufacturer's instructions. Curve-fitting was obtained by Graph Pad Prism 8.0 software (GraphPad, La Jolla, CA, USA).

3. 12 Respiratory chain complexes activity and ATP content

Experiments were conducted on 4 samples per group. Because of the small amount of tissue available, each sample was obtained by pooling hippocampus from 2 animals (for a total of 8 mice per group). Mitochondria were isolated as previously described by using a gradient of Percoll[230]. The specific activity of NADH-decylubiquinone oxidoreductase (NQR) (complex I), succinate decylubiquinone DCPIP reductase (SQR) (complex II) and cytochrome c oxidase (complex IV) were measured using a Beckman Coulter Spectrophotometer. Briefly, to disrupt the mitochondrial membranes for complex I measurement, 100 µg of mitochondrial suspension was first lysed by 3 min incubation in distilled water. Rotenone-sensitive complex I activity was measured in assay medium with final volume of 1 ml (50 mM TRIS, pH 8.1, 2.5 mg/ml BSA, 0.3 mM KCN, 0.1 mM NADH, 50 µM decylubiquinone without and with 3 µM rotenone) and followed the decrease in absorbance at

340 nm due to the NADH oxidation (ε = 6.22 mM−1 cm−1). Complex II activity was measured in 1 ml of assay medium containing 10 mM potassium phosphate pH 7.8, 2 mM EDTA, 1 mg/ml BSA, 200 µg of mitochondrial protein, 0.3 mM KCN, 10 mM succinate, 3 µM rotenone, 0.2 mM ATP, 80uM DCPIP (2,6-dichlorophenolindophenol), 1 µM Antimycin, 50 µM decylubiquinone). The decrease in absorbance at 600 nm due to the oxidation of DCPIP at 600 nm (ε = 20.1 mM−1 cm−1) was recorded. Complex IV activity was measured by incubating 100 µg of mitochondrial protein in 1 ml of assay medium (40 mM potassium phosphate, pH 7.0; 1 mg/ml BSA; 25 µM reduced cytochrome c) by following the oxidation of cytochrome c (II) at 550 nm (ε = 19.6 mM−1 cm−1). All assays were performed at 37 °C. FoF1-ATPase activity was measured following ATP hydrolysis with an ATP-regenerating system coupled to nicotinamide adenine dinucleotide phosphate (NADPH) oxidation, as previously reported[231]. Measurement of ATP concentration in the total homogenates from hippocampal area was performed by using a commercial bioluminescent assay kit (Sigma-Aldrich, St. Louis, MO, USA).

3.13 Statistical Analysis

Statistical analyses were performed using Student t test for the evaluation of differences between 2 groups and a non-parametric 1-way ANOVA with *post-hoc* Bonferroni t-test for the evaluation of differences between more than two group. To determine the influence of genotype (Ts2Cje; Ts2) and treatment (Thiamet G; TMG) we performed a 2-way ANOVA analysis. Data are expressed as mean ± SEM per group. All statistical analyses were performed using Graph Pad Prism 8.0 software (GraphPad, La Jolla, CA, USA).

4 RESULTS

4.1 Project 1: The dysregulation of OGT/OGA cycle mediates tau and APP neuropathology in Down syndrome

4.1.1 Ts2Cje mice show an aberrant and tissue-specific O-GlcNAcylation profile at 6 months of age.

In the last few years, a strong correlation between reduced protein O-GlcNAcylation and AD-associated pathological features was established[160,161,232,233]. We exploited the Ts2Cje (Ts2) mouse model to investigate the O-GlcNAcylation profile and its relevance in DS neurodegeneration. At first, we conducted an age-dependent study with the aim to assess putative changes of the total levels of O-GlcNAcylated proteins in the hippocampus from 3, 6, 9 and 12-months-old Ts2 compared with aged-matched euploids (Eu). We observed, in Ts2 mice, a premature reduction of O-GlcNAcylated proteins as early as at 6 months of age. Indeed, we found a trend of increase of total O-GlcNAc levels in 3 months-old Ts2 hippocampus, compared to aged-matched euploids, but a sudden significant switch is shown at 6-months of age (Fig. 7A; **$p<0.01$, Eu vs Ts2: -18%). A trend of reduced O-GlcNAc levels persisted also in Ts2 hippocampus at 9-months of age and 12-months of age compared to respective euploids, suggesting the progressive reduction of O-GlcNAc levels during aging. Accordingly, we observed by

immunofluorescence microscopy, a diffuse reduction of O-GlcNAcylated proteins in the entire hippocampus area of Ts2 mice at 6 months of age compared to respective euploids (Fig. 7E-F;**p<0.01, Eu vs Ts2: -10%). Considering the significant alteration of protein O-GlcNAcylation in 6 months old DS mice, we focused our following experiments on this age group. To investigate the interplay between O-GlcNAcylation and O-phosphorylation on serine-threonine residues[234–237], we evaluated the levels of total protein phosphorylation on these residues only. As postulated, we detected a significant increase of total protein phosphorylation in Ts2 hippocampus compared to respective euploids at 6 months of age (Fig. 7C-D; *p<0.05, Eu vs Ts2: +44%). Several studies supported that in AD and metabolic diseases the reduction of protein O-GlcNAcylation is a brain specific effect associated with reduced glucose uptake, altered HBP flux and/or aberrant phosphorylation process[53,159,162,221,238–240]. In contrast, peripheral organs often demonstrate an increased trend of O-GlcNAcylated proteins which correlates hyperglycaemia and contributes to impaired insulin signalling and glucose toxicity[232,241]. Our analysis of liver samples from 6-months-old Ts2 mice compared to relative euploids demonstrated a significant increase of global protein O-GlcNAcylation (Fig. 7G-H; *p<0.05, Eu vs Ts2: +74%), thus confirming the tissue specificity of this PTMs. Further, the early presence of alterations both in the central nervous system and the liver of 6-months old Ts2Cje mice suggest that aberrant protein O-GlcNAcylation contributes to DS pathogenesis promoting, in different organs, peculiar mechanisms of disease development.

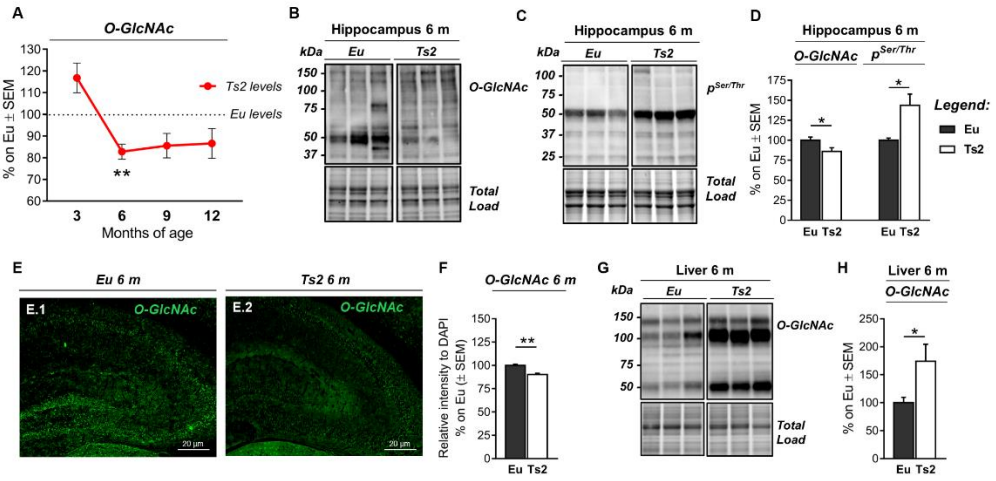

Figure 7: Early alteration of O-GlcNAcylation and phosphorylation profile in Ts2Cje mice. A: Longitudinal study of the O-GlcNAcylation profile in the hippocampus of differently aged Ts2Cje mice compared to respective euploids. A premature impairment of protein O-GlcNAcylation was observed in 6-months-old Ts2 mice compared to aged-matched euploids. A pronounced dropping of O-GlcNAcylated protein levels was detected also at 9 and 12 months of age. **B-D**: O-GlcNAcylation/phosphorylation profile in 6-months Ts2Cje mice hippocampus compared to respective euploids. The reduction of protein O-GlcNAcylation in the hippocampus of 6-months-old Ts2 mice was in line with a mutual inverse increase in the global phosphorylation of serine and threonine residues compared to aged-matched controls. Representative blots are reported in (**B**) and (**C**). **E-F**: Immunofluorescence analysis of O-GlcNAcylated proteins in the hippocampus of 6-months-old Ts2Cje and respective euploid mice. A diffuse impairment of O-GlcNAcylated proteins was detected in the entire hippocampal region from Ts2 mice compared to aged-matched euploids. Relative intensity quantification is reported in (**F**). **G-H**: O-GlcNAcylation profile in 6-months Ts2Cje mice liver compared to respective euploids. Increased levels of O-GlcNAcylated proteins were observed in the liver of Ts2 mice compared to euploid animals of the same age, confirming a global imbalance of O-GlcNAcylation homeostasis. Representative blot is reported in (**G**). Number of animals for each condition were as follow: n=6/group for western blot and n=3/group for immunofluorescence staining. All bar charts reported in (**A**), (**D**), (**F**) and (**H**) show mean ± SEM. *p<0.05, **p<0.01, using Student's t test.

4.1.2 The reduction of O-GlcNAcylated proteins in the hippocampus of 6-months old Ts2Cje mice is area and cell-type specific.

Although almost all cerebral tissues contain O-GlcNAcylated proteins, O-GlcNAc and OGT are particularly abundant in the hippocampal region[242]. Furthermore, O-GlcNAcylation plays a role in regulating hippocampal synaptic transmission and plasticity, thus influencing learning and memory processes[243,244]. Considering the relevance of protein O-GlcNAcylation in this brain area, we further examined the distribution of O-GlcNAcylated proteins in different subregions of Ts2 hippocampus at 6 months of age. As expected, Ts2 mice showed a general impairment of protein O-GlcNAcylation compared to respective euploids in each of the hippocampal subregions analysed (Fig. 2A1-2). In details, a relevant reduction of O-GlcNAc fluorescent signal was observed in the CA1 area (Fig. 8B1-6, E; **p<0.01, Eu vs Ts2: -20%), in the CA3 area (Fig. 8C1-6, E; *p<0.05, Eu vs Ts2: -70%) and in the dentate gyrus (DG) region (Fig. 8D1-6, E; *p<0.05, Eu vs Ts2: -30%) of the hippocampus from Ts2 mice compared to the respective euploid mice. Besides, Ts2 mice showed a different distribution of O-GlcNAcylated proteins reduction, with a higher decrease O-GlcNAc levels in the CA3 subregion compared both to the DG area and the CA1 area (Fig. 8E).

In the second instance, we evaluated cell-type distribution of O-GlcNAcylated proteins in the CA3 subregion, which has proved to be the area most affected by the reduction of O-GlcNAc fluorescence intensity in Ts2 mice. We determined that protein O-GlcNAcylation occurs primarily in neurons in Ts2Cje (Fig 9A5-8). Indeed, co-localization analysis showed significant O-GlcNAc signal (green) that overlaps with the neuronal marker

NeuN-1 (red) (Fig.9A5-8), while partial or no overlap between O-GlcNAc and microglia (IBA-1) or astrocytes (GFAP) occurs (Fig. 9B5-8, C5-8 respectively) in the CA3 of 6-months-old Ts2 mice. Costes' and Manders' coefficient (M1 and M2) analysis of co-localization showed that 90% of the O-GlcNAc signal co-localized with neurons[245]. In Eu mice, colocalization analysis demonstrated a strong correlation as well with NeuN-1 and O-GlcNAc that, although with lower values, persists also in microglia and astrocytes. These results suggest a cell-type specific impairment of O-GlcNAcylated proteins in Ts2Cje at 6 months of age and a consistent reduction of protein O-GlcNAcylation in neurons and astrocytes.

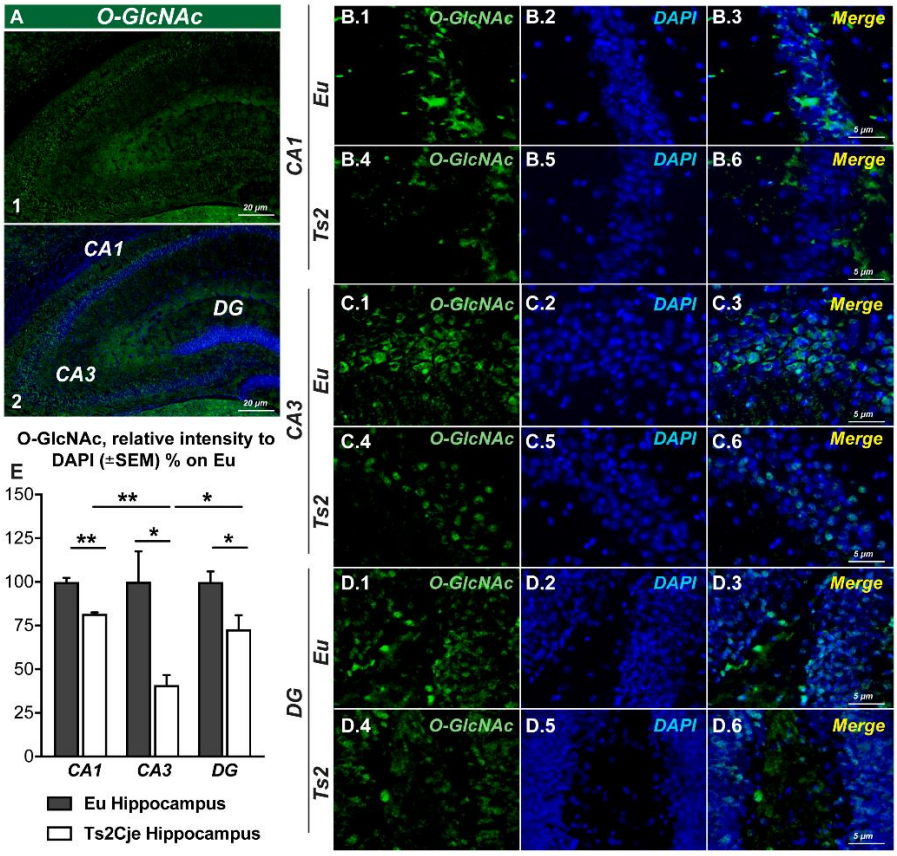

Figure 8: The reduction of O-GlcNAcylated proteins is area specific in the hippocampus of Ts2Cje mice. A1-2: O-GlcNAc staining of the entire hippocampus from 6-months-old Ts2Cje mice. **B-6**: O-GlcNAc staining of the CA1 area of the hippocampus from Ts2 and respective euploids. A significant impairment of global protein O-GlcNAcylation in the CA1 area of Ts2 mice (**B1-3**) was observed in comparison with the fluorescent signal of the same area from aged-matched euploids (**B4-6**); O-GlcNAc (green); DAPI (blue). **C1-6**: O-GlcNAc staining of the CA3 area of the hippocampus from Ts2 and respective euploids. Ts2 mice showed a massive reduction of global protein O-GlcNAcylation in the CA3 hippocampal area (**C1-3**) compared to respective euploids (**C4-6**); O-GlcNAc (green); DAPI (blue). **D1-6**: O-GlcNAc staining of the DG area of the hippocampus from Ts2 and respective euploids. A similar impairment was observed in the dentate gyrus from Ts2 mice (**D1-3**) compared to the same brain region from euploid animals (**D4-6**); O-GlcNAc (green); DAPI (blue). **E**: Related quantification of O-GlcNAc fluorescence intensity normalized on DAPI signal is reported for each hippocampal region from Ts2 and Eu animals. Number of animals for each condition were as follow: n=3/group for immunofluorescence staining. All bar charts reported in (**E**) show mean ± SEM. *p<0.05, **p<0.01, using Student's t test.

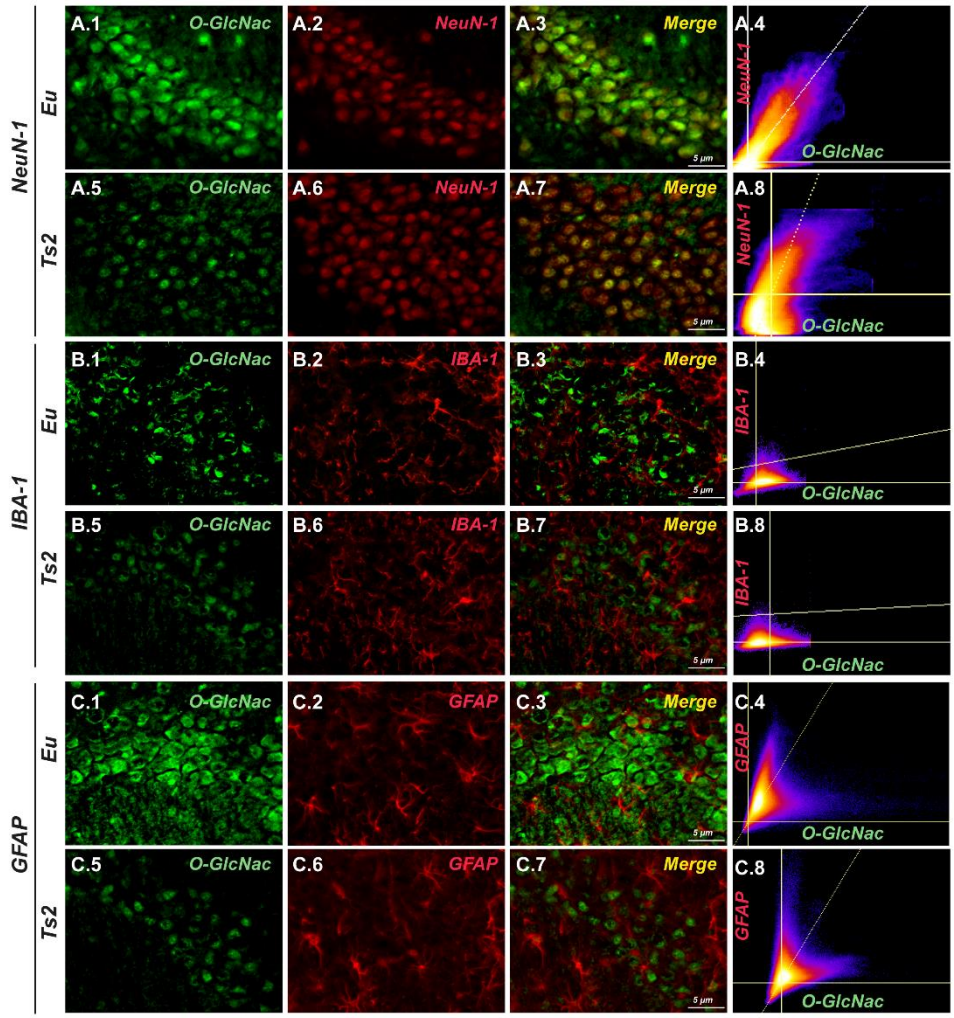

Figure 9: The reduction of O-GlcNAcylated proteins is cell-type specific in the hippocampus of Ts2Cje mice. A1-8: O-GlcNAc co-localization with the neuronal marker NeuN-1 in the CA3 hippocampal area from Ts2 and respective euploid mice. O-GlcNAc signal seems to broadly overlap with neuronal marker NeuN-1 in both CA3 area from euploid animals (**A1-4**) and Ts2 mice (**A5-8**). Co-localization graphs are reported for both Eu (**A4**) and Ts2 (**A8**) mice; O-GlcNAc (green); NeuN-1 (red); Co-localization (yellow). **B1-8**: O-GlcNAc co-localization with glial marker IBA-1 in the CA3 hippocampal area from Ts2 and respective euploid mice. Partial co-localization was observed between O-GlcNAcylated proteins and fluorescent signal from the glial marker IBA-1 in Ts2 CA3 subregion (**B1-4**) and a comparable result was obtained in the same region of euploid animals (**B5-8**). Co-localization graphs are reported for both Eu (**B4**) and Ts2 (**B8**) mice; O-GlcNAc (green); IBA-1 (red); Co-localization (yellow). C1-8: O-GlcNAc co-localization with the astrocytic marker

GFAP in the CA3 hippocampal area from Ts2 and respective euploid mice. Consistent colocalization of O-GlcNAc signal and GFAP was detected in the CA3 area of euploid animals (**C1-4**), while apparently no signal has been identified in the same area of Ts2 hippocampus (**C5-8**). Colocalization graphs are reported for both Eu (**C4**) and Ts2 (**C8**) mice; O-GlcNAc (green); GFAP (red); Co-localization (yellow). Number of animals for each condition were as follow: n=3/group for immunofluorescence staining.

4.1.3 Reduced O-GlcNAcylation results from the dys-regulation of OGT/OGA cycle.

Considering the relevance of O-GlcNAcylation cycle homeostasis, many regulatory mechanisms exist to balance OGA/OGT activity, thus calibrating protein O-GlcNAc levels according to cellular status[246]. We investigated OGA/OGT functionality in the hippocampus of Ts2 mice to test whether a dysfunctional cycling could be responsible for the observed reduction of global O-GlcNAcylation. Ts2 mice showed no difference in both OGT protein expression (Fig. 10A-B) and transcript (Fig. 10C) compared to the aged-matched Eu group. Since OGT itself undergoes to O-GlcNAcylation and phosphorylation on different sites, we performed an immunoprecipitation assay to analyse OGT PTMs that could potentially affect its ability to transfer O-GlcNAc moiety[240,247]. We noticed a significant reduction in $^{O\text{-}GlcNAc}$OGT/OGT levels in Ts2 mice compared to the Eu group (Fig. 10D-E; **p<0.01, Eu vs Ts2: -73%) and a trend on increase in $^{pSer/Thr}$OGT/OGT levels (Fig. 10D-E; Eu vsTs2: +20%). The reduction in the O-GlcNAc/phosphorylation ratio of OGT (Fig. 10D-E; **p<0.01, Eu vs Ts2: -75%) in Ts2 hippocampus suggests that the global reduction of O-GlcNAcylation might results from OGT altered functionality. Subsequently, we analysed the removal process of the O-GlcNAc moiety, measuring both OGA levels and enzymatic activity. OGA resulted significantly more

expressed in the hippocampus of 6-months old Ts2 mice (Fig. 10F-G; **p<0.01. Eu vs Ts2: +15%) in comparison with the control group. Furthermore, OGA protein levels also reflect the difference in mRNA transcript, which is significantly increased in Ts2 mice (Fig. 10H; *p<0.05. Eu Vs Ts2: +1.20-fold change), confirming an upregulation of OGA in Ts2 mice at 6 months of age. The analysis of OGA activity also demonstrated an upregulation of the global removal process of O-GlcNAc moiety (Fig. 10I, left panel; **p<0.01. Eu vs Ts2: +29%), although no changes in enzyme-specific hydrolytic activity was detected (Fig. 10I, right panel). In details, our data suggests that O-GlcNAc removal process is markedly increased in Ts2 hippocampus at 6-months of age compared to euploids as effect of increased OGA protein levels but not of OGA-specific hydrolytic activity increase. Therefore, we support that increased OGA levels promote the aberrant subtraction of O-GlcNAc moiety from serine and threonine residues, thus leading to the global reduction of O-GlcNAcylated proteins in Ts2Cje mice.

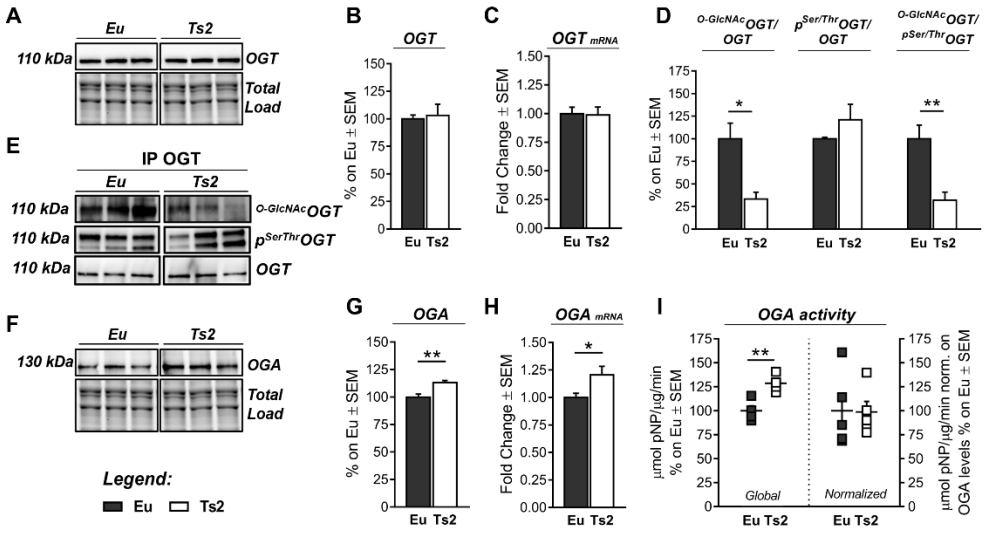

Figure 10: Reduced O-GlcNAcylation rely on aberrant OGT/OGA cycling. A-C: Analysis of OGT protein levels and transcript in Ts2 mice compared to respective euploids. OGT showed no alteration neither in protein expression nor mRNA levels in Ts2 hippocampus compared to the control group. Representative blot is reported in (**A**). **D-E**: Evaluation of OGT's PTMs by immunoprecipitation analysis. A significant reduction in $^{O\text{-}GlcNAc}$OGT/OGT levels together with a trend of increase in its $^{pSer/Thr}$OGT/OGT levels were observed in Ts2 mice compared to the respective euploid group. Representative blots are reported in (**E**). **F-H**: Analysis of OGA protein levels and transcript in Ts2 mice compared to respective euploids. Both OGA protein and mRNA levels were found significantly increased Ts2 mice in comparison to respective control group. Representative blot is reported in (**F**). **I**: OGA activity assay. Global OGA activity is significantly increased in Ts2 mice compared to respective control group. However, the enzyme-specific hydrolytic activity of OGA obtained through normalization on respective protein levels do not show relevant changes in the two groups. Number of animals for each condition were as follow: n=6/group for western blot and RT-qPCR, n=3/group for immunoprecipitation analysis and n=5/group for OGA activity assay. All bar charts reported in (**B**), (**C**), (**D**), (**G**), (**H**) and (**I**) show mean ± SEM. *p<0.05, **p<0.01, using Student's t test.

4.1.4 The aberrant O-GlcNAc/phosphorylation ratio of tau and APP drives Alzheimer-like neurodegeneration in Ts2Cje mice.

The abnormal hyperphosphorylation of tau, on specific serine and threonine residues, induces protein self-assembly and gives rise to toxic NFTs, a well-established hallmark of AD-like pathology[159,248]. Recent studies highlighted that tau phosphorylation is inversely regulated by O-GlcNAc and that tau O-GlcNAcylation plays a key role in hindering its aggregation[171,239,240,249]. Our data confirmed the aberrant phosphorylation of tau protein in 6-months old Ts2 mice compared to Eu group on both Ser202-Thr205 residues (Fig. 5A-B, AT8/tau; *p<0.05. Eu vs Ts2: +75%) and Ser404 (Fig. 5A-B; *p<0.05. Eu vs Ts2: +14%). Furthermore, through immunoprecipitation analysis, we found that increased phosphorylation of tau is associated with a significant reduction of its O-GlcNAcylated levels (Fig. 11C-D; *p<0.05. Eu vs Ts2: -20%). These results suggest a role for O-GlcNAc levels in the early disturbance of tau PTMs and confirm, in Ts2 neuropathology, the mutual inverse relationship between tau reduced O-GlcNAcylated levels and its increased phosphorylation. It was largely proven that APP undergoes O-GlcNAcylation[250] and recent advances demonstrated how increased $^{O\text{-}GlcNAc}$APP/APP levels could switch its processing from the amyloidogenic pathway to the non-amyloidogenic via, thus reducing the production of Aβ plaques[165]. Since APP is encoded on chromosome 21, the role of O-GlcNAcylation in APP processing could be further exacerbated in DS neuropathology. As expected, APP protein levels were significantly higher in Ts2 mice compared to respective Eu controls (Fig. 11E, G; **p<0.01. Eu vs Ts2: +60%). Subsequently, $^{O\text{-}GlcNAc}$APP/APP levels demonstrated to be significantly reduced in 6-months old Ts2 mice compared to Eu group (Fig.

11F, H; **p<0.01. Eu vs Ts2: -35%) and in parallel a significant increase in $^{pSer/Thr}$APP/APP levels (Fig. 11F, H; *p<0.05. Eu vs Ts2: +45%) was observed.

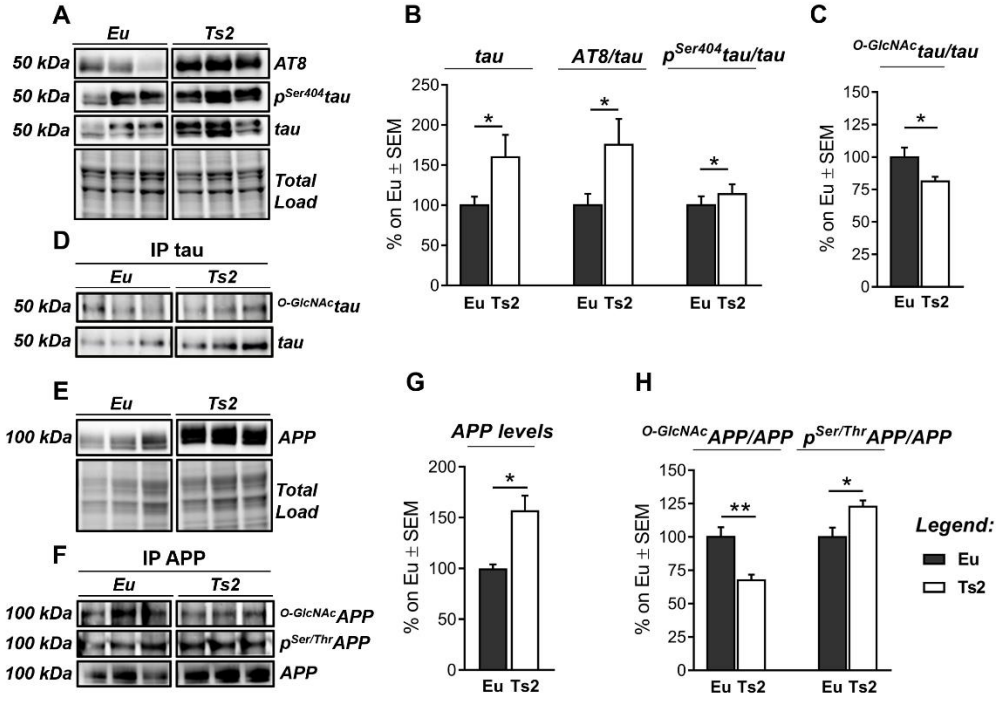

Figure 11: Aberrant O-GlcNAc/phosphorylation ratio of AD-related proteins in Ts2Cje mice. A-B: Analysis of tau phosphorylated levels in Ts2 mice compared to respective euploids. Tau protein levels were significantly higher in our DS model compared to controls. Moreover, increased levels of Ser202-Thr205tau/tau (AT8) and Ser404tau/tau were found in Ts2. Representative blots are reported in (**A**). **C-D**: Evaluation of $^{O\text{-}GlcNAc}$tau levels by immunoprecipitation analysis. A significant impairment in $^{O\text{-}GlcNAc}$tau /tau levels was observed in Ts2. Representative blots are reported in (**D**). **E, G**: Analysis of APP protein levels in Ts2 mice compared to respective euploids. We confirmed that APP is significantly more expressed in Ts2 mice. Representative blot is reported in (**E**). **F, H:** Evaluation of $^{O\text{-}GlcNAc}$APP and $^{pSer/Thr}$APP levels by immunoprecipitation analysis. $^{O\text{-}GlcNAc}$APP/APP impairment is related with increased $^{pSer/Thr}$APP/APP levels in the hippocampus of Ts2 mice compared to respective euploids. Representative blots are reported in (**F**). Number of animals for each condition were as follow: n=6/group for western blot and n=3/group for immunoprecipitation analysis. All bar charts reported in (**B**), (**C**), (**G**) and (**H**) show mean ± SEM. *p<0.05, **p<0.01, using Student's t test.

4.1.5 Ts2Cje mice show alteration of the HBP and the induction of the insulin cascade.

Since DS is characterized by a significant altered metabolic profile, with a prevalence of less efficient fermentative metabolism[121,251], we decided to analyse the activation state of AMP-activated protein kinase (AMPK) in our Ts2 model and its relevance in the control of HBP at early stage of disease. A significant increase in AMPK protein levels was observed in the hippocampus of 6-months-old Ts2 compared to the Eu group (Fig. 11A-B; **p<0.01, Eu vs Ts2: +78%), together with a significant reduction of AMPK activation measured by its ^{pThr172}AMPK levels normalized on respective protein levels (Fig. 11A-B; **p<0.01, Eu vs Ts2: +40%). The analysis of GFAT1 protein levels showed a significant difference among the two groups (Fig. 11C-D; *p<0.05, Eu vs Ts2: +50%), while GFAT1 phosphorylation on Ser 243, which is controlled by AMPK and regulates the inhibition of its catalytic activity, showed a significant reduction in Ts2 mice compared to euploids (Fig. 11C-D; *p<0.05; Eu Vs Ts2: +34%). In order to evaluate GFAT1 activation state, we exploited an HPLC-based method to measure its direct enzymatic product. According with the lack of AMPK inhibitory effect, a trend of increase was observed in GFAT1 global ability to synthetize glucosamine-6-phosphate in Ts2 mice compared to Eu group (Fig. 11E-G). However, since GFAT1 protein levels changes between Ts2 and Eu animals the activity was also normalized on respective protein levels demonstrating no significant alterations. To fully clarify if Ts2 show metabolic alteration that can impact the HBP and the O-GlcNAcylation process we evaluated the insulin cascade and/or glucose uptake. At first, we analysed in 6 months old animals the phosphorylated levels of IR on Tyr1146-1150-1151 to assess its activation state: a significant increase

in the phosphorylated levels of IR/IR was observed in Ts2 hippocampus compared to respective euploids (Fig. 11H-I; *p<0.05, Eu vs Ts2: +130%), while no significant changes were noticed on IR protein levels in the two groups. The evaluation of IR's direct substrate, IRS-1, demonstrated a significant increase in ^{pTyr632}IRS-1 (activator site) compared to ^{pSer636}IRS (inhibitory site) in Ts2 mice compared to Eu group (Fig. 11H,L; *p<0.05, Eu vs Ts2: +60%). No relevant differences were observed in IRS-1 protein levels between the two groups. According to our results, Ts2 mice at 6 months of age suggest the increased activation of the insulin cascade compared to respective euploids. The observed increased activation of the insulin cascade in Ts2 mice was anyhow associated with unaltered levels of brain glucose transporters but with an increase of GLUT4 translocation to the membrane as suggested by the increased total phosphorylation of AS160 (data not shown).

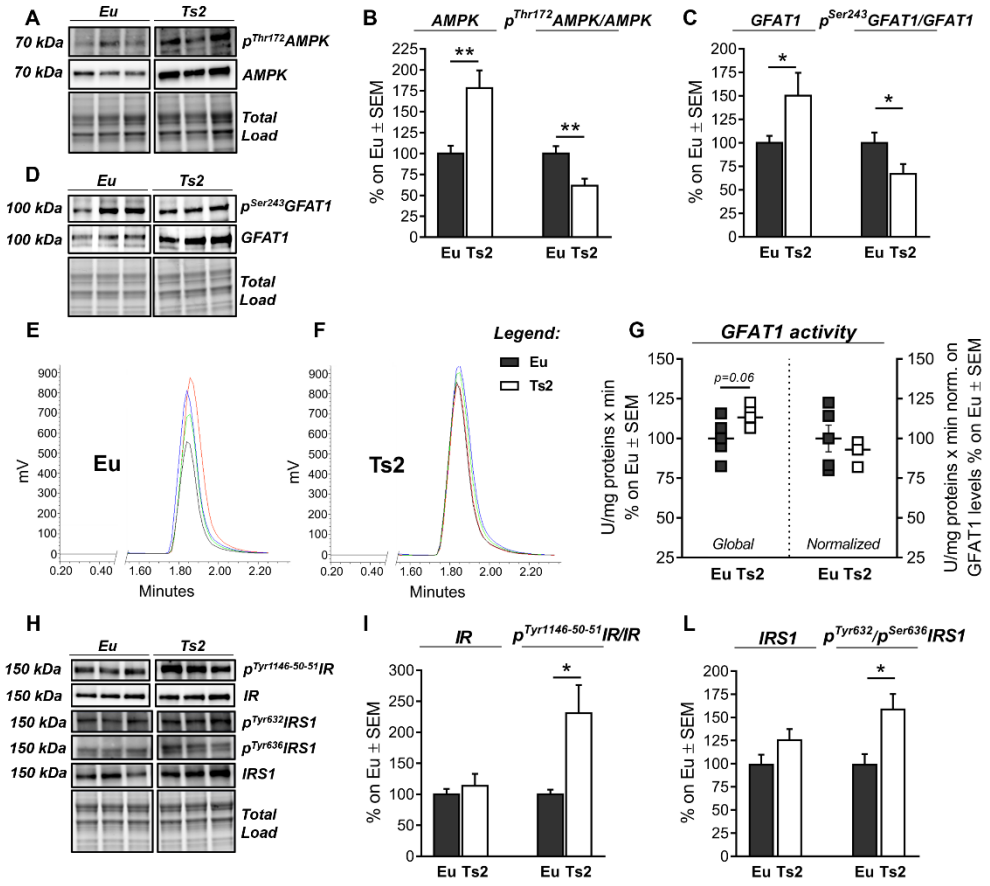

Figure 11: HBP flux is impaired in Ts2Cje mice together with an hyperactivation of the insulin cascade. A-B: Analysis of AMPK activation status in Ts2 mice compared to respective euploids. A significant increase in the AMPK protein levels was observed in Ts2 mice compared to Eu, together with a significant impairment in ^{pThr172}AMPK/AMPK levels, thus resulting in reduced AMPK activation. Representative blots are reported in (**A**). **C-D**: Analysis of GFAT1 activation status in Ts2 mice compared to respective euploids. A significant increase in GFAT1 levels was observed in Ts2 mice compared to control group, together with an impairment of ^{pSer243}GFAT1/GFAT1 ratio, resulting in reduced GFAT1 inhibition. Representative blots are reported in (**D**). **E-G**: GFAT1 activity assay. GFAT1 global activity showed a trend of increase in Ts2 hippocampus compared to respective euploids, while GFAT1 enzymatic normalized on corresponding protein expression levels showed no alteration. Representative spectra of GFAT1-synthetized glucosamine-6-phosphate for both Ts2 and euploid animals are reported in (**E**) and (**F**) and respective bar graph of global and normalized activity (**G**). **H-L**: Analysis of the insulin cascade in Ts2

mice compared to respective euploids. A significant increase in the phosphorylated levels of insulin receptor (Tyr1146-1150-1151)/IR was observed in Ts2 mice compared to Eu (**I**). Ts2 mice also showed an increase in the activation of the insulin receptor substrate (IRS-1), with increased ratio between phosphorylated levels on activator site (Tyr632) and inhibitory site (Ser636) (**L**). Representative blots are reported in (**H**). Number of animals for each condition were as follow: n=6/group for both western blot analysis and GFAT1 activity assay. All bar charts reported in (**B**), (**C**), (**G**), (**I**) and (**L**) show mean ± SEM. *p<0.05, **p<0.01, using Student's t test.

4.1.6 Intranasal Thiamet-G rescued aberrant protein O-GlcNAcylation and OGA activity in 6-months-old Ts2Cje mice.

Our results demonstrated that aberrant protein O-GlcNAcylation occurs in Ts2 mice because of increased OGA expression, which plays a significant role in the onset of AD-related markers. Hence, to question the possible neuroprotective effects of rescuing protein O-GlcNAcylation in Ts2 neuropathology, we performed a short-term intranasal treatment with Thiamet-G (TMG), a potent and selective OGA inhibitor. 6-months-old Ts2 and respective Eu were administered by intranasal route with vehicle solution (Veh) or 25 μg of TMG (Fig. 12A), with the aim to directly target the brain and avoid effects on peripheral organs[252] that might behave differently in term of O-GlcNAcylation. After 5 days of treatment, we observed that TMG treatment was able to rescue lower levels of O-GlcNAcylated proteins in Ts2 hippocampus, restoring euploid-physiological levels (Fig. 12B,D; **p<0.01, Ts2 Veh vs Ts2 TMG: +46%), without affecting neither OGT protein levels (Fig. 12C, E) nor transcript (Fig. 12F) Accordingly, 2-way ANOVA analysis support the effect of TMG treatment in rising O-GlcNAcylated protein levels [Table 3; F (1;21) =21.25, ***p<0.001]. In agreement with our hypothesis, the

analysis of OGA enzymatic activity demonstrated the efficacy of the intranasal TMG administration in inhibiting the aberrant removal of O-GlcNAc moiety from serine and threonine residues of hippocampal proteins. Indeed, TMG treatment induced a significant reduction of OGA specific activity in Ts2-treated mice compared to respective Ts2 treated with vehicle solution (Fig. 12I, right panel; *p<0.05: Ts2 Veh Vs Ts2 TMG: -24%). Anyhow, due to increased OGA expression levels in treated Ts2Cje mice we did not observed reduction on global OGA enzyme activity. Furthermore, we confirmed a genotype-dependent upregulation of both OGA protein levels (Fig. 12C, G) and transcript (Fig.12H) in Ts2 mice compared to euploids treated with vehicle, [Table 3; OGA protein: F (1;22) =3.7, *p<0.05; OGA mRNA: F (1;20) =5.3, *p<0.05]. Intriguingly, as described elsewhere[253,254], TMG treatment was able to trigger a significant increase of OGA protein levels in both Eu (Fig. 12C, G; *p<0.05, Eu Veh vs Eu TMG: +27%) and Ts2 animals (Fig. 12C, G; ***p<0.001, Ts2 Veh vs Ts2 TMG: +20%). Furthermore, an effect of TMG treatment in increasing OGA protein levels was also assessed by 2-way ANOVA analysis [Table 3; F (1;22) =16.8, ***p<0.001]. Surprisingly, upregulated OGA protein levels did not significantly reflect OGA mRNA levels both in Eu and Ts2 mice treated with TMG (Fig. 12H). The effect of TMG on OGA protein levels has been already observed by others[255], suggesting the occurrence of TMG-induced compensatory mechanisms during the inhibition of OGA catalytic activity.

Table 3: 2-way ANOVA analysis in Eu and Ts2 mice treated with Veh and TMG

2-Way ANOVA Analysis			
Target of interest	**Genotype (Eu vs Ts2)**	**Treatment (Veh vs TMG)**	**Interaction**
O-GlcNAc	F (1;21) = 2.055 p=0.1665	**F (1;21) = 21.25 ***p=0.0002**	F (1;21) = 1.327 p=0.2622
OGA activity/OGA	F (1;17) = 0.0001521 p=0.9903	F (1;17) = 3.468 p=0.0799	F (1:17) = 0.1305 p=0.7224
OGT	F (1;19) = 0.3515 p=0.5602	F (1;19) = 0.3289 p=0.5730	F (1;19) = 0.8781 p=0.3605
OGA	**F (1;22) = 3.710 *p=0.0498**	**F (1;22) = 16.83 ***p=0.0005**	F (1;22) = 0.4029 p=0.5321
OGT *mRNA*	F (1;20) = 0.9879 p=0.3321	F (1;20) = 1.047 p=0.3184	F (1;20) = 1.427 p=0.2462
OGA *mRNA*	**F (1;20) = 5.337 *p=0.0317**	F (1;20) = 0.02546 p=0.8748	F (1;20) = 1.985 p=0.1742
AT8/tau	**F (1;19) = 4.441 *p=0.0486**	F (1;19) = 0.08656 p=0.7718	F (1;19) = 1.069 p=0.3141
p^{Ser404}/tau	F (1;21) = 0.1369 p=0.7150	F (1;21) = 1.131 p=0.2997	**F (1;21) = 7.610 *p=0.0118**
β-CTF/α-CTF	**F (1;17) = 24.06 ***p=0.0001**	**F (1;17) = 9.043 **p=0.0079**	F (1;17) = 0.001069 p=0.9743
Aβ 42	F (1;20) = 0.6361 p=0.4345	**F (1;20) = 8.009 *p=0.0103**	F (1;20) = 0.01148 p=9157
PSD95	F (1;18) = 0.08181 p=0.7781	**F (1;18) = 7.727 *p=0.0124**	F (1;18) = 0.0691 p=0.7956
Syntaxin 1A	F (1;18) = 2.324 p=0.1448	**F (1;18) = 16.26 ***p=0.0008**	F (1;18) = 1.398 p=0.2524
BDNF	F (1;19) = 1.115 p=0.3043	**F (1;19) = 14.05 **p=0.0014**	**F (1;19) = 23.08 ***p=0.0001**
Atg7	F (1;21) = 0.05321 p=0.8198	**F (1;21) =14.48 **p=0.0010**	F (1;21) = 0.1.574 p=0.2234
Beclin-1	F (1;23) = 0.005176 p=0.9433	**F (1;23) = 16.48 ***p=0.0005**	F (1;23) = 2.745 p=0.1111
LC3-II/I	**F (1;21) = 7.926 *p=0.0104**	**F (1;21) = 5.861 *p=0.0246**	**F (1;21) = 13.85 **p=0.0013**
SQSTM1	F (1;23) = 2.521 p=0.1260	F (1;23) = 0.9074 p=0.3507	**F (1; 23) = 6.288 *p=0.0197**
3-NT	F (1;21) = 2.401 p=0.1362	F (1;21) =1.65 p=0.2130	**F (1;21) = 5.68 *p=0.0180**
HNE-adducts	**F (1;22) = 18.75 ***p=0.0003**	F (1;22) = 2.289 p=0.1445	F (1;22) = 0.09204 p=0.7644

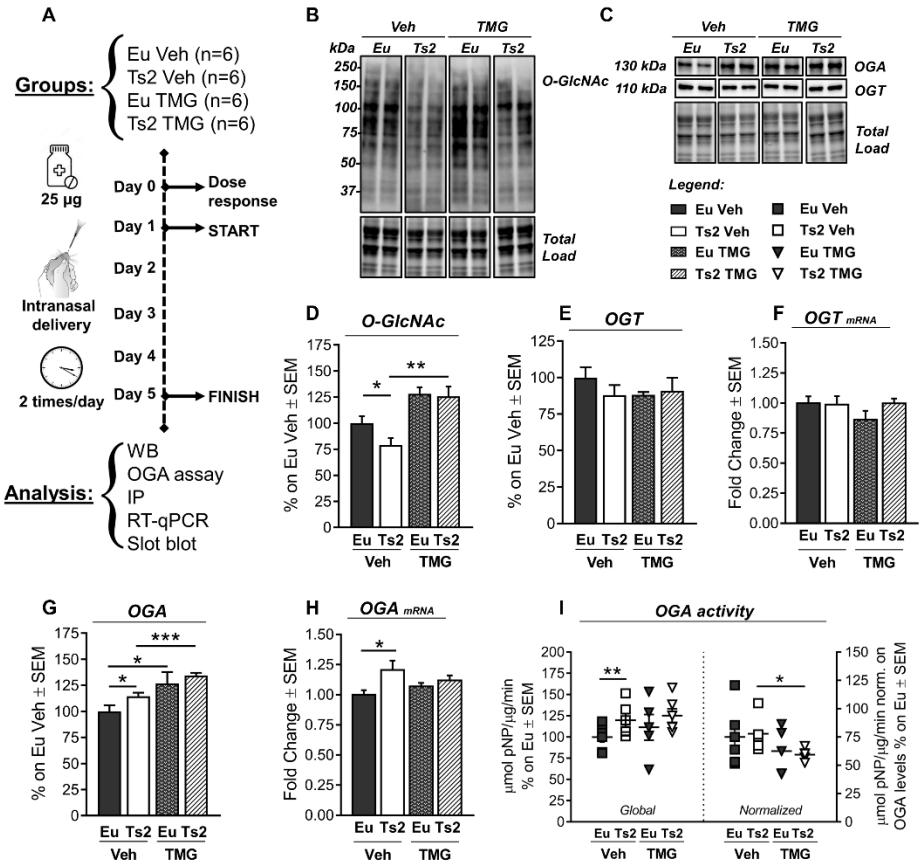

Figure 12: Short-term TMG intranasal treatment rescued protein O-GlcNAcylation and OGA activity in 6-months-old Ts2Cje mice. A: Schematic representation of the short-term TMG intranasal treatment. After a single dose-response study to assess the correct TMG dose (data not shown), 6-months-old animals were treated twice a day with vehicle solution (Veh; PBS 1X solution) or TMG (25 µg Thiamet-G solution) for 5 days. Animals were divided according to their genotype and intranasal treatment received in the following groups: Eu Veh, Ts2 Veh, Eu TMG, Ts2 TMG. Samples were then collected for subsequent analysis. **B, D**: Analysis of protein O-GlcNAcylation levels after TMG treatment. TMG intranasal treatment rescued protein O-GlcNAcylation in Ts2 TMG compared to Ts2 Veh. An increase of protein O-GlcNAcylation levels was also observed in Eu treated with TMG in comparison to Eu Veh. Representative blot is reported in (**B**). **C**: Representative blots of OGA and OGT protein levels after TMG treatment. **E-F:** Analysis of OGT protein levels and transcript after TMG treatment. No changes in OGT protein levels (**E**) and transcript (**F**) were observed in treated mice. Representative blot is reported in (**C**). **G-H**: Analysis of OGA protein levels and transcript after treatment. TMG treated triggered a significant increase in OGA protein

levels both in Eu and Ts2 mice (**G**), while no changes were observed in OGA transcript levels, following TMG administration (**H**). Representative blot is reported in (**C**). **I**: Analysis of OGA activity after treatment. TMG induced a significant reduction of OGA enzyme-specific activity in TMG-treated Ts2 mice compared to Ts2 mice treated with vehicle. OGA enzyme-specific activity was obtained for each group though normalization on corresponding protein expression levels. Number of animals for each condition were as follow: n=6/group for western blot analysis, RT-qPCR and OGA activity assay. All bar charts reported in (**D**), (**E**), (**F**), (**G**), (**H**) and (**I**) show mean ± SEM. *p<0.05, **p<0.01, ***p<0.001, using Student's t test.

4.1.7 Intranasal Thiamet-G rescued aberrant APP and tau PTMs in Ts2Cje hippocampus.

Subsequently, we evaluated the consequence of TMG treatment on tau PTMs. We observed a considerable increase of $^{O\text{-}GlcNAc}$tau/tau levels in TMG-treated Ts2 mice compared to Ts2 administered with vehicle solution (Fig. 13A-B; ***p<0.001, Ts2 Veh vs Ts2 TMG: +113%). Since pharmacological elevation of $^{O\text{-}GlcNAc}$tau/tau trough OGA inhibitors was related with reduced toxic forms of tau[177], we then measured the levels of phosphorylated tau. A significant reduction of the levels of tau phosphorylated on Ser404 was detected in Ts2 TMG-treated mice compared to respective trisomic animals treated with vehicle (Fig. 13C, E; *p<0.05, Ts2 Veh vs Ts2 TMG: -35%) with a mutual interaction between genotype and treatment described by 2-way ANOVA analysis [Table 3; F (1;21) = 7.6, *p<0.05]. On the contrary, no changes in Ser202-Thr205 phosphorylation were observed in TMG-treated Ts2 compared with Ts2 Veh (Fig. 13D-E: AT8/tau). As regard of APP, we observed that the short-term intranasal treatment with TMG induced a significant increase in the levels of $^{O\text{-}GlcNAc}$APP/APP in Ts2 mice compared to corresponding vehicle group (Fig. 13F, H; *p<0.05, Ts2 Veh vs Ts2 TMG: +35%), which was in line with a significant reciprocal inverse reduction of $^{pSer/Thr}$APP/APP levels (Fig. 13F, H; ***p<0.001, Ts2 Veh vs Ts2 TMG: -30%). Since site-specific phosphorylation on serine and threonine residues are known to influence APP fate[256–258], we presumed that TMG intranasal

treatment could exert beneficial effects on APP cleavage on Ts2Cje, as reported for AD murine models[167,259]. To confirm our hypothesis, we analysed APP cleavage products measuring both β-CTF and α-CTF. As expected, Ts2 Veh mice showed a significant increase in β-CTF/α-CTF ratio compared to respective euploids (Fig. 13G, I; **p<0.01, Eu Veh Vs Ts2 Veh: +40%) with a relevant contribution of genotype [Table 3; F (1;17) =24.1, ***p<0.0001] that confirms a tendency toward the APP-amyloidogenic processing in our DS model. According to our result, TMG intranasal administration induced a significant reduction of β-CTF/α-CTF ratio in the euploid group (Fig. 13G, I; *p<0.05, Eu Veh vs Eu TMG: -24%) but only a trend of decrease in Ts2-treated mice (Fig. 13G, I). Anyhow, an effect of TMG treatment in reducing β-CTF/α-CTF ratio was confirmed by 2-way ANOVA analysis [Table 3; F (1;17) =9.1, **p<0.01]. Our data suggest that the reduction of β-CTF/α-CTF ratio in the treated groups is mainly due to an increase of the α-CTF fragment rather than a significant reduction in β-CTF levels (data not shown), indicating that the increase in $^{O\text{-}GlcNAc}$APP/APP levels favours the non-amyloidogenic cleavage of the protein. Further, to account for the ability of Thiamet-G on reducing Aβ formation we analysed soluble Aβ 1-42 after intranasal treatment. To note, previous studies on DS models demonstrated that mice do not exhibit Aβ plaques within the brain, while the increase of soluble Aβ might occurs after mice middle age[260,261]. Our analysis demonstrates a slight but not significant increase of Aβ 1-42 in Ts2 mice compared to respective euploids (Fig.8L; Eu Veh vs Ts2 Veh: +1.9 pg/mL), while the treatment with Thiamet G showed a trend of decrease in both Eu (Fig. 8L; p=0.06, Eu Veh vs Eu TMG: -8.2 pg/mL) and Ts2 animals (Fig. 8L; p=0.07, Ts2 Veh vs Ts2 TMG: -7.6 pg/mL) suggesting the potential efficacy of the compound. In line with this trend, an effect of TMG treatment on Aβ 1-42 peptide was also confirmed by 2-way ANOVA analysis [Table 3; F (1;20) =8.0, *p<0.05].

In order to further characterize the possible neuroprotective effects of our treatment, we also analysed the expression of synapse-related proteins in TMG-treated mice. In details, TMG treatment proved to significantly raise PSD95 protein

expression levels in the hippocampus of Ts2 TMG mice (Fig. 8M-N; *p<0.05, Ts2 Veh vs Ts2 TMG: +31%) and induce the same significant increase of Syntaxin 1A protein levels in TMG-treated mice compared to Ts2 Veh group (Fig. 8M, O; **p<0.01, Ts2 Veh vs Ts2 TMG: +72%). Consistent with the above data, 2-way ANOVA analysis confirmed an effect of TMG treatment for both PSD95 and Syntaxin 1A [Table 3; PSD95: F (1;18) = 7.7, *p<0.05; Syntaxin 1A: F (1;18) = 16.3, ***p<0.001]. Interestingly, previous studies on the Ts65Dn model correlated reduced brain-derived neurotrophic factor (BDNF) with poor spatial memory in 6-months-old animals[262] and BDNF-mimetic therapy proved to rescue synaptic plasticity and memory deficits in Ts65Dn mice[263]. In this scenario, our analysis on 6-months-old Ts2 animals confirmed a significant reduction of BDNF protein levels in the hippocampal region of trisomic mice treated with Veh compared to equally treated Eu (Fig. 8M, P; ***p<0.001, Eu Veh vs Ts2 Veh: -37%). Furthermore, TMG-treated Ts2 mice showed significant higher levels of BDNF protein in comparison to respective Ts2 treated with vehicle (Fig. 8M, P; ***p<0.001, Ts2 Veh vs Ts2 TMG: +83%). This effect of TMG treatment was also demonstrated by 2-way ANOVA analysis [Table 3; F (1;19) = 14,.05 **p<0.01] and also a synergic effect of both treatment and genotype was observed [Table 2; F (1;19) = 23,0 ***p<0.001]. Overall, these data suggest that TMG treatment could exert its benefits also trough the induction of synapses-related proteins, possibly recovery Ts2 cognitive deficits.

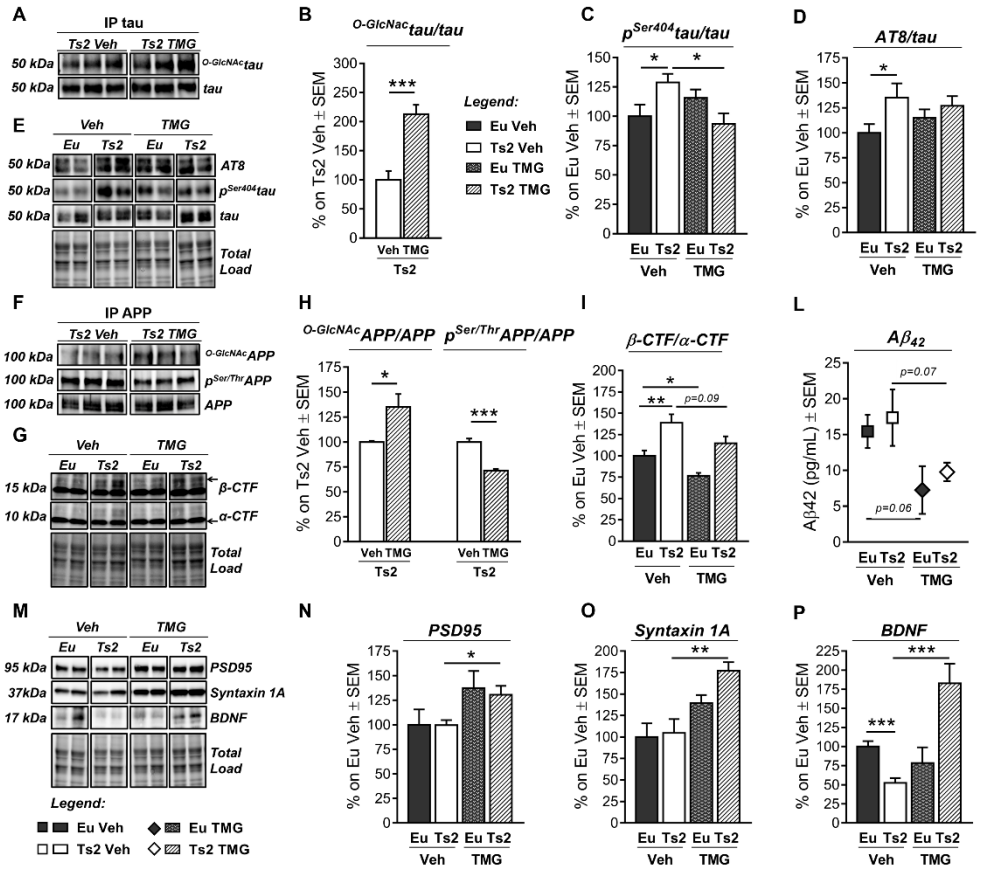

Figure 13: Short-term TMG intranasal treatment rescued aberrant tau and APP PTMs and increased synaptic proteins expression in Ts2Cje mice. **A-B**: Evaluation of $^{O\text{-}GlcNAc}$tau levels by immunoprecipitation analysis after TMG treatment. TMG intranasal treatment induced a significant increase in $^{O\text{-}GlcNAc}$tau/tau levels of TMG-treated Ts2 compared to vehicle-administered Ts2 mice. Representative blots are reported in (**A**). **C-E**: Analysis of tau phosphorylated levels after TMG treatment. No changes were observed in tau phosphorylation levels on Ser-202-Thr208tau/tau of TMG-treated Ts2 (**C**), while a significant reduction was reported in Ser404tau/tau of Ts2 TMG compared to Ts2 Veh (**D**). Representative blots are reported in (**E**). **F, H**: Evaluation of $^{O\text{-}GlcNAc}$APP and $^{pSer/Thr}$APP levels after TMG treatment. A significant increase in $^{O\text{-}GlcNAc}$APP/APP levels was measured, together with a significant reduction of $^{pSer/Thr}$APP/APP levels in Ts2 TMG compared to Ts2 Veh. Representative blots are reported in (**F**). **G, L**: Evaluation of APP cleavage by the measure of β-CTF/α-CTF ratio and soluble Aβ after TMG treatment. A significant increase in β-CTF/α-CTF was observed in Ts2 Veh compared to Eu Veh, confirming the preferential amyloidogenic processing of APP in our DS model. The increased $^{O\text{-}}$

^{GlcNAc}APP/APP levels reflects the reduction of β-CTF/α-CTF ratio in treated Ts2 mice, confirming the ability of TMG treatment to favour the non-amyloidogenic cleavage of APP. Furthermore, evaluation of soluble Aβ 1-42 peptide by ELISA showed a trend of reduction in both Euploid and Ts2 mice treated with TMG in comparison to respective group administered with Veh, confirming the effect of intranasal TMG treatment in modulating APP's fate. Representative blots are reported in (**G**). **M-P**: Evaluation of PSD95, Syntaxin 1A and BDNF protein levels after TMG treatment. A significant increase in both PSD95 and Syntaxin 1A protein levels was observed in Ts2 mice treated with TMG compared to Ts2 animals treated with Veh. Interestingly, TMG treatment was also able to rescue the impairment of BDNF protein levels that was observed in Ts2 Veh compared to Eu Veh. Indeed, TMG-treated Ts2 mice showed a significant increase in BDNF protein levels in comparison to Ts2 Veh group, confirming an effect of TMG treatment in inducing synaptic-related proteins and neurotrophic factors. Representative blots are reported in (M). Number of animals for each condition were as follow: n=6/group for western blot and ELISA analysis, n=4/group for immunoprecipitation analysis. All bar charts reported in (**B**), (**C**), (**D**), (**H**), (**I**), (**L**), (**N**), (**O**) and (**P**) show mean ± SEM. *p<0.05, **p<0.01, ***p<0.001 using Student's t test.

4.1.8 Thiamet-G treatment boosts autophagic clearance and reduces oxidative damage in 6-months-old Ts2Cje mice.

Further, we evaluated the influence of O-GlcNAc rescue on autophagy induction and protein oxidative damage. Considering recent findings by Zhu *et al.* regarding the ability of Thiamet-G to boost autophagy[223], we evaluated possible implications of our intranasal TMG treatment in Ts2 mice. We observed a relevant increase in Atg7 protein levels both in Eu mice treated with TMG (Fig. 14A-B; **p<0.01, Eu Veh vs Eu TMG: +14%) and Ts2 equally treated (Fig. 14A-B; *p<0.05, Ts2 Veh vs Ts2 TMG: +27%). In line with the promotion of initial autophagic steps, TMG treatment also stimulated a significant increase in Beclin-1 protein levels both in euploids mice (Fig. 14A, D; *p<0.01, Eu Veh vs Eu TMG: +60%) and respective Ts2 animals (Fig. 14A, D; *p<0.05, Ts2 Veh vs Ts2 TMG: +25%). Consistent with the above data, 2-

way ANOVA confirmed that Atg7 and Beclin-1 are increased as an effect of the treatment [Table 3; Atg7: F (1,22) =14.5 **p<0.001; Beclin-1: F (1,22) =16.5 ***p<0.001]. Subsequently, we analysed changes in LC3 protein by measuring its cleaved forms as index of autophagosome maturation[264]. Interestingly, TMG treatment proved to significantly increase LC3II/I ratio in Ts2 mice (Fig. 14E-F; **p<0.01, Ts2 Veh vs Ts2 TMG: +20%) as a result of treatment administration [Table 3; F (1;21) = 5.7, *p<0.05] together with a synergistic effect of treatment and genotype [Table 3; F (1;21) =13.9, **p<0.01]. Afterwards, we evaluated the possible effects of TMG treatment in autolysosomal degradation efficacy, measuring SQSTM1 levels. We observed a relevant accumulation of SQSTM1 protein in Ts2 mice compared to age-matched controls treated with Veh solution (Fig. 14D-E; *p<0.05, Eu Veh vs Ts2 Veh: +50%), suggesting a failure in autolysosomal clearance in our DS model. Intriguingly, TMG treatment proved to boost autophagic flux by significantly reducing SQSTM1 levels in TMG-treated Ts2 mice (Fig. 14D-E; **p<0.01, Ts2 Veh vs Ts2 TMG: -43%), reactivating autolysosomal degradation. Moreover, 2-way ANOVA analysis revealed a combined effect of both genotype and treatment in the observed changes of SQSTM1 protein levels [Table 3; F (1;23) =6.3, *p<0.05].

Among all the different characteristics of DS neuropathology, an increase of protein oxidative damage was observed[82,151,265,266]. Since autophagy induction is considered one of the strategy able to promote the degradation of toxic aggregates[266], we evaluated the benefits of our TMG treatment in reducing oxidatively modified proteins is Ts2 mice. As expected, 6-months-old Ts2 mice showed high levels of 3-nitrotyrosine (3-NT) compared to age-matched controls (Fig. 14G; *p<0.05, Eu Veh vs Ts2 Veh:

+51%). Intriguingly, TMG treatment showed was able to reduce 3-NT levels in the hippocampus of Ts2 treated mice (Fig. 14G; *p<0.05, Ts2 Veh vs Ts2 TMG: -48%). Moreover, 2-way ANOVA analysis point out a combined effect of both genotype and treatment on 3-NT levels [Table1; F (1;21) =5.7 *p<0.05]. In line with this result, also HNE-adducts levels were higher in Ts2 mice compared to respective euploids (Fig. 14H; **p<0.01, Eu Veh vs Ts2 Veh: +25%), with a remarkable effect of the genotype [Table 3; F (1;22) =18.8, ***p<0.001]. However, TMG treatment was not able to rescue HNE adducts levels in Ts2 animals. Our data suggest a possible implication of TMG-induced autophagy in the clearance of nitrated proteins. A schematic summary on the role of altered O-GlcNAcylation in Ts2Cje neuropathology and the effects of TMG treatment in our DS model is reported in figure 15.

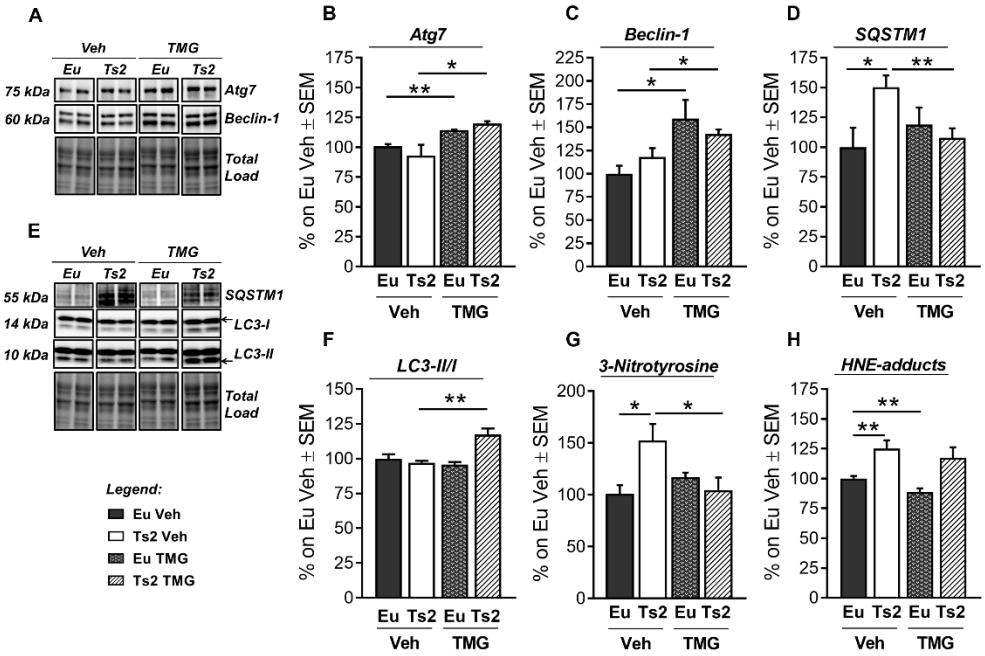

Figure 14: Short-term TMG intranasal treatment boosted autophagic clearance and reduced oxidative damage in Ts2Cje mice. A-C: Analysis of the initial steps of autophagy machinery after TMG treatment. TMG intranasal treatment proved to induce initial steps of autophagic flux by significantly increasing Atg7 (**B**) and Beclin-1 (**C**) protein levels in TMG-treated mice compared to animals treated with vehicle solution, independently form the genotype. Representative blots are reported in (**A**). **D-F**: Analysis of autophagic flux efficiency after TMG treatment. 6-months old Ts2 mice showed an accumulation of SQSTM1 protein levels compared to respective euploid treated with vehicle, suggesting a failure in autolysosomal degradation. TMG showed to significantly reduce SQSTM1 levels, reactivating the autophagic flux in Ts2 mice (**D**). Furthermore, our treatment significantly increased LC3II/I ratio in TMG-treated Ts2 compared to Ts2 administered with Veh, confirming an amelioration of autophagosome maturation (**F**). Representative blots are reported in (**E**). **G**: Analysis of 3-nitrotyrosine levels after TMG treatment. Intriguingly, high levels of oxidatively-modified proteins are decreased by the administration of TMG in Ts2 mice which proved to reduce 3-NT levels in comparison to Ts2 administered with vehicle solution. Global 3-NT levels are measured by slot blot technique. **H**: Analysis of HNE-adducts levels after TMG treatment. High levels of HNE-adducts characterized Ts2 animals compared to respective Eu Veh. TMG treatment proved to significantly reduce HNE-adducts in euploid animals together with a trend of reduction in TMG-treated Ts2 group. Global HNE-adducts are measured by slot blot technique. Number of animals for each condition were as follow: n=6/group for western blot analysis and slot blot analysis. All bar charts reported in (**B**), (**C**), (**D**), (**F**), (**G**) and (**H**) show mean ± SEM. *p<0.05, **p<0.01 using Student's t test.

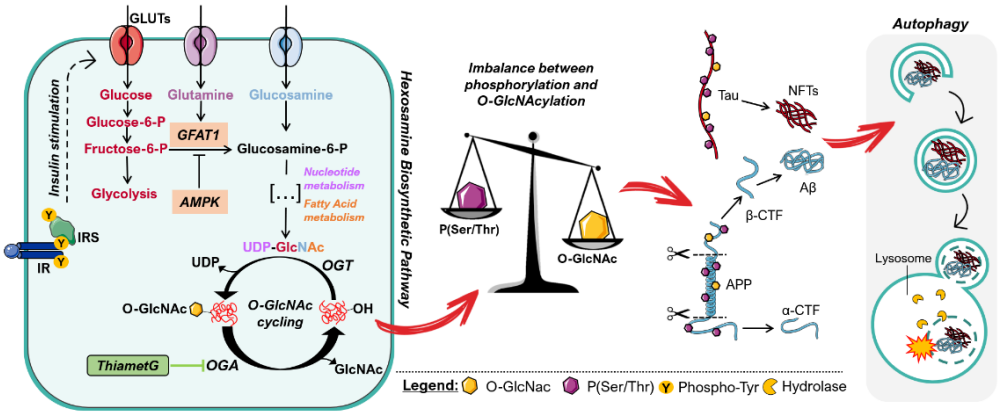

Figure 15: Role of disrupted O-GlcNAcylation homeostasis in DS neuropathology. The hexosamine biosynthetic pathway (HBP) is a minor branch of the glycolytic pathway that results in the production of UDP-GlcNAc, the activated substrate for protein O-GlcNAcylation. As the HBP flux integrates molecules from carbohydrate (fructose-6-phosphate), amino acid (glutamine/glucosamine), nucleotide (UTP) and lipid (Acetyl-CoA) metabolism, the production of UDP-GlcNAc is considered a valuable intracellular sensor of cell metabolic status. An early upregulation of the insulin cascade (IR-IRS) is present in our DS murine model, which could reasonably imply an increase in glucose availability. In line with that, the HBP rate-limiting enzyme GFAT1 by lack the inhibitory action of the metabolic-sensor kinase AMPK. Therefore, the altered OGT functionality and, mostly, and aberrant increase of OGA-driven hydrolysis of O-GlcNAc seems to be the main cause for reduced protein O-GlcNAcylation in our DS model. The loss of protein O-GlcNAcylation is known to give rise to an aberrant increase of protein phosphorylation, because of the mutual inverse relationship between these two modifications. This process acquires relevance when it comes to the post-translational modifications of proteins implicated in the DS neurodegenerative process. Indeed, the unbalanced O-GlcNAcylation/phosphorylation ratio of tau is known to promotes its aggregated forms (NTFs, neurofibrillary tangles) while the aberrant increase of phosphorylated-APP favours its amyloidogenic cleavage that results in the formation of β-CTF and thus, to β-amyloid accumulation. In this scenario, data collected on our model confirm the relevance of O-GlcNAcylation disruption in the appearance of AD-related hallmarks. Furthermore, Thiamet-G mediated inhibition of OGA proved to restore protein O-GlcNAcylation and further exert its neuroprotective effects by boosting autophagic clearance of toxic aggregates.

4.2 Project 2: High fat diet leads to aberrant protein O-GlcNAcylation and to the development of Alzheimer's Disease signatures in mice

4.2.1 HFD mice show an aberrant and tissue-specific O-GlcNAcylation profile.

Studies on the high-fat-diet (HFD) model have largely demonstrated a strong correlation between the consumption of an hypercaloric diet and consequent alterations in brain functionality[194,210,267]. However, the exact molecular mechanisms that link perturbations of peripheral metabolism with brain alterations driving cognitive decline are still under discussion. Within this context, protein O-GlcNAcylation is extremely sensitive to nutrients fluctuations and it is widely recognized as a key linkage between nutrient sensing, energy metabolism and cellular functions[8,268]. Considering these evidences, in the second part of our work we explored the impact of nutrients overload in driving putative changes of protein O-GlcNAcylation in the brain and liver of mice fed with a diet rich in fat content (HFD) in comparison to aged-matched animals that have received a standard feeding (SD). Our analysis revealed a significant reduction of global O-GlcNAcylated proteins in the hippocampus of HFD mice if compared to the total O-GlcNAcylation levels observed in the same brain region from SD mice (Fig. 16A-C; *$p<0.05$, SD vs HFD: -28%). In line with the well-known competition occurring between protein O-GlcNAcylation and phosphorylation[54,269], together with the reduction of O-GlcNAcylated proteins we also observed an inverse increase of total serine/threonine phosphorylation in the hippocampus of HFD mice compared to the respective brain region of SD animals (Fig. 16A-C; *$p<0.02$, SD vs HFD: +52%). These results suggest that diet-induced changes can drive alterations in brain regions widely involved in cognition, as the hippocampus. Since HFD is a well-established model of diet-induced obesity and insulin resistance[195], we also evaluated the O-GlcNAcylation of hepatic proteins from HFD mice in order to assess putative involvement of this PTM in driving

pathological changes that occurs also in the peripheral organs. In this context, we observed an O-GlcNAcylation profile that was completely opposite to that examined in the hippocampus. Indeed, a significant increase in the total O-GlcNAcylated protein levels was observed in the liver of HFD mice in comparison to the control group (Fig. 16D-F; *$p<0.02$, SD vs HFD: +38%). Furthermore, a trend of decrease was observed in serine/threonine phosphorylation of hepatic proteins from HFD mice compared to SD mice (Fig.16-D-F; SD vs HFD: -20%). These results are in agreement with the notion that an aberrant increase of O-GlcNAcylation in peripheral organs is directly linked to insulin resistance and to hyperglycaemia-induced glucose toxicity[212], confirming a role of altered O-GlcNAcylation in driving pathological mechanisms in HFD mice.

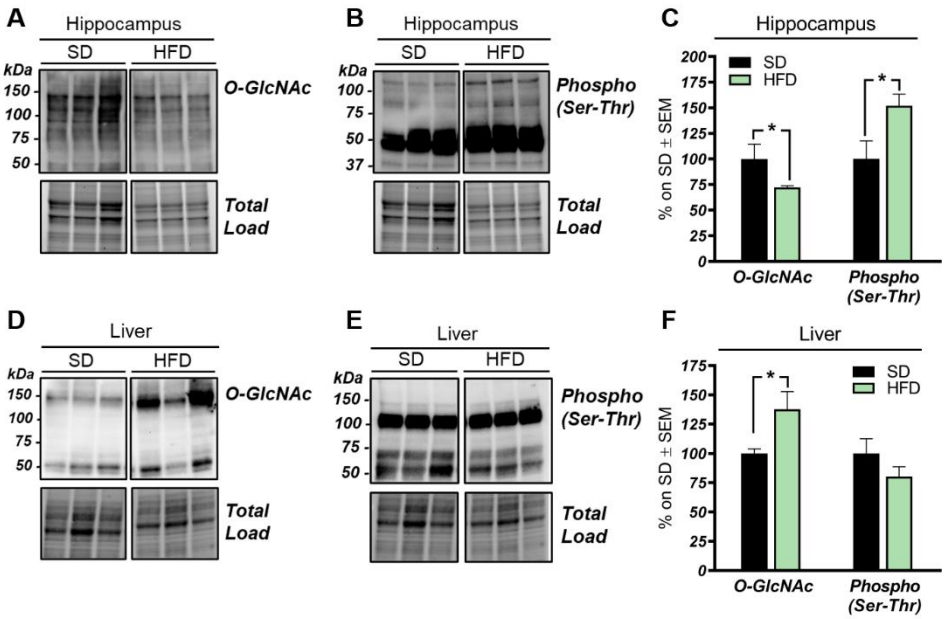

Figure 16: O-GlcNAcylation and phosphorylation profile in the hippocampus and liver from HFD mice. A-C: O-GlcNAcylation/phosphorylation profile in the hippocampus from HFD mice compared to respective SD animals. The reduction of protein O-GlcNAcylation in the hippocampus of HFD mice was in line with a mutual inverse increase in the global phosphorylation of serine and threonine residues compared to SD controls. Representative blots are reported in (**A**) and (**B**). **D-E**: O-GlcNAcylation/phosphorylation profile in the liver of HFD mice compared to respective control group. Increased levels of O-GlcNAcylated proteins were observed in the liver of HFD compared to animals fed with SD, confirming a global imbalance of O-GlcNAcylation homeostasis in peripheral organs of our model. A trend of increased was observed in the phosphorylation of serine and threonine of hepatic proteins from HFD in comparison to SD mice. Representative blots are reported in (**D**) and (**E**). Number of animals for each condition were as follow: n=6/group for western blot. All bar charts reported in (**C**) and (**F**) show mean ± SEM. *$p<0.05$, **$p<0.01$, using Student's t test.

Afterwards, we evaluated possible alterations occurring on the O-GlcNAc enzymatic machinery with the aim of assessing whether the reduction of O-GlcNAcylated protein levels in the hippocampus of HFD mice could be the result of an altered OGT/OGA functionality. In details, we did not observe any relevant changes neither in OGT nor OGA protein expression levels in the hippocampus of our HFD model (Fig. 17A, C). Consistent with the role of OGT as a sensor of cellular metabolic state[33,34], we further analysed OGT PTMs trough immunoprecipitation to evaluate the effects of nutrients surplus on its functionality. Interestingly, we observed a significant reduction of $^{O\text{-}GlcNAc}$OGT levels in HFD hippocampus (Fig. 17B, D; *p<0.05, SD vs HFD: -57%) together with a substantial increase of $^{pSer/Thr}$OGT levels in our HFD model compared to the same brain region of SD animals (Fig. 17B, D; **p<0.01, SD vs HFD: +193%). This aberrant changes in OGT PTMs suggest an imbalance in the regulative mechanisms of the enzyme that may affect its enzymatic ability to transfer O-GlcNAc moiety. Furthermore, OGA did not show any variation in its enzymatic functionality in the two experimental groups examined (Fig. 17E), excluding that the observed reduction in O-GlcNAcylation levels may due to an increase in O-GlcNAc moiety removal in HFD mice.

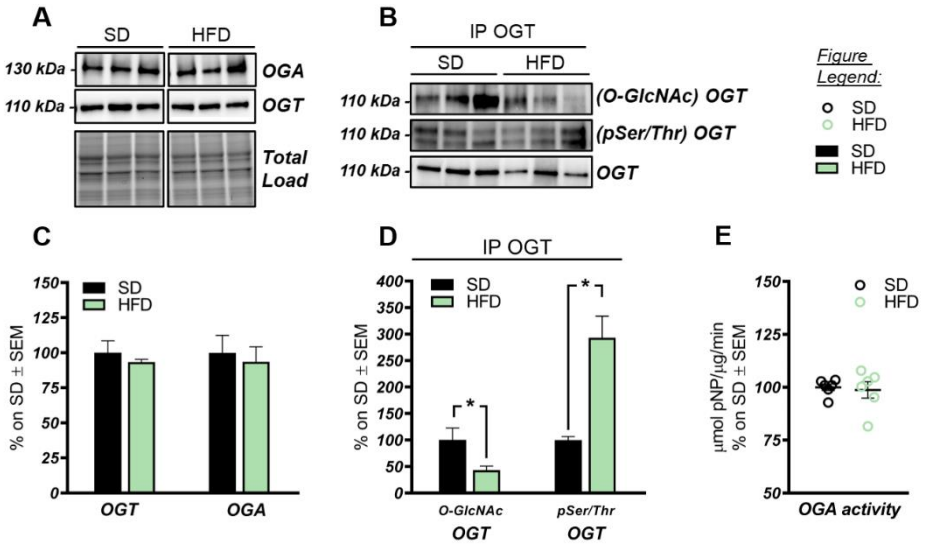

Figure 17: OGT/OGA functionality in the hippocampus of HFD mice. A, C: OGT and OGA protein levels in HFD mice hippocampus compared to respective SD animals. No relevant changes were observed in the protein expression levels of the enzymes controlling O-GlcNAc cycle. Representative blots are reported in (**A**). **B, D**: Evaluation of OGT's PTMs by immunoprecipitation analysis. A significant reduction in $^{O\text{-}GlcNAc}$OGT/OGT levels together with a consistent increase in its $^{pSer/Thr}$OGT/OGT levels were observed in HFD hippocampus in comparison to the same brain region from SD mice. Representative blots are reported in (**B**). **E**: OGA assay analysis. No changes were observed in OGA enzymatic activity between the two experimental groups. Number of animals for each condition were as follow: n=6/group for western blot and OGA assay analysis while n=3/group was used for immunoprecipitation analysis. All bar charts reported in (**C**), (**D**) and (**E**) show mean ± SEM. *p<0.05, **p<0.01, using Student's t test.

4.2.2 The HBP flux is impaired in HFD mice compared to SD.

The HBP pathway integrates multiple metabolic pathways into the synthesis of UDP-GlcNAc, proving feedback on overall cellular energy levels and nutrients availability[214]. In this scenario, increased flux of metabolites into the HBP have already been highlighted as a key point driving metabolic alterations in the skeletal muscle of a fat-induced insulin resistance model[270]. However, the role of the HBP in driving the reduction of O-GlcNAcylated protein levels in the brain of HFD mice has not yet been clarified. As GFAT1 is the rate-limiting enzyme that coordinates nutrients entrance into the HBP flux, we analysed its activation state in HFD mice hippocampus together with that of AMPK, a key GFAT1 inhibitor[271,272]. We observed a significant increase in Ser243 phosphorylation of GFAT1 in HDF hippocampus compared to respective control group (Fig. 18A-B; *$p<0.05$, SD vs HFD: +65%), index of an inhibition of GFAT1 activity. No relevant changes were observed in GFAT1 protein expression levels between the two groups (Fig. 18A-B). Most interestingly, testing GFAT1 ability to synthetise glucosamine-6-phosphate *in vitro* by measuring its fluorescent derivative by HPLC, we did not observe significant changes between HFD hippocampal extract and respective SD controls (Fig. 18D-E). As GFAT1 activity assay is carried out in large excess of substrates[228], the reduced GFAT1 activation (measured as increased p^{Ser243}GFAT1/GFAT1 levels) may be the result of reduced substrates availability in the intracellular environment. In line with this hypothesis, HFD mice showed a remarkable increase in AMPK activatory phosphorylation on Thr172 compared to animals that have been fed with the standard diet (Fig. 18A, C; ***$p<0.001$, SD vs HFD: +255%) together with a significant increase in AMPK protein levels in HFD mice (Fig. 18A, C; *$p<0.03$, SD vs HFD:

+20%). In line with these data, AMPK is known to inhibit GFAT1 activity under nutrient depletion or stress conditions via its phosphorylation on Ser243, in order to reduce the amount of nutrients entering the HBP flux[271,272]. All together these findings suggest that HFD-driven reduction of nutrition uptake (e.g. glucose) at brain level may drive AMPK-mediated inhibition of GFAT1, finally resulting in reduced synthesis of UDP-GlcNAc through the HBP and impaired protein O-GlcNAcylation in the hippocampus of HFD mice.

The reduction of brain insulin sensitivity is one of the most well-known mediators of HFD-induced cognitive decline[208]. Since our HFD model showed reduced HBP flux, we tested the hypothesis that insulin resistance could favour nutrients depletion and consequently induce AMPK-mediated inhibition of GFAT1 in the hippocampus of HFD mice. As expected, we observed a significant increase in the phosphorylation levels of IRS-1 on its inhibitory sites. In details, a marked increase of p^{Ser307}IRS-1 levels was observed in the hippocampal region of HFD mice in comparison to the control group (Fig. 18F-G; **p<0.01, SD vs. HFD: +70%) together with a significant increase of p^{Ser636}IRS-1 levels in HFD mice compared to standard-fed animals (Fig. 18F-G; **p<0.01, SD vs. HFD: +38%). Furthermore, a substantial rise of p^{Ser473}Akt levels was detected in the hippocampus of the model examined compared to the control group (Fig. 18F, H; **p<0.003, SD vs. HFD: +73%) without affecting Akt protein expression levels between the two groups (Fig. 18F, H). All together these data confirm a uncoupling of the proteins involved in the insulin cascade related to an insulin resistance condition, suggesting that HFD-driven depletion of glucose intake could drive the reduction of HBP flux in the brain of HFD mice.

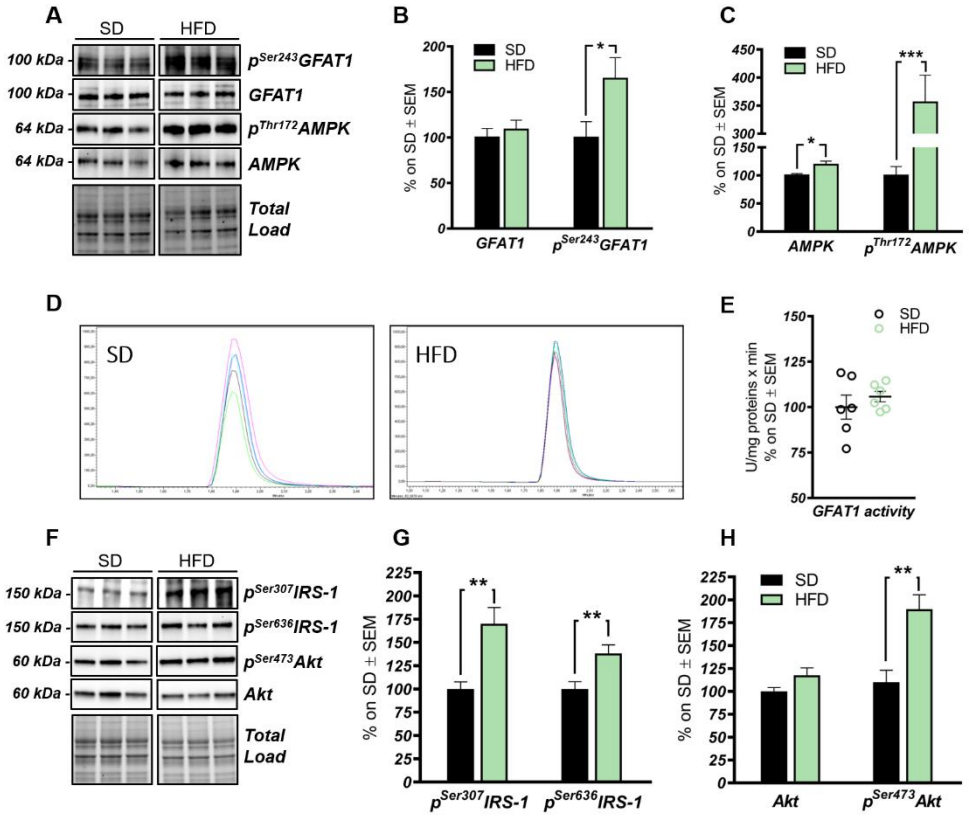

Figure 18: The HBP flux is impaired in the hippocampus of HFD mice. A-B: Analysis of GFAT1 activation status in HFD mice compared to respective controls. A significant increase p^{Ser243}GFAT1/GFAT1 ratio was observed in HFD mice compared to SD, thus resulting in the inhibition of GFAT1 activity. Representative blots are reported in (**A**). **A, C**: Analysis of AMPK activation status in HFD mice compared to respective SD animals. A significant increase in the AMPK protein levels was observed in HFD mice compared to SD, together with a relevant increase in p^{Thr172}AMPK/AMPK levels, thus resulting in increased AMPK activation. Representative blots are reported in (**A**). **D-E**: GFAT1 activity assay. No relevant changes were observed in GFAT1 ability to synthetise glucosamine-6-phosphate *in vitro* between the HFD group and SD mice. Representative spectra of GFAT1-synthetized glucosamine-6-phosphate for both HFD and SD animals are reported in (**E**). **F-G**: Analysis of IRS-1 activation state in the hippocampus of HFD mice compared to standard-fed animals. A relevant increase in both p^{Ser307}IRS-1 and p^{Ser636}IRS-1 levels was observed, suggesting a reduction in IRS-1 activation in HFD

mice compared to SD. Representative blots are reported in (**F**). **F, H**: Analysis of Akt activation status in HFD mice compared to respective controls. p^{Ser473}Akt/Akt ratio is significantly increase in HFD hippocampal region compared to the same brain area of SD mice. Number of animals for each condition were as follow: n=6/group for both western blot analysis and GFAT1 activity assay. All bar charts reported in (**B**), (**C**), (**G**) and (**H**) show mean ± SEM. *p<0.05, **p<0.01, ***p<0.001 using Student's t test.

4.2.3 Alzheimer's disease hallmarks in HFD mouse brain.

A study by Kothari *et al.* have recently proved that cognitive decline associated with high fat/sugar consumption is related to increased amyloid beta deposition and neurofibrillary tangle formation in the brain of wild type mice fed with a hypercaloric diet[208]. Considering these evidences, we evaluated tau and APP PTMs to assess the role of reduced O-GlcNAcylation in the appearance of AD-related hallmarks in HFD mice. In the first instance, we confirmed the hyperphosphorylated state of tau in the hippocampus of our murine model. Indeed, a trend of increase was observed on Ser202-Th205 residues (Fig. 19A-B; AT8: SD vs HFD: +16%) together with a massive increase in Ser404 phosphorylation in HFD mice compared to respective standard-fed animals (Fig. 19A-B; ****$p<0.0001$, SD vs HFD: +98%). Furthermore, the analysis of tau PTMs trough immunoprecipitation highlighted the inverse relationship between O-GlcNAcylation and phosphorylation, at least for Ser404. Indeed, the p^{Ser404}tau increase in HFD mice corresponded to a significant reduction in its O-GlcNAcylated levels when compared to SD animals (Fig. 19C-D; *$p<0.03$, SD vs HFD: -37%). Considering APP PTMs, we also observed a significant reduction of $^{O\text{-}GlcNAc}$APP levels in the brain of HFD mice compared to SD levels (Fig. 19E-F; *$p<0.03$, SD vs HFD: -56%) that was not supported by an inverse increase in its phosphorylation state (Fig. 19E-F). According to our results, the impairment of protein O-GlcNAcylation observed in the hippocampus of HFD mice partially contributes to the formation of AD-hallmarks, with a more evident involvement for tau than for APP.

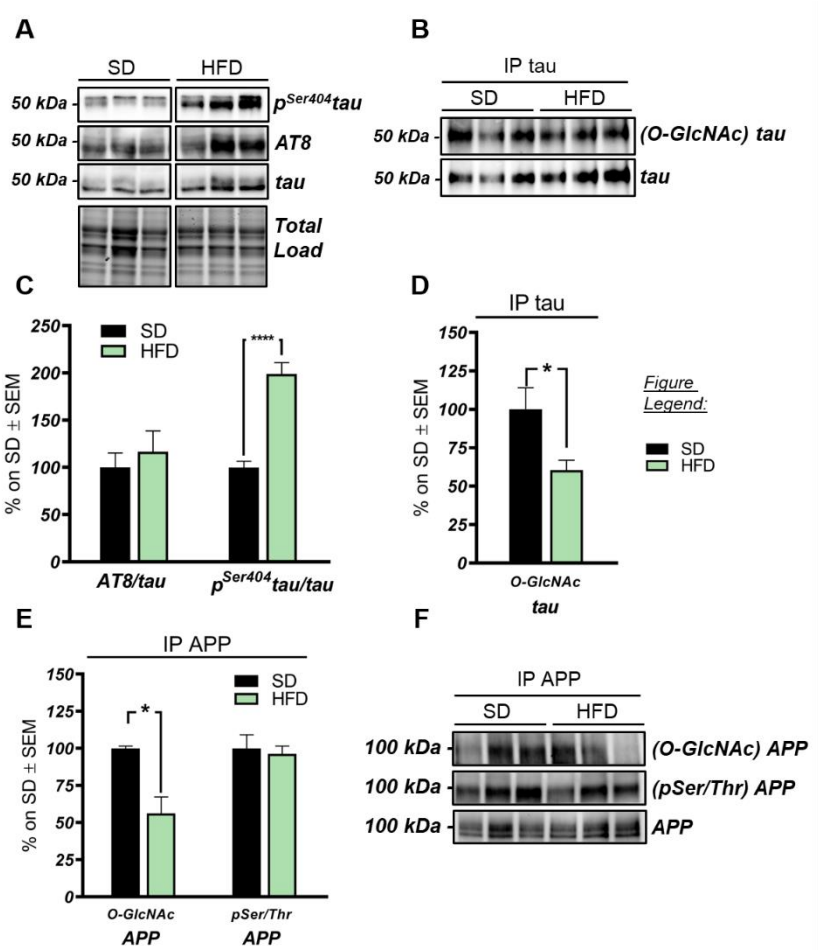

Figure 19: Role of altered protein O-GlcNAcylation in the onset of AD hallmarks in the brain of HFD mice. A-B: Analysis of tau phosphorylated state in HFD hippocampus compared to SD. A trend of increase in Ser202-Thr205tau/tau (AT8) together with a significant increase in Ser404tau/tau was observed in HFD mice compared to respective controls. Blots are reported in (**A**). **B-C**: Evaluation of $^{O\text{-}GlcNAc}$tau levels by immunoprecipitation analysis. $^{O\text{-}GlcNAc}$tau/tau levels were remarkably reduced in HFD hippocampus in comparison to SD. Blots are reported in (**D**). **E-F**: Evaluation of $^{O\text{-}GlcNAc}$APP and $^{pSer/Thr}$APP levels by immunoprecipitation analysis. $^{O\text{-}GlcNAc}$APP/APP was significantly reduced in HFD mice in comparison to SD, not supported by an inverse increase in its phosphorylated levels. Blots are reported in (**E**). Number of animals for each condition were as follow: n=6/group for western blot and n=3/group for immunoprecipitation. All bar charts reported in (**A**), (**C**), and (**D**) show mean ± SEM. *p<0.05, **p<0.01, ***p<0.001, ****p<0.0001 using Student's t test.

4.2.4 High-fat-diet affects mitochondrial function

Mitochondrial dysfunction and impaired mitochondrial dynamics are well-known driving force for the development of AD[273]. Interestingly, abnormal mitochondrial density and morphology, together with altered mitochondrial dynamics, reduced respiratory chain complexes activity and increased AMP/ATP ratio have also been observed in rats fed with HFD[274]. In this scenario, defective mitochondrial function might be the link between impaired bioenergetic and HFD-induced neurodegeneration. According to our analysis, HFD consumption induced an impairment in the expression levels of most respiratory chain complexes in comparison to that of standard-fed mice. In details, a consistent reduction of Complex I subunit NDUFB8 was observed in the hippocampus of HFD mice compared to respective SD animals (Fig. 20A-B; ****$p<0.0001$, SD vs HFD: -32%). A similar even if not significant trend of reduction was observed for Complex II subunit SDHB (Fig. 20A-B; SD vs HFD: -16%) and Complex IV subunit MTCO1 (Fig. 20A-B; SD vs HFD: -18%). Instead no considerable variation has been observed in Complex III subunit UQCRC2 between the two groups (Fig. 20A-B). In addition, a significant reduction of Complex V subunit ATP5A was observed in the hippocampal region of HFD mice compared to the same brain region from SD animals (Fig. 20A-B; *$p<0.02$, SD vs HFD: -16%). Most interestingly, reduced protein expression levels of specific respiratory chain complexes were perfectly in line with a correspondingly reduced functionality. Indeed, a significant reduction of Complex-I activity was detected by means of a specific spectrophotometric assay in HFD mice compared to respective control group (Fig. 20E; *$p<0.03$, SD vs HFD: -0.053 mmol/mg/min). In line with these results, a trend of reduction of Complex II-III activity was observed in the mitochondrial extract from HFD mice in comparison to SD group (Fig. 20F;

SD vs HFD: -0.16 mmol/mg/min) together with a trend of reduction of Complex V activity between the same group of comparison (Fig. 20H; SD vs HFD: -0.10 mmol/mg/min). Perfectly in line with our hypothesis of HFD driving an impairment of mitochondrial bioenergetic function, a significant reduction of ATP content was observed in the total homogenate from HFD mice in comparison to standard-fed animals (Fig. 20I; *$p<0.04$, SD vs HFD: -7.22 mmol/mg tissue). To further demonstrate a possible role of protein O-GlcNAcylation in mediating the detrimental effects of high-fat consumption on mitochondrial function, we performed an immunoprecipitation analysis on Complex I subunit NDUFB8, which seems to be the one with most altered functionality. As expected, we found a relevant reduction of NDUFB8 O-GlcNAcylated levels in HFD mice hippocampal area in respect to SD control group (Fig. 20C-D; *$p<0.02$, SD vs HFD: -14%), supporting the idea of altered protein O-GlcNAcylation as a possible determining cause of mitochondrial defective function in HFD mice.

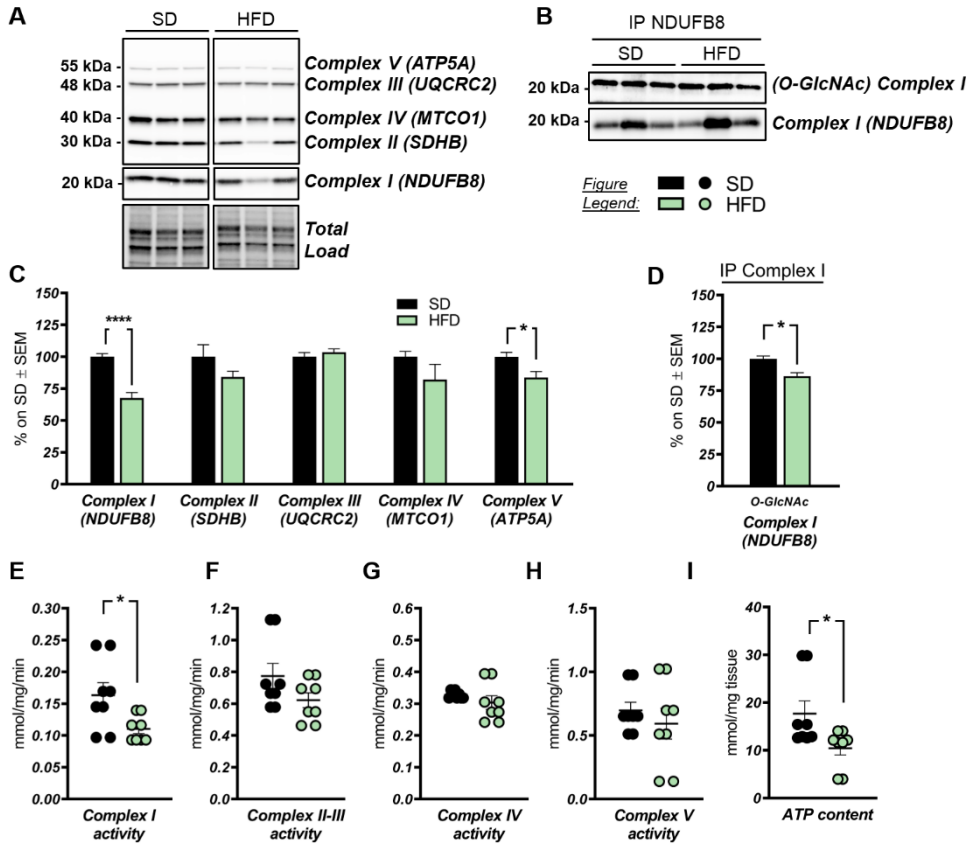

Figure 20: High-fat-diet affects respiratory chain complexes expression and mitochondrial functionality. A, C: Analysis of respiratory chain complexes subunits expression in HFD hippocampus compared to standard-fed animals. A significant reduction in Complex I subunit NDUFB8 was observed in HFD mice compared to SD controls. A trend of impairment was found for Complex II subunit SDHB and Complex IV subunit MTCO1 between HFD and respective controls, while no relevant changes have been observed in Complex III subunit UQCRC2 between the two groups of comparison. Finally, a significant decreased of Complex V subunit ATP5A was found in HFD hippocampus in comparison to respective SD mice. Representative blots are reported in (**A**). **B, D**: Analysis of Complex I subunit NDUFB8 O-GlcNAcylated levels by immunoprecipitation in HFD mice compared to controls. A significant reduction in $^{O\text{-}GlcNAc}$NDUFB8/NDUFB8 levels was observed in the hippocampus from HFD mice compared to respective standard-fed mice. Representative blots are reported in (**B**). **E-H**: Evaluation of specific respiratory chain complexes activity in HFD mice compared to controls. A significant reduction of

Complex I activity was reported in HFD mice compared to SD animals (**E**). A trend of reduction was also observed in Complex II-III activity (**F**) and Complex V activity (**G**) in HFD mice compared to controls. **I**: Analysis of overall ATP content in HFD mice compared to correspondent SD animals. A relevant impairment of ATP content was observed in HFD animals compared to respective standard-fed mice. Number of animals for each condition were as follow: n=6/group for western blot analysis, n=3/group for immunoprecipitation analysis and n=8/group for Complexes activity and ATP content evaluation. All bar charts reported in (**C**), (**D**), (**E**), (**F**), (**G**), (**H**) and (**I**) show mean ± SEM. *p<0.05, **p<0.01, ***p<0.001, ****p<0.0001 using Student's t test.

5. DISCUSSION

In the last decade, a great deal of effort has been made to investigate the role of protein O-GlcNAcylation in neurodegenerative diseases, however no evidence is available on its possible implications in DS neuropathology. Our analysis on Ts2Cje mice showed a persistent reduction of total GlcNAc bound to protein in each area of the hippocampal region, suggesting the alteration of O-GlcNAcylation homeostasis as an early molecular event that could increase susceptibility to neurodegenerative phenotypes. Previous reports demonstrated that decreased protein O-GlcNAcylation in the hippocampal region drives synaptic and cognitive decline in aging brain, facilitating later onset of dementia[275]. Among the proposed mechanisms through which loss of O-GlcNAcylation promotes neurodegenerative processes, the extensive interplay of this PTM with protein phosphorylation has special relevance[53]. In agreement, our analysis showed increased global protein phosphorylation on Ser/Thr residues and the imbalance of the O-GlcNAcylation/phosphorylation equilibrium in the hippocampal area, recapitulating the alterations observed in the brain of both AD humans and murine models[161,162,233,276]. Most interestingly, the reciprocal interplay between protein O-GlcNAcylation and phosphorylation is not only related to the competitive modification of the same residues but also to the ability of each modification to regulate the other's enzymatic machinery. Recently, insulin stimulation of 3T3-L1 adipocytes was proved to increase both OGT tyrosine phosphorylation and catalytic activity[29]. Furthermore, Kaasik *et al*. found that GSK3β can enhance OGT activity by its phosphorylation on Ser residues[240]. In line with this, the decreased O-GlcNAcylation of OGT observed in our model may alter the sites available for phosphorylation, thus affecting its

activity. Among control mechanisms of O-GlcNAc cycling, fluctuations in protein O-GlcNAcylation are known to affect both OGT and OGA transcription in physiological context, in the direction of compensating the imbalance[255]. On to the other hand, an uncoupling of OGT/OGA levels and altered O-GlcNAcylation has been reported in different disease, suggesting a role in pathology progression[277,278]. In Ts2 mice, the relevant reduction in protein O-GlcNAcylation was concomitant with a significant increase of both OGA transcript and protein levels, hinting a lack of compensation for O-GlcNAc imbalance. Taken together our data suggest that the overall removal process of O-GlcNAc moiety is markedly increased in young DS animals as effect of OGA overexpression. We cannot exclude that increased gene dosage, occurring in DS both human and mice, might directly or indirectly drive the overexpression of OGA transcript and protein. However, no interaction between triplicated genes in DS and OGA gene sequence or product has been observed yet and further studies in that sense are needed.

Molecular pathways regulating the O-GlcNAcylation of proteins include the HBP, an offshoot of the glycolytic flux that integrates several major metabolic pathways into the synthesis of UDP-GlcNAc. Zibrova *et al.* demonstrated that GFAT1, the first rate-limiting enzyme of the HBP, undergoes to negative regulation through increased phosphorylation on Ser243, by the action of AMPK, one of the master sensors of cellular energy. Moreover, AMPK itself was found to be O-GlcNAcylated on several residues, allowing to theorize further feedback mechanisms between these systems[271,272]. In line with the reduced AMPK activation (Thr172 phosphorylation), GFAT1 inhibitory phosphorylation decreases and a trend of increase is observed for GFAT1 enzyme activity in our model. In addition,

HBP is finely regulated by nutrients availability and brain metabolic changes, and many studies demonstrated that DS brain is characterized by the early presence of insulin resistance markers, which precede and favour the development of AD-like brain damage[279]. We demonstrate in 6-months-old Ts2 mice that reduced GlcNAc levels couple with the overactivation of insulin signal and with no massive defects in glucose uptake. These events suggest not to consider the alteration of glucose utilization as a possible negative regulator of the HBP flux. Despite this, prolonged IR stimulation is known to result in IRS-1 inhibition through negative feedback mechanisms[280]. Though, the early alteration of O-GlcNAcylation cycling may interfere with correct insulin signaling in young Ts2 mice, as observed in AD mice[233], paving the way for the onset of an insulin resistance condition observed in DS brain[133,252,281]. Accordingly, streptozotocin-treated rats showed decreased global O-GlcNAcylation before the appearance of commonly recognized markers of insulin resistance, confirming the relevance of O-GlcNAcylation disturbances in the onset of insulin signaling defects[282].

In the last decade, OGA inhibitors have been proposed as a promising approach to recover the pathological implications of reduced O-GlcNAcylation in neurodegenerative diseases. Growing evidence in murine models of AD have shown that rescuing brain GlcNAc levels, by OGA inhibition, reduces the levels of pathological tau[170,175,177,283], limits APP amyloidogenic processing and Aβ accumulation[167,171], boosts mitochondrial activity[161] and promotes the removal of toxic aggregates trough macro-autophagy[223]. Data collected in Ts2 mice support a role of dysregulated OGT/OGA cycle in promoting unbalanced O-GlcNAcylation/phosphorylation ratio of tau and APP, thus favouring the accumulation of their resulting toxic

aggregates. Further, previous data in Ts65Dn mice, which share the same genetic background as Ts2, demonstrate altered mitochondrial function and impaired autophagy[155,252]. In this scenario, Ts2 mice describe a pathological context that strongly encourage the administration of OGA inhibitors to rescue GlcNAc levels and protect the brain from AD-like neurodegeneration. Yet, our analysis of liver samples in Ts2 mice showed an opposite profile in terms of O-GlcNAcylated/phosphorylated ratio, as observed in diabetes[284], advising for a brain-specific targeting of OGA with the aim to directly object the brain and avoid possible disturbances in other organs. The intranasal administration of TMG proved positive outcomes in rescuing protein O-GlcNAcylation levels through the inhibition of OGA activity in Ts2 hippocampus. Such effect was followed by the recovery of $^{O\text{-}GlcNAc}$tau deficiency and site-specific reduction of tau phosphorylation. Indeed, upon TMG administration, a reduction on Ser404 phosphorylation was observed while Ser202 and Thr205 were not affected in our model. However, the site-specific effect on tau phosphorylation should not be considered a surprise since compelling evidence indicated that the neuroprotective effect of increased $^{O\text{-}GlcNAc}$tau levels is not necessarily associated with the reduction of each tau phosphorylation sites[171]. In agreement, a previous study by Yang Yu *et al*. regarding the effects of acute TMG treatment observed a reduction in tau phosphorylation on Ser404, while an increase in Ser202 was reported together with a time-dependent effect on Thr205[283]. As a matter of fact, a site-specific reciprocity between O-GlcNAcylation and phosphorylation was described for Ser404[248,285]. As regard of APP, TMG has proved to compensate for reduced $^{O\text{-}GlcNAc}$APP levels that characterized DS mice and was able to further reduce its aberrant hyper-phosphorylation. TMG-driven modulation of APP PTMs acquires special relevance in DS neuropathology. Indeed, DS-affected subjects have increased

APP gene dosage and overexpress APP, showing early signs of Aβ build-up[286,287]. Among APP residues that can be O-GlcNAcylated, Thr576 is known to regulate APP trafficking and processing, attenuating Aβ generation[166]. Conversely, increased levels of phosphorylated APP on Thr668 are found in AD brains and seem to facilitate BACE1 cleavage of APP, that results in higher Aβ production[256,257]. In line with this neuroprotective role of APP O-GlcNAcylation, our TMG treatment has directed APP towards a non-amyloidogenic processing, reducing β-CTF/α-CTF ratio and theoretically cutting down the formation process of Aβ that underlies DS neuropathology. Although we have shown the positive effects of increasing O-GlcNAcylated levels of both tau and APP, this is not the only mechanisms through which TMG exerts its neuroprotective purposes. A recent study by Zhu *et al.* strongly indicates that TMG acts in the brain inducing the disposal of toxic aggregates though the enhancement of autophagy[223]. The ability of TMG to modulate autophagy holds particular importance in DS, where defective degradative systems are known to exacerbate the neurodegenerative phenotype by preventing proper aggregates clearance[252,281,288,289]. Despite Ts2 mice did not show signs of massive autophagy impairment at 6 months of age, an increase of SQSTM1 was observed, possibly indicating insufficient autolysosmal degradation[264]. TMG treatment demonstrated to boost autophagic flux in our DS mice both at initial and later steps. Indeed, increased levels of Atg7 and Beclin-1 support an effect of TMG treatment at the level of autophagic induction, while increased LC3-II/I ratio and the reduction of SQSTM1 levels suggest a TMG-driven increased of autophagosome maturation and lysosomal degradation in DS mice. The valuable interplay between O-GlcNAcylation and autophagy was also observed in a number of different *in vitro* and *in vivo* models, where authors showed how reducing protein O-GlcNAcylation by

genetic and pharmacological manipulation of OGT or OGA resulted in increased autophagy[223,290–292]. In this scenario, our results support the idea that recovering protein O-GlcNAcylation in an altered phenotype such as DS, could be an effective strategy to activate autophagic flux. To note, TMG treatment was also able to ameliorate the increased 3-NT levels, which characterize the pathological alterations occurring in the brain of DS human and mice[82,150,151]. Several lines of evidence demonstrated a role of autophagy in the removal of oxidized proteins[252,266,293–295] and our data from TMG treatment support this hypothesis. However, the decreased burden of nitrated proteins might be also associated with the reduced formation of toxic tau and APP aggregates and/or with the induction/modulation of antioxidant pathways regulated by the O-GlcNAcylation process.

The crucial aspect that has emerged from the analysis of our DS model strongly indicates that impaired protein O-GlcNAcylation, altered brain metabolism and AD-hallmarks manifestation are intrinsically related and influence each other in the neurodegenerative course. However, the ability of protein O-GlcNAcylation to relate cellular metabolic status to well-known aspects of AD-like neurodegeneration challenged us to investigate the contribution of metabolic-induced changes in protein O-GlcNAcylation profile with the aim of discerning common and divergent aspects of HFD-driven neurodegeneration. Many evidences have emphasized the role of aberrantly increased protein O-GlcNAcylation in driving glucose toxicity and chronic hyperglycaemia-induced insulin resistance[212,214], major hallmarks of type 2 diabetes and obesity. In this regard, the HFD model closely recapitulates molecular changes occurring in the so-called metabolic syndrome that precede obesity, T2DM and dementia, which manifests as hyperglycaemia,

hyperinsulinemia, and insulin resistance[195,197,207]. In this scenario, our analysis of liver samples from HFD mice perfectly summarizes the increase in protein O-GlcNAcylation already observed in peripheral organs of diabetic individuals, confirming O-GlcNAcylation as a major trigger of glucose toxicity[212,213,296]. A completely different analysis as to be carried out for the role of O-GlcNAcylation in the brain. A wide range of evidences have already demonstrated how hypercaloric diet affects cognitive performances promoting metabolic dysregulation in the brain, in a way similar to diabetes[196,197,201,267].In agreement, epidemiological and molecular studies suggest that T2DM, obesity and general defects in brain glucose metabolism predispose to poorer cognitive performance and rapid cognitive decline during ageing, favouring the onset of dementia[145,183,232]. In this scenario, the alteration of protein O-GlcNAcylation that we observed in the hippocampus from HFD mice, coupled with the aberrant increase in Ser/Thr phosphorylation levels, perfectly fits with the neurodegenerative context observed in the brain of AD individuals[142,160,161,222,233], as well as, in our DS model. The analysis of brain samples from animals fed with HFD demonstrated also the increase of Aβ deposition, p-tau and decreased synaptic plasticity, suggesting common molecular mechanism underling the onset of cognitive decline in HFD mice[205]. Our analysis of tau and APP PTMs clearly showed that the alteration of O-GlcNAcylation/phosphorylation ratio of these proteins are prominent molecular mechanism in HFD-driven neurodegeneration. In particular, the significant reduction of its O-GlcNAcylated levels, associated with the pathological increase in Ser404 phosphorylation of tau, further support the idea of a site-specific competition[114,169]. Such outcome was already highlighted in TMG-treated Ts2 mice, confirming the relevance of altered O-GlcNAcylation as a driving force underling different forms of neurodegeneration. Although

the pathological alterations observed in HFD mice are similar to those of other neurodegeneration models, it cannot be excluded that the mechanisms underlying disturbances of O-GlcNAc homeostasis in the brain of HFD mice have different origins. Unlike what is found in the hippocampus of Ts2 mice, our HFD mice did not show any significant hyperactivation of OGA, excluding that the same mechanism of increased removal of O-GlcNAc moiety determines the reduction of O-GlcNAcylated proteins and supporting the hypothesis of a distinctive gene dosage effect in our DS model. Rather the attention must be placed on the well-proved alteration of the insulin signal that we observed in the hippocampus of HFD mice. Indeed, both human and rodent data support diet-induced insulin resistance as one of the main mediators of cognitive deficit associated with high fat consumption[205,207,208]. In support of this, mice fed with HFD exhibit a significant increase in obesity, lower glucose and insulin tolerance as compared to animals fed with standard diet. These changes parallel the consistent alterations of the insulin signalling in the brain characterized by reduced insulin receptor activation together with increase inhibitory phosphorylation of the insulin receptor substrate (IRS-1)[207,208]. Our data, by reporting the inhibition of IRS1 in the hippocampus of our HFD mice, overlaps with the above-mentioned mechanisms of insulin resistance. Interestingly, inhibitory serine residues of IRS1 can also be O-GlcNAcylated[216], leading to the possibility of reduced O-GlcNAcylation as a leading cause for IRS-1 hyperphosphorylation on inhibitory sites. Although it seems clear that the disruption of the balance between O-GlcNAcylation and phosphorylation contributes to the unproper functioning of the insulin cascade, it should also be considered that the onset of insulin resistance may affect O-GlcNAc homeostasis by altering the amount of nutrients available for the synthesis of UDP-GlcNAc. In line with a metabolic profile characterized by

low nutrients availability and increased AMP/ATP ratio, HFD mice showed a significant increase in AMPK activation (increased pThr172AMPK levels). Most interestingly, AMPK-mediated inhibition of GFAT1 activity by its direct phosphorylation on Ser243 seems to appear one of the best characterized mechanisms to reduce the amount of nutrients entering the HBP flux under nutrient depletion conditions[12,271], perfectly matching the variations observed in HFD mice brain. In addition, also OGT can be phosphorylated by AMPK on Thr444, regulating both OGT selectivity and nuclear localization. Furthermore, glucose-deprivation has proved to favour OGT cytosolic localization upon AMPK activation[31]. In this context, several AMPK subunits have shown to be dynamically modified by O-GlcNAc and AMPK activation itself seems to be sensitive to global O-GlcNAc perturbation[31], showing a complex interplay between these enzymes. Most interestingly, OGT has shown an aberrant alteration of its O-GlcNAcylation/phosphorylation ratio in the hippocampus of HFD mice that may indicate an additional mechanism by which AMPK mediates the alteration of O-GlcNAc cycling, further exacerbating the metabolic-induced impairment of protein O-GlcNAcylation. According to these evidences, HFD-driven alterations of protein O-GlcNAcylation seems to be linked to reduced HBP flux and altered OGT PTMs tiggered by AMPK activation in response to nutrients deprivation. Together with insulin resistance, HFD rodents also show altered mitochondrial functionality, oxidative stress, and reduced brain cortex bioenergetic[203,210,274]. Indeed, among the possible mechanisms by which nutrients overload exert negative effects within the brain, the alteration of mitochondrial functionalities is among the most impactful. A recent study by Chen et al. have shown an impaired expression of protein involved in mitochondrial dynamics, reduced Complex I-III activity and decreased mitochondrial respiration in HFD-treated

rats[274]. Furthermore, a reduced AMP/ATP ratio in HFD rats demonstrated how diet-induced impairment of mitochondrial activity is reflected by the reduced ability to synthetise ATP as a source of energy[274]. In this context, our data on the hippocampal region of HFD mice perfectly fits with the current knowledge on the topic which clearly indicates that high fat consumption can affect mitochondria functionality resulting in reduced respiratory capacity, decreased oxygen consumption and reduced ATP production[203,210]. Indeed, our HFD model showed a significant reduction in both the expression levels and the activity of most respiratory chain complexes, especially regarding Complex I, finally resulting in impaired ATP content in comparison to standard-fed mice. In this context, sustained alterations in O-GlcNAcylation either by pharmacological or genetic manipulation are known to reprogram mitochondrial function and may underlie reduced cellular respiration and ROS generation[297]. Furthermore, marked reduction of global O-GlcNAcylation strongly correlates with hampered mitochondrial bioenergetic function and disrupted mitochondrial network in AD models, while TMG-mediated restoration of overall O-GlcNAcylation have shown neuroprotective effects[298]. Withing this scenario, the impairment of O-GlcNAcylated levels of the Complex I subunit NDUFB8 supports the idea of altered protein O-GlcNAcylation as another possible element triggering mitochondrial defects in HFD mice, thus demonstrating a pivotal role of this PTM in mediating the detrimental effects of high-fat consumption.

6. Conclusions

Overall, our study supports the pathological role of impaired protein O-GlcNAcylation as a common driving force in neurodegenerative processes. On one hand, our DS model seems to pose the dysregulation of OGT/OGA cycle as a central contributor to tau and APP hyperphosphorylation. In this scenario, the brain-targeted OGA inhibition might represent a valuable therapeutic strategy to ameliorate AD-like neurodegeneration in DS subjects by the recovery of global and specific O-GlcNAcylation of AD-hallmarks and through the induction of autophagy. On to the other hand, diet-driven cognitive decline is favoured, as well, by aberrant protein O-GlcNAcylation, but different molecular mechanism seems to be involved in respect to DS. Indeed, reduced HBP flux, impaired O-GlcNAcylation and defective insulin signalling appear to cooperate in the progression of the neurodegenerative process of HFD mice, eventually resulting in mitochondrial defects, reduced energy consumption and in the development of typical AD signatures.

7. References

1. C R Torres, G W Hart. Topography and polypeptide distribution of terminal N-acetylglucosamine residues on the surfaces of intact lymphocytes. Evidence for O-linked GlcNAc. *J Biol Chem* **10**, 3308–17 (1984).

2. G D Holt; G W Hart. The subcellular distribution of terminal N-acetylglucosamine moieties. Localization of a novel protein-saccharide linkage, O-linked GlcNAc. *J Biol Chem* **261**, 8049–57 (1986).

3. Gerald W. Hart, Michael P. Housley & Chad Slawson. Cycling of O-linked β-N-acetylglucosamine on nucleocytoplasmic proteins. *Nature* **446**, 1017–1022 (2007).

4. Xiaoyong Yang & Kevin Qian. Protein O-GlcNAcylation: emerging mechanisms and functions. *Nat. Rev. Mol. Cell Biol.* **18**, 452–465 (2017).

5. Robert G. Spiro. Protein glycosylation: nature, distribution, enzymatic formation, and disease implications of glycopeptide bonds. *Glycobiology* **12**, 43R–56R (2002).

6. L Wells; K Vosseller; G W Hart. Glycosylation of nucleocytoplasmic proteins: signal transduction and O-GlcNAc. *Science (80-.).* **291**, 2376–7 (2001).

7. Dona C. Love and John A. Hanover. The Hexosamine Signaling Pathway: Deciphering the 'O-GlcNAc Code'. *Sci. STKE* **2005**, re13 (2005).

8. Katryn R. Harwood, John A. Hanover. Nutrient-driven O-GlcNAc cycling – think globally but act locally. *J. Cell Sci.* **127**, 1857–67 (2014).

9. Kornfeld, R. Studies on l-glutamine d-fructose 6-phosphate amidotransferase. I. Feedback inhibition by uridine diphosphate-N-acetylglucosamine. *J. Biol. Chem.* **242**, 3135–41 (1967).

10. Tourian, A.; Callahan, M. & Hung, W. l-glutamine d-fructose-6-P aminotransferase regulation by glucose-6-P and UDP-N-acetylglucosamine. *Neurochem. Res.* **8**, 1589–1595 (1983).

11. Satoshi Eguchi *et al*. AMP-activated protein kinase phosphorylates glutamine : fructose-6-phosphate amidotransferase 1 at Ser243 to modulate its enzymatic activity. *Genes to cells* **14**, 179–189 (2009).

12. Darya Zibrova *et al*. GFAT1 phosphorylation by AMPK promotes VEGF-induced angiogenesis. *Biochem J.* **474**, 983–1001 (2017).

13. Chiaradonna F; Ricciardiello F; Palorini R. The nutrient-sensing hexosamine biosynthetic pathway as the hub of cancer metabolic rewiring. *Cells* **7**, 53 (2018).

14. Moremen KW; Tiemeyer M; Nairn AV; Vertebrate protein glycosylation: diversity, synthesis and function. *Nat Rev Mol Cell Biol* **13**, 448–62 (2012).

15. Gerald W Hart, Chad Slawson, Genaro Ramirez-Correa, Olof Lagerlof. Cross talk between O-GlcNAcylation and phosphorylation: roles in signaling, transcription, and chronic disease. *Annu Rev Biochem* **80**, 825–58 (2011).

16. Alexis K. Nagel and Lauren E. Ball. O-GlcNAc transferase and O-GlcNAcase: achieving target substrate specificity. *Amino Acids* **46**, 2305–2316 (2014).

17. Lubas WA; Frank DW; Krause M; Hanover JA. O-Linked Glc-NAc transferase is a conserved nucleocytoplasmic protein containing tetratricopeptide repeats. *J Biol Chem.* **272**, 9316– 9324 (1997).

18. Dagmar Nolte, Ulrich Müller. Human O-GlcNAc transferase (OGT): genomic structure, analysis of splice variants, fine mapping in Xq13.1. *Mamm. Genome* **13**, 62–64 (2002).

19. Hanover JA *et al.* Mitochondrial and nucleocytoplasmic isoforms of O-linked GlcNAc transferase encoded by a single mammalian gene. *Arch Biochem Biophys* **409**, 287–297 (2003).

20. Tracey M Gloster, David J Vocadlo. Mechanism, structure, and inhibition of O-GlcNAc processing enzymes. *Curr Signal Transduct Ther* **5**, 74–91 (2010).

21. Lubas WA; Hanover JA. Functional expression of O-linked GlcNAc transferase. Domain structure and substrate specificity. *J Biol Chem* **275**, 10983–10988 (2000).

22. Comer FI; Hart GW. Reciprocity between O-GlcNAc and O-phosphate on the carboxyl terminal domain of RNA polymerase II. *Biochemistry* **40**, 7845–7852 (2001).

23. Akimoto Y; Kreppel LK; Hirano H; Hart GW. Localization of the O-linked N-acetylglucosamine transferase in rat pancreas. *Diabetes* **48**, 2407–2413 (1999).

24. Haltiwanger RS; Blomberg MA; Hart GW. Glycosylation of nuclear and cytoplasmic proteins. Purification and characterization of a uridine diphospho-N-acetylglucosamine:polypeptide beta-Nacetylglucosaminyltransferase. *J Biol Chem* **267**, 9005–9013 (1992).

25. Kreppel LK; Blomberg MA; Hart GW. Dynamic glycosylation of nuclear and cytosolic proteins. Cloning and characterization of a unique O-GlcNAc transferase with multiple tetratricopeptide repeats. *J Biol Chem.* **272**, 9308–9315 (1997).

26. Kreppel LK; Hart GW. Regulation of a cytosolic and nuclear O-GlcNAc transferase. Role of the tetratricopeptide repeats. *J Biol Chem.* **274**, 32015–

32022 (1999).

27. Jinek M; Rehwinkel J; Lazarus BD; Izaurralde E; Hanover JA; Conti E; The superhelical TPR-repeat domain of O-linked GlcNAc transferase exhibits structural similarities to importin alpha. *Nat Struct Mol Biol* **11**, 1001–1007 (2004).

28. L K Kreppel *et al.* Dynamic glycosylation of nuclear and cytosolic proteins. Cloning and characterization of a unique O-GlcNAc transferase with multiple tetratricopeptide repeats. *J Biol Chem.* **272**, 9308–9315 (1997).

29. Whelan SA; Lane MD; Hart GW. Regulation of the O-linked beta-N-acetylglucosamine transferase by insulin signaling. *J Biol Chem.* **283**, 21411–21417 (2008).

30. Krista Kaasik *et al.* Glucose Sensor O-GlcNAcylation Coordinates with Phosphorylation to Regulate Circadian Clock. *Cell Metab.* **17**, 291–302 (2013).

31. John W Bullen; Jeremy L Balsbaugh; Dipanjan Chanda; Jeffrey Shabanowitz; Donald F Hunt; Dietbert Neumann; Gerald W Hart; Cross-talk between two essential nutrient-sensitive enzymes: O-GlcNAc transferase (OGT) and AMP-activated protein kinase (AMPK). *J Biol Chem* **289**, 10592–606 (2014).

32. Kazemi, Z., Chang, H., Haserodt, S., McKen, C. & Zachara, N. E. O-linked β-N-acetylglucosamine (O-GlcNAc) regulates stress-induced heat shock protein expression in a GSK-3β-dependent manner. *J. Biol. Chem.* (2010). doi:10.1074/jbc.M110.131102

33. Xiaoyong Yang *et al.* Phosphoinositide signalling links O-GlcNAc transferase to insulin resistance. *Nature* (2008).

34. Cheung, W. D. & Hart, G. W. AMP-activated protein kinase and p38 MAPK activate O-GlcNAcylation of neuronal proteins during glucose deprivation. *J. Biol. Chem.* (2008). doi:10.1074/jbc.M801222200

35. Zachara, N. E. & Hart, G. W. O-GlcNAc a sensor of cellular state: The role of nucleocytoplasmic glycosylation in modulating cellular function in response to nutrition and stress. *Biochimica et Biophysica Acta - General Subjects* (2004). doi:10.1016/j.bbagen.2004.03.016

36. Zachara, N. E. *et al.* Dynamic O-GlcNAc modification of nucleocytoplasmic proteins in response to stress: A survival response of mammalian cells. *J. Biol. Chem.* (2004). doi:10.1074/jbc.M403773200

37. Boss, G. R. & Seegmiller, J. E. Age-related physiological changes and their clinical significance. *West. J. Med.* (1981).

38. López-Otín, C., Blasco, M. A., Partridge, L., Serrano, M. & Kroemer, G. The hallmarks of aging. *Cell* (2013). doi:10.1016/j.cell.2013.05.039

39. Banerjee, P. S., Lagerlöf, O. & Hart, G. W. Roles of O-GlcNAc in chronic diseases of aging. *Molecular Aspects of Medicine* (2016). doi:10.1016/j.mam.2016.05.005

40. Comtesse, N., Maldener, E. & Meese, E. Identification of a nuclear variant of MGEA5, a cytoplasmic hyaluronidase and a β-A-acetylglucosaminidase. *Biochem. Biophys. Res. Commun.* (2001). doi:10.1006/bbrc.2001.4815

41. Dong, D. L. Y. & Hart, G. W. Purification and characterization of an O-GlcNAc selective N-acetyl-β-D- glucosaminidase from rat spleen cytosol. *J. Biol. Chem.* (1994).

42. Gao, Y., Wells, L., Comer, F. I., Parker, G. J. & Hart, G. W. Dynamic O-glycosylation of nuclear and cytosolic proteins: cloning and characterization of a neutral, cytosolic beta-N-acetylglucosaminidase from human brain. *J Biol Chem* **276**, 9838–9845 (2001).

43. Wells, L. *et al.* Dynamic O-glycosylation of nuclear and cytosolic proteins: Further characterization of the nucleocytoplasmic β-N-acetylglucosaminidase, O-GlcNAcase. *J. Biol. Chem.* (2002). doi:10.1074/jbc.M109656200

44. Heckel, D. *et al.* Novel immunogenic antigen homologous to hyaluronidase in meningioma. *Hum. Mol. Genet.* (1998). doi:10.1093/hmg/7.12.1859

45. Toleman, C., Paterson, A. J., Whisenhunt, T. R. & Kudlow, J. E. Characterization of the histone acetyltransferase (HAT) domain of a bifunctional protein with activable O-GlcNAcase and HAT activities. *J. Biol. Chem.* (2004). doi:10.1074/jbc.M410406200

46. Rao, F. V. *et al.* Structure of a bacterial putative acetyltransferase defines the fold of the human O-GlcNAcase C-terminal domain. *Open Biol.* (2013). doi:10.1098/rsob.130021

47. Khidekel, N. *et al.* Probing the dynamics of O-GlcNAc glycosylation in the brain using quantitative proteomics. *Nat. Chem. Biol.* (2007). doi:10.1038/nchembio881

48. Thomas R Whisenhunt, Xiaoyong Yang, Damon B Bowe, Andrew J Paterson, Brian A Van Tine, Jeffrey E Kudlow. Disrupting the enzyme complex regulating O-GlcNAcylation blocks signaling and development. *Glycobiology* **16**, 551–563 (2006).

49. Lazarus, B. D., Love, D. C. & Hanover, J. A. Recombinant O-GlcNAc transferase isoforms: Identification of O-GlcNAcase, yes tyrosine kinase, and tau as isoform-specific substrates. *Glycobiology* (2006).

50. Love, D. C., Krause, M. W. & Hanover, J. A. O-GlcNAc cycling: Emerging roles in development and epigenetics. *Seminars in Cell and Developmental Biology* (2010). doi:10.1016/j.semcdb.2010.05.001

51. Sinclair, D. A. R. *et al.* Drosophila O-GlcNAc transferase (OGT) is encoded by the Polycomb group (PcG) gene, super sex combs (sxc). *Proc. Natl. Acad. Sci. U. S. A.* (2009). doi:10.1073/pnas.0904638106

52. Zhang, Z., Tan, E. P., VandenHull, N. J., Peterson, K. R. & Slawson, C. O-GlcNAcase expression is sensitive to changes in O-GlcNAc homeostasis. *Front. Endocrinol. (Lausanne).* (2014). doi:10.3389/fendo.2014.00206

53. Wang, Z., Gucek, M. & Hart, G. W. Cross-talk between GlcNAcylation and phosphorylation: site-specific phosphorylation dynamics in response to globally elevated O-GlcNAc. *Proc Natl Acad Sci U S A* **105**, 13793–13798 (2008).

54. Van der Laarse, S. A. M., Leney, A. C. & Heck, A. J. R. Crosstalk between phosphorylation and O-GlcNAcylation: friend or foe. *FEBS Journal* (2018). doi:10.1111/febs.14491

55. Leney, A. C., El Atmioui, D., Wu, W., Ovaa, H. & Heck, A. J. R. Elucidating crosstalk mechanisms between phosphorylation and O-GlcNAcylation. *Proc. Natl. Acad. Sci. U. S. A.* (2017). doi:10.1073/pnas.1620529114

56. Zeidan, Q. & Hart, G. W. The intersections between O-GlcNAcylation and phosphorylation: Implications for multiple signaling pathways. *J. Cell Sci.* (2010). doi:10.1242/jcs.053678

57. Trinidad, J. C. *et al.* Global identification and characterization of both O-GlcNAcylation and phosphorylation at the murine synapse. *Mol. Cell. Proteomics* (2012). doi:10.1074/mcp.O112.018366

58. Copeland, R. J., Bullen, J. W. & Hart, G. W. Cross-talk between GlcNAcylation and phosphorylation: Roles in insulin resistance and glucose toxicity. *American Journal of Physiology - Endocrinology and Metabolism* (2008). doi:10.1152/ajpendo.90281.2008

59. Wani, W. Y., Chatham, J. C., Darley-Usmar, V., McMahon, L. L. & Zhang, J. O-GlcNAcylation and neurodegeneration. *Brain Research Bulletin* (2017). doi:10.1016/j.brainresbull.2016.08.002

60. Ballard, C., Mobley, W., Hardy, J., Williams, G. & Corbett, A. Dementia in Down's syndrome. *Lancet Neurol* **15**, 622–636 (2016).

61. Sherman, S. L., Allen, E. G., Bean, L. H. & Freeman, S. B. Epidemiology of Down syndrome. *Ment Retard Dev Disabil Res Rev* **13**, 221–227 (2007).

62. Neale, N., Padilla, C., Fonseca, L. M., Holland, T. & Zaman, S. Neuroimaging and other modalities to assess Alzheimer's disease in Down syndrome. *Neuroimage Clin* **17**, 263–271 (2018).

63. Wiseman, F. K. *et al.* A genetic cause of Alzheimer disease: mechanistic insights from Down syndrome. *Nat Rev Neurosci* **16**, 564–574 (2015).

64. Antonarakis, S. E. *et al.* Down syndrome. *Nat Rev Dis Prim.* **6**, 9 (2020).

65. Bittles, A. H., Bower, C., Hussain, R. & Glasson, E. J. The four ages of Down syndrome. *Eur J Public Heal.* **17**, 221–225 (2007).

66. De Graaf, G., Buckley, F. & Skotko, B. G. Estimation of the number of people with Down syndrome in the United States. *Genet Med* **19**, 439–447 (2017).

67. Strauss, D. & Eyman, R. K. Mortality of people with mental retardation in California with and without Down syndrome, 1986-1991. *Am. J. Ment. Retard.* (1996).

68. Elizabeth Head, Wayne Silverman, David Patterson, and I. T. L. Aging and Down Syndrome. *Curr. Gerontol. Geriatr. Res.* (2012).

69. Hartley, D. *et al.* Down syndrome and Alzheimer's disease: Common pathways, common goals. *Alzheimers Dement* **11**, 700–709 (2016).

70. Perluigi, M., Di Domenico, F. & Buttterfield, D. A. Unraveling the complexity of neurodegeneration in brains of subjects with Down syndrome: insights from proteomics. *Proteomics Clin Appl* **8**, 73–85 (2014).

71. Head, E., Lott, I. T., Wilcock, D. M. & Lemere, C. A. Aging in Down Syndrome and the Development of Alzheimer's Disease Neuropathology. *Curr. Alzheimer Res.* **13**, 18–29 (2016).

72. Glasson, E. J. *et al.* The changing survival profile of people with Down's syndrome: Implications for genetic counselling. *Clin. Genet.* (2002). doi:10.1034/j.1399-0004.2002.620506.x

73. Franceschi, M., Comola, M., Piattoni, F., Gualandri, W. & Canal, N. Prevalence of dementia in adult patients with trisomy 21. *Am. J. Med. Genet.* (1990). doi:10.1002/ajmg.1320370760

74. Prasher, V. P. & Filer, A. Behavioural disturbance in people with Down's syndrome and dementia. *J. Intellect. Disabil. Res.* (1995). doi:10.1111/j.1365-2788.1995.tb00547.x

75. Holland, A. J., Hon, J., Huppert, F. A. & Stevens, F. Incidence and course of dementia in people with Down's syndrome: Findings from a population-based study. *J. Intellect. Disabil. Res.* (2000). doi:10.1046/j.1365-2788.2000.00263.x

76. Oliver, C., Crayton, L., Holland, A., Hall, S. & Bradbury, J. A four year prospective study of age-related cognitive change in adults with Down's syndrome. *Psychol. Med.* (1998). doi:10.1017/S0033291798007417

77. Oliver, C., Holland, T., Hall, S. & Crayton, L. Effects of increasing task load on memory impairment in adults with Down syndrome. *Am. J. Ment. Retard.* (2005). doi:10.1352/0895-8017(2005)110[339:EOITLO]2.0.CO;2

78. Collacott, R. A. & Cooper, S. A. A five-year follow up study of adaptive behaviour in adults with Down syndrome. *J. Intellect. Dev. Disabil.* (1997). doi:10.1080/13668259700033401

79. Lott, I. T. & Head, E. Dementia in Down syndrome: unique insights for Alzheimer disease research. *Nat Rev Neurol* **15**, 135–147 (2019).

80. Lao, P. J. *et al.* Alzheimer-Like Pattern of Hypometabolism Emerges with Elevated Amyloid-β Burden in Down Syndrome. *J. Alzheimer's Dis.* (2017). doi:10.3233/JAD-170720

81. De-Paula, V. J., Radanovic, M., Diniz, B. S. & Forlenza, O. V. Alzheimer's disease. *Subcell. Biochem.* (2012). doi:10.1007/978-94-007-5416-4_14

82. Di Domenico, F. *et al.* Redox proteomics analysis of HNE-modified proteins in Down syndrome brain: clues for understanding the development of Alzheimer disease. *Free Radic Biol Med* **71**, 270–280 (2014).

83. Zana, M. Oxidative stress : A bridge between Down ' s syndrome and Alzheimer ' s disease. *Neurobiol. Aging* **28**, 648–676 (2007).

84. Doran, E. *et al.* Down Syndrome, Partial Trisomy 21, and Absence of Alzheimer's Disease: The Role of APP. *J. Alzheimer's Dis.* (2017). doi:10.3233/JAD-160836

85. Prasher, V. P. *et al.* Molecular mapping of Alzheimer-type dementia in Down's syndrome. *Ann. Neurol.* (1998). doi:10.1002/ana.410430316

86. Cataldo, A. M. *et al.* Down syndrome fibroblast model of Alzheimer-related endosome pathology: Accelerated endocytosis promotes late endocytic defects. *Am. J. Pathol.* (2008). doi:10.2353/ajpath.2008.071053

87. Shukkur, E. A. *et al.* Mitochondrial dysfunction and tau hyperphosphorylation in Ts1Cje, a mouse model for Down syndrome. *Hum. Mol. Genet.* (2006). doi:10.1093/hmg/ddl211

88. Drewes, G. *et al.* Dephosphorylation of tau protein and Alzheimer paired helical filaments by calcmeurin and phosphatase-2A. *FEBS Lett.* (1993). doi:10.1016/0014-5793(93)80850-T

89. Wieslaw K. Dowjata,, Tatyana Adayevb, Izabela Kuchnaa, Krzysztof

Nowickia, Sonia Palminielloc, Yu Wen Hwangb, and J. W. Trisomy-driven overexpression of DYRK1A kinase in the brain of subjects with Down syndrome. *Neurosci Lett* **413**, 77–81 (2008).

90. Liu, F. *et al.* Overexpression of Dyrk1A contributes to neurofibrillary degeneration in Down syndrome. *FASEB J.* (2008). doi:10.1096/fj.07-104539

91. Busciglio, J. & Yankner, B. A. Apoptosis and increased generation of reactive oxygen species in down's syndrome neurons in vitro. *Nature* (1995). doi:10.1038/378776a0

92. Picard, M. & McEwen, B. S. Mitochondria impact brain function and cognition. *Proceedings of the National Academy of Sciences of the United States of America* (2014). doi:10.1073/pnas.1321881111

93. Brooksbank, B. W. L., Martinez, M. & Balazs, R. Altered Composition of Polyunsaturated Fatty Acyl Groups in Phosphoglycerides of Down's Syndrome Fetal Brain. *J. Neurochem.* (1985). doi:10.1111/j.1471-4159.1985.tb12896.x

94. Odetti, P. *et al.* Early glycoxidation damage in brains from Down's syndrome. *Biochem. Biophys. Res. Commun.* (1998). doi:10.1006/bbrc.1998.8186

95. Cenini, G. *et al.* Association between frontal cortex oxidative damage and beta-amyloid as a function of age in Down syndrome. *Biochim. Biophys. Acta - Mol. Basis Dis.* (2012). doi:10.1016/j.bbadis.2011.10.001

96. DeHaan, J. B. et al. Elevation in the ratio of Cu/Zn-superoxide dismutase to glutathione peroxidase activity induces features of cellular senescence and this effect is mediated by hydrogen peroxide. *Hum. Mol. Genet.* **5**, 283–292 (1996).

97. Shariati, S. A. M. & De Strooper, B. Redundancy and divergence in the amyloid precursor protein family. *FEBS Letters* (2013). doi:10.1016/j.febslet.2013.05.026

98. Zhang, Y. W., Thompson, R., Zhang, H. & Xu, H. APP processing in Alzheimer's disease. *Molecular Brain* (2011). doi:10.1186/1756-6606-4-3

99. Choi, J. H. K. *et al.* Age-dependent dysregulation of brain amyloid precursor protein in the Ts65Dn Down syndrome mouse model. *J. Neurochem.* (2009). doi:10.1111/j.1471-4159.2009.06277.x

100. Cheon, M. S., Dierssen, M., Kim, S. H. & Lubec, G. Protein expression of BACE1, BACE2 and APP in Down syndrome brains. *Amino Acids* (2008). doi:10.1007/s00726-007-0618-9

101. Seo, H. & Isacson, O. Abnormal APP, cholinergic and cognitive function in Ts65Dn Down's model mice. *Exp. Neurol.* (2005).

102. Teller, J. K. *et al.* Presence of soluble amyloid β-peptide precedes amyloid plaque formation in Down's syndrome. *Nat. Med.* (1996). doi:10.1038/nm0196-93

103. Murray, A. *et al.* Brief report: Isogenic induced pluripotent stem cell lines from an adult with mosaic down syndrome model accelerated neuronal ageing and neurodegeneration. *Stem Cells* (2015). doi:10.1002/stem.1968

104. Shi, Y. *et al.* A human stem cell model of early Alzheimer's disease pathology in down syndrome. *Sci. Transl. Med.* (2012). doi:10.1126/scitranslmed.3003771

105. Fabio Di Domenico, Raffaella Coccia, Annalisa Cocciolo, M. Paul Murphy, Giovanna Cenini, Elizabeth Head, D. Allan Butterfield, Alessandra Giorgia, M. E. & Schinina, Cesare Mancuso, Chiara Cini, and M. P. Impairment of proteostasis network in Down syndrome prior to the development of Alzheimer's disease neuropathology: Redox proteomics analysis of human brain. *Biochim Biophys Acta* **1832**, 1249–1259 (2014).

106. Perluigi, M., Di Domenico, F. & Butterfield, D. A. mTOR signaling in aging and neurodegeneration: At the crossroad between metabolism dysfunction and impairment of autophagy. *Neurobiol. Dis.* **84**, 39–49 (2015).

107. Witman, G. B., Cleveland, D. W., Weingarten, M. D. & Kirschner, M. W. Tubulin requires tau for growth into microtubule initiating sites. *Proc. Natl. Acad. Sci. U. S. A.* (1976). doi:10.1073/pnas.73.11.4070

108. Rodríguez-Martín, T. *et al.* Tau phosphorylation affects its axonal transport and degradation. *Neurobiol. Aging* (2013). doi:10.1016/j.neurobiolaging.2013.03.015

109. Mann, D. M. A., Yates, P. O., Marcyniuk, B. & Ravindra, C. R. The topography of plaques and tangles in down's syndrome patients of different ages. *Neuropathol. Appl. Neurobiol.* (1986). doi:10.1111/j.1365-2990.1986.tb00053.x

110. Hof, P. R. *et al.* Age-Related Distribution of Neuropathologic Changes in the Cerebral Cortex of Patients with Down's Syndrome: Quantitative Regional Analysis and Comparison with Alzheimer's Disease. *Arch. Neurol.* (1995). doi:10.1001/archneur.1995.00540280065020

111. Rahmani, Z., Lopes, C., Rachidi, M. & Delabar, J. M. Expression of the mnb (dyrk) protein in adult and embryonic mouse tissues. *Biochem. Biophys. Res. Commun.* (1998). doi:10.1006/bbrc.1998.9803

112. Martí, E. *et al.* Dyrk1A expression pattern supports specific roles of this kinase in the adult central nervous system. *Brain Res.* (2003).

113. Guimera, J., Casas, C., Estivill, X. & Pritchard, M. Human minibrain homologue (MNBH/DYRK1): Characterization, alternative splicing, differential tissue expression, and overexpression in Down syndrome. *Genomics* (1999). doi:10.1006/geno.1999.5775

114. Woods, Y. L. *et al.* The kinase DYRK phosphorylates protein-synthesis initiation factor elF2Bε at Ser539 and the microtubule-associated protein tau at Thr212: Potential role for DYRK as a glycogen synthase kinase 3-priming kinase. *Biochem. J.* (2001). doi:10.1042/bj3550609

115. Ryoo, S. R. *et al.* DYRK1A-mediated hyperphosphorylation of Tau: A functional link between down syndrome and Alzheimer disease. *J. Biol. Chem.* (2007). doi:10.1074/jbc.M707358200

116. Lu, T. *et al.* REST and stress resistance in ageing and Alzheimer's disease. *Nature* (2014). doi:10.1038/nature13163

117. Cardenas, A. M. . et al. Role of tau protein in neuronal damage in Alzheimer's disease and Down syndrome. *Arch Med Res* **43**, 645–654 (2012).

118. Harris, C. D. . G. E. and K. J. D. RCAN1-1L is overexpressed in neurons of Alzheimer's disease patients. *FEBS J.* **274**, 1715–24 (2007).

119. Kimura, R. . et al. The DYRK1A gene, encoded in chromosome 21 Down syndrome critical region, bridges between beta-amyloid production and tau phosphorylation in Alzheimer disease. *Hum Mol Genet* **16**, 15–23 (2007).

120. Lloret, A., et al. Amyloid-beta toxicity and tau hyperphosphorylation are linked via RCAN1 in Alzheimer's disease. *J Alzheimers Dis* **27**, 701–9 (2011).

121. Caracausi, M. *et al.* Plasma and urinary metabolomic profiles of Down syndrome correlate with alteration of mitochondrial metabolism. *Sci. Rep.* (2018). doi:10.1038/s41598-018-20834-y

122. Obeid, R. *et al.* Blood biomarkers of methylation in Down syndrome and metabolic simulations using a mathematical model. *Mol. Nutr. Food Res.* (2012). doi:10.1002/mnfr.201200162

123. Škovierová, H. *et al.* The molecular and cellular effect of homocysteine metabolism imbalance on human health. *International Journal of Molecular Sciences* (2016). doi:10.3390/ijms17101733

124. Panagaki, T., Randi, E. B., Augsburger, F. & Szabo, C. Overproduction of H2S, generated by CBS, inhibits mitochondrial Complex IV and suppresses oxidative phosphorylation in down syndrome. *Proc. Natl. Acad. Sci. U. S. A.* (2019). doi:10.1073/pnas.1911895116

125. Adelekan, T., Magge, S., Shults, J., Stallings, V. & Stettler, N. Lipid profiles

of children with Down syndrome compared with their siblings. *Pediatrics* (2012). doi:10.1542/peds.2011-1262

126. Buonuomo, P. S. *et al.* Lipid profiles in a large cohort of Italian children with Down syndrome. *Eur. J. Med. Genet.* (2016). doi:10.1016/j.ejmg.2016.06.005

127. Zamorano, A., Guzmán, M., Aspillaga, M., Avendaño, A. & Gatica, M. [Concentrations of serum lipids in children with Down's syndrome]. *Arch. Biol. Med. Exp. (Santiago).* (1991).

128. Sobey, C. G. *et al.* Risk of major cardiovascular events in people with down syndrome. *PLoS One* (2015). doi:10.1371/journal.pone.0137093

129. Yu, Q. *et al.* Lipidome alterations in human prefrontal cortex during development, aging, and cognitive disorders. *Mol. Psychiatry* (2018). doi:10.1038/s41380-018-0200-8

130. Hwang, S. *et al.* Suppressing Aneuploidy-Associated Phenotypes Improves the Fitness of Trisomy 21 Cells. *Cell Rep.* (2019). doi:10.1016/j.celrep.2019.10.059

131. Pietrini, P. *et al.* Low glucose metabolism during brain stimulation in older Down's syndrome subjects at risk for Alzheimer's disease prior to dementia. *Am. J. Psychiatry* (1997). doi:10.1176/ajp.154.8.1063

132. Schapiro, M. B. *et al.* Decline in cerebral glucose utilisation and cognitive function with aging in Down's syndrome. *J. Neurol. Neurosurg. Psychiatry* (1987). doi:10.1136/jnnp.50.6.766

133. Tramutola, A. *et al.* Brain insulin resistance triggers early onset Alzheimer disease in Down syndrome. *Neurobiol. Dis.* (2020). doi:10.1016/j.nbd.2020.104772

134. Labudova, O., Cairns, N., Kitzmüller, E. & Lubec, G. Impaired brain glucose metabolism in patients with Down Syndrome. *J. Neural Transm. Suppl.* (1999). doi:10.1007/978-3-7091-6380-1_16

135. Annerén, K. G., Korenberg, J. R. & Epstein, C. J. Phosphofructokinase activity in fibroblasts aneuploid for chromosome 21. *Hum. Genet.* (1987). doi:10.1007/BF00283052

136. Peled-Kamar, M., Degani, H., Bendel, P., Margalit, R. & Groner, Y. Altered brain glucose metabolism in transgenic-PFKL mice with elevated L-phosphofructokinase: In vivo NMR studies. *Brain Res.* (1998). doi:10.1016/S0006-8993(98)00899-3

137. Elson, A., Levanon, D., Weiss, Y. & Groner, Y. Overexpression of liver-type phosphofructokinase (PFKL) in transgenic-PFKL mice: Implication for gene

dosage in trisomy 21. *Biochem. J.* (1994). doi:10.1042/bj2990409

138. Pelleri, M. C. *et al.* Integrated quantitative transcriptome maps of human trisomy 21 tissues and cells. *Front. Genet.* (2018). doi:10.3389/fgene.2018.00125

139. Szablewski, L. Glucose Transporters in Brain: In Health and in Alzheimer's Disease. *Journal of Alzheimer's Disease* (2017). doi:10.3233/JAD-160841

140. Simpson, I. A., Chundu, K. R., Davies-Hill, T., Honer, W. G. & Davies, P. Decreased concentrations of GLUT1 and GLUT3 glucose transporters in the brains of patients with Alzheimer's disease. *Ann. Neurol.* (1994). doi:10.1002/ana.410350507

141. Kalaria, R. H. N. & Harik, S. I. Reduced Glucose Transporter at the Blood-Brain Barrier and in Cerebral Cortex in Alzheimer Disease. *J. Neurochem.* (1989). doi:10.1111/j.1471-4159.1989.tb07399.x

142. Liu, Y., Liu, F., Iqbal, K., Grundke-Iqbal, I. & Gong, C. X. Decreased glucose transporters correlate to abnormal hyperphosphorylation of tau in Alzheimer disease. *FEBS Lett.* (2008). doi:10.1016/j.febslet.2007.12.035

143. Arnold, S. E. *et al.* Brain insulin resistance in type 2 diabetes and Alzheimer disease: Concepts and conundrums. *Nature Reviews Neurology* (2018). doi:10.1038/nrneurol.2017.185

144. Haeusler, R. A., McGraw, T. E. & Accili, D. Metabolic Signalling: Biochemical and cellular properties of insulin receptor signalling. *Nature Reviews Molecular Cell Biology* (2018). doi:10.1038/nrm.2017.89

145. Butterfield, D. A., Di Domenico, F. & Barone, E. Elevated risk of type 2 diabetes for development of Alzheimer disease: A key role for oxidative stress in brain. *Biochimica et Biophysica Acta - Molecular Basis of Disease* (2014). doi:10.1016/j.bbadis.2014.06.010

146. Bomfim, T. R. *et al.* An anti-diabetes agent protects the mouse brain from defective insulin signaling caused by Alzheimer's disease-associated Aβ oligomers. *J. Clin. Invest.* (2012). doi:10.1172/JCI57256

147. Lourenco, M. V. *et al.* TNF-α mediates PKR-dependent memory impairment and brain IRS-1 inhibition induced by Alzheimer's β-amyloid oligomers in mice and monkeys. *Cell Metab.* (2013). doi:10.1016/j.cmet.2013.11.002

148. Barone, E. *et al.* Impairment of biliverdin reductase-A promotes brain insulin resistance in Alzheimer disease: A new paradigm. *Free Radic. Biol. Med.* **91**, 127–142 (2016).

149. Chen, Z. & Zhong, C. Decoding Alzheimer's disease from perturbed cerebral

glucose metabolism: Implications for diagnostic and therapeutic strategies. *Progress in Neurobiology* (2013). doi:10.1016/j.pneurobio.2013.06.004

150. Coskun, P. E. & Busciglio, J. Oxidative stress and mitochondrial dysfunction in Down's syndrome: Relevance to aging and dementia. *Current Gerontology and Geriatrics Research* (2012). doi:10.1155/2012/383170

151. Butterfield, D. A., Di Domenico, F., Swomley, A. M., Head, E. & Perluigi, M. Redox proteomics analysis to decipher the neurobiology of Alzheimer-like neurodegeneration: Overlaps in Down's syndrome and Alzheimer's disease brain. *Biochem. J.* (2014). doi:10.1042/BJ20140772

152. Valenti, D. *et al.* Mitochondria as pharmacological targets in Down syndrome. *Free Radical Biology and Medicine* (2018). doi:10.1016/j.freeradbiomed.2017.08.014

153. Valenti, D. *et al.* Impairment of F1F0-ATPase, adenine nucleotide translocator and adenylate kinase causes mitochondrial energy deficit in human skin fibroblasts with chromosome 21 trisomy. *Biochem. J.* (2010). doi:10.1042/BJ20100581

154. Valenti, D., Manente, G. A., Moro, L., Marra, E. & Vacca, R. A. Deficit of complex I activity in human skin fibroblasts with chromosome 21 trisomy and overproduction of reactive oxygen species by mitochondria: Involvement of the cAMP/PKA signalling pathway. *Biochem. J.* (2011). doi:10.1042/BJ20101908

155. Valenti, D. *et al.* The polyphenols resveratrol and epigallocatechin-3-gallate restore the severe impairment of mitochondria in hippocampal progenitor cells from a Down syndrome mouse model. *Biochim Biophys Acta* **1862**, 1093–1104 (2016).

156. Piccoli, C. *et al.* Chronic pro-oxidative state and mitochondrial dysfunctions are more pronounced in fibroblasts from down syndrome foeti with congenital heart defects. *Hum. Mol. Genet.* (2013). doi:10.1093/hmg/dds529

157. Perluigi, M. & Butterfield, D. A. Oxidative stress and down syndrome: A route toward Alzheimer-like dementia. *Current Gerontology and Geriatrics Research* (2012). doi:10.1155/2012/724904

158. Kandimalla, R., Thirumala, V. & Reddy, P. H. Is Alzheimer's disease a Type 3 Diabetes? A critical appraisal. *Biochimica et Biophysica Acta - Molecular Basis of Disease* (2017). doi:10.1016/j.bbadis.2016.08.018

159. Gong, C. X., Liu, F. & Iqbal, K. O-GlcNAcylation: A regulator of tau pathology and neurodegeneration. *Alzheimers Dement* **12**, 1078–1089 (2016).

160. Liu, F. *et al.* Reduced O-GlcNAcylation links lower brain glucose metabolism

and tau pathology in Alzheimer's disease. *Brain* **132**, 1820–1832 (2009).

161. Pinho, T. S., Verde, D. M., Correia, S. C., Cardoso, S. M. & Moreira, P. I. O-GlcNAcylation and neuronal energy status: Implications for Alzheimer's disease. *Ageing Res Rev* **46**, 32–41 (2018).

162. Zhu, Y., Shan, X., Yuzwa, S. A. & Vocadlo, D. J. The emerging link between O-GlcNAc and Alzheimer disease. *J Biol Chem* **289**, 34472–34481 (2014).

163. Oh, H., Madison, C., Baker, S., Rabinovici, G. & Jagust, W. Dynamic relationships between age, amyloid-β deposition, and glucose metabolism link to the regional vulnerability to Alzheimer's disease. *Brain* (2016). doi:10.1093/brain/aww108

164. Griffith, L. S., Mathes, M. & Schmitz, B. Beta-amyloid precursor protein is modified with O-linked N-acetylglucosamine. *J Neurosci Res* **41**, 270–278 (1995).

165. Jacobsen, K. T. & Iverfeldt, K. O-GlcNAcylation increases non-amyloidogenic processing of the amyloid-beta precursor protein (APP). *Biochem Biophys Res Commun* **404**, 882–886 (2011).

166. Chun, Y. S., Kwon, O. H. & Chung, S. O-GlcNAcylation of amyloid-beta precursor protein at threonine 576 residue regulates trafficking and processing. *Biochem Biophys Res Commun* **490**, 486–491 (2017).

167. Kim, C. *et al.* O-linked beta-N-acetylglucosaminidase inhibitor attenuates beta-amyloid plaque and rescues memory impairment. *Neurobiol Aging* **34**, 275–285 (2013).

168. Shane Arnold, C. *et al.* The microtubule-associated protein tau is extensively modified with O- linked N-acetylglucosamine. *J. Biol. Chem.* (1996). doi:10.1074/jbc.271.46.28741

169. Yuzwa, S. A. *et al.* Mapping O-GlcNAc modification sites on tau and generation of a site-specific O-GlcNAc tau antibody. *Amino Acids* (2011). doi:10.1007/s00726-010-0705-1

170. Yuzwa, S. A. *et al.* Increasing O-GlcNAc slows neurodegeneration and stabilizes tau against aggregation. *Nat. Chem. Biol.* (2012). doi:10.1038/nchembio.797

171. Yuzwa, S. A. *et al.* Pharmacological inhibition of O-GlcNAcase (OGA) prevents cognitive decline and amyloid plaque formation in bigenic tau/APP mutant mice. *Mol. Neurodegener.* **9**, 42 (2014).

172. Deng, Y. *et al.* Dysregulation of insulin signaling, glucose transporters, O-GlcNAcylation, and phosphorylation of tau and neurofilaments in the brain:

Implication for Alzheimer's disease. *Am. J. Pathol.* (2009). doi:10.2353/ajpath.2009.090157

173. Li, X., Lu, F., Wang, J. Z. & Gong, C. X. Concurrent alterations of O-GlcNAcylation and phosphorylation of tau in mouse brains during fasting. *Eur. J. Neurosci.* (2006). doi:10.1111/j.1460-9568.2006.04735.x

174. Lefebvre, T. *et al.* Effect of okadaic acid on O-linked N-acetylglucosamine levels in a neuroblastoma cell line. *Biochim. Biophys. Acta - Gen. Subj.* (1999). doi:10.1016/S0304-4165(99)00105-1

175. Graham, D. L. *et al.* Increased O-GlcNAcylation reduces pathological tau without affecting its normal phosphorylation in a mouse model of tauopathy. *Neuropharmacology* **79**, 307–313 (2014).

176. Y.K. Lim, S.; Haque, M. M.; Nam, G.; Ryoo, N.; Rhim, H. . & K. Monitoring of intracellular tau aggregation regulated by OGA/OGT inhibitors. *Int. J. Mol. Sci.* **16**, 20212–20224 (2015).

177. Hastings, N. B. *et al.* Inhibition of O-GlcNAcase leads to elevation of O-GlcNAc tau and reduction of tauopathy and cerebrospinal fluid tau in rTg4510 mice. *Mol. Neurodegener.* **12**, (2017).

178. Frisardi, V. *et al.* Metabolic-cognitive syndrome: A cross-talk between metabolic syndrome and Alzheimer's disease. *Ageing Research Reviews* (2010). doi:10.1016/j.arr.2010.04.007

179. Solfrizzi, V. *et al.* Lifestyle-related factors in predementia and dementia syndromes. *Expert Review of Neurotherapeutics* (2008). doi:10.1586/14737175.8.1.133

180. Biessels, G. J., Staekenborg, S., Brunner, E., Brayne, C. & Scheltens, P. Risk of dementia in diabetes mellitus: A systematic review. *Lancet Neurology* (2006). doi:10.1016/S1474-4422(05)70284-2

181. Van Der Flier, W. M. & Scheltens, P. Epidemiology and risk factors of dementia. *Neurology in Practice* (2005). doi:10.1136/jnnp.2005.082867

182. Janson, J. *et al.* Increased Risk of Type 2 Diabetes in Alzheimer Disease. *Diabetes* (2004). doi:10.2337/diabetes.53.2.474

183. Koekkoek, P. S., Kappelle, L. J., van den Berg, E., Rutten, G. E. H. M. & Biessels, G. J. Cognitive function in patients with diabetes mellitus: Guidance for daily care. *The Lancet Neurology* (2015). doi:10.1016/S1474-4422(14)70249-2

184. Haroon, N. N. *et al.* Risk of dementia in seniors with newly diagnosed diabetes: A Population-Based study. *Diabetes Care* (2015). doi:10.2337/dc15-

185. Crane, P. K. *et al.* Glucose levels and risk of dementia. *N. Engl. J. Med.* (2013). doi:10.1056/NEJMoa1215740

186. Beydoun, M. A., Beydoun, H. A. & Wang, Y. Obesity and central obesity as risk factors for incident dementia and its subtypes: A systematic review and meta-analysis. *Obesity Reviews* (2008). doi:10.1111/j.1467-789X.2008.00473.x

187. Whitmer, R. A., Gunderson, E. P., Barrett-Connor, E., Quesenberry, C. P. & Yaffe, K. Obesity in middle age and future risk of dementia: A 27 year longitudinal population based study. *Br. Med. J.* (2005). doi:10.1136/bmj.38446.466238.E0

188. Hassing, L. B. *et al.* Overweight in midlife and risk of dementia: A 40-year follow-up study. *Int. J. Obes.* (2009). doi:10.1038/ijo.2009.104

189. Hassing, L. B., Dahl, A. K., Pedersen, N. L. & Johansson, B. Overweight in midlife is related to lower cognitive function 30 years later: A prospective study with longitudinal assessments. *Dement. Geriatr. Cogn. Disord.* (2010). doi:10.1159/000314874

190. Whitmer, R. A. *et al.* Central obesity and increased risk of dementia more than three decades later. *Neurology* (2008). doi:10.1212/01.wnl.0000306313.89165.ef

191. Jagust, W., Harvey, D., Mungas, D. & Haan, M. Central obesity and the aging brain. *Arch. Neurol.* (2005). doi:10.1001/archneur.62.10.1545

192. Molteni, R. *et al.* Exercise reverses the harmful effects of consumption of a high-fat diet on synaptic and behavioral plasticity associated to the action of brain-derived neurotrophic factor. *Neuroscience* (2004). doi:10.1016/j.neuroscience.2003.09.020

193. Noble, E. E. & Kanoski, S. E. Early life exposure to obesogenic diets and learning and memory dysfunction. *Current Opinion in Behavioral Sciences* (2016). doi:10.1016/j.cobeha.2015.11.014

194. Alzoubi, K. H., Mayyas, F. A., Mahafzah, R. & Khabour, O. F. Melatonin prevents memory impairment induced by high-fat diet: Role of oxidative stress. *Behav. Brain Res.* (2018). doi:10.1016/j.bbr.2017.08.047

195. Heydemann, A. An Overview of Murine High Fat Diet as a Model for Type 2 Diabetes Mellitus. *Journal of Diabetes Research* (2016). doi:10.1155/2016/2902351

196. McLean, F. H. *et al.* Rapid and reversible impairment of episodic memory by

a high-fat diet in mice. *Sci. Rep.* (2018). doi:10.1038/s41598-018-30265-4

197. Cordner, Z. A. & Tamashiro, K. L. K. Effects of high-fat diet exposure on learning & memory. *Physiology and Behavior* (2015). doi:10.1016/j.physbeh.2015.06.008

198. Sivanathan, S., Thavartnam, K., Arif, S., Elegino, T. & McGowan, P. O. Chronic high fat feeding increases anxiety-like behaviour and reduces transcript abundance of glucocorticoid signalling genes in the hippocampus of female rats. *Behav. Brain Res.* (2015). doi:10.1016/j.bbr.2015.02.036

199. Zemdegs, J. *et al.* High-fat diet-induced metabolic disorders impairs 5-HT function and anxiety-like behavior in mice. *Br. J. Pharmacol.* (2016). doi:10.1111/bph.13343

200. Beilharz, J. E., Maniam, J. & Morris, M. J. Short exposure to a diet rich in both fat and sugar or sugar alone impairs place, but not object recognition memory in rats. *Brain. Behav. Immun.* (2014). doi:10.1016/j.bbi.2013.11.016

201. Davidson, T. L. *et al.* The effects of a high-energy diet on hippocampal-dependent discrimination performance and blood-brain barrier integrity differ for diet-induced obese and diet-resistant rats. *Physiol. Behav.* (2012). doi:10.1016/j.physbeh.2012.05.015

202. Molteni, R., Barnard, R. J., Ying, Z., Roberts, C. K. & Gómez-Pinilla, F. A high-fat, refined sugar diet reduces hippocampal brain-derived neurotrophic factor, neuronal plasticity, and learning. *Neuroscience* (2002). doi:10.1016/S0306-4522(02)00123-9

203. Miotto, P. M., LeBlanc, P. J. & Holloway, G. P. High-fat diet causes mitochondrial dysfunction as a result of impaired ADP sensitivity. *Diabetes* (2018). doi:10.2337/db18-0417

204. Wu, H. W., Ren, L. F., Zhou, X. & Han, D. W. A high-fructose diet induces hippocampal insulin resistance and exacerbates memory deficits in male Sprague-Dawley rats. *Nutr. Neurosci.* (2015). doi:10.1179/1476830514Y.0000000133

205. Calvo-Ochoa, E., Hernández-Ortega, K., Ferrera, P., Morimoto, S. & Arias, C. Short-term high-fat-and-fructose feeding produces insulin signaling alterations accompanied by neurite and synaptic reduction and astroglial activation in the rat hippocampus. *J. Cereb. Blood Flow Metab.* (2014). doi:10.1038/jcbfm.2014.48

206. Woodie, L. & Blythe, S. The differential effects of high-fat and high-fructose diets on physiology and behavior in male rats. *Nutr. Neurosci.* (2018). doi:10.1080/1028415X.2017.1287834

207. Greenwood, C. E. & Winocur, G. High-fat diets, insulin resistance and declining cognitive function. in *Neurobiology of Aging* (2005). doi:10.1016/j.neurobiolaging.2005.08.017

208. Kothari, V. *et al.* High fat diet induces brain insulin resistance and cognitive impairment in mice. *Biochim. Biophys. Acta - Mol. Basis Dis.* (2017). doi:10.1016/j.bbadis.2016.10.006

209. Gerozissis, K. Brain insulin, energy and glucose homeostasis; genes, environment and metabolic pathologies. *European Journal of Pharmacology* (2008). doi:10.1016/j.ejphar.2008.01.050

210. Cavaliere, G. *et al.* High-Fat Diet Induces Neuroinflammation and Mitochondrial Impairment in Mice Cerebral Cortex and Synaptic Fraction. *Front. Cell. Neurosci.* (2019). doi:10.3389/fncel.2019.00509

211. Yang, Y. *et al.* O-GlcNAc transferase inhibits visceral fat lipolysis and promotes diet-induced obesity. *Nat. Commun.* (2020). doi:10.1038/s41467-019-13914-8

212. M.a., J. & Hart, G. W. Protein O-GlcNAcylation in diabetes and diabetic complications. *Expert Review of Proteomics* (2013). doi:10.1586/14789450.2013.820536

213. Park, K., Saudek, C. D. & Hart, G. W. Increased expression of β-N-acetylglucosaminidase in erythrocytes from individuals with pre-diabetes and diabetes. *Diabetes* (2010). doi:10.2337/db09-1086

214. Myslicki, J. P., Belke, D. D. & Shearer, J. Role of O-GlcNAcylation in nutritional sensing, insulin resistance and in mediating the benefits of exercise. *Applied Physiology, Nutrition and Metabolism* (2014). doi:10.1139/apnm-2014-0122

215. Whelan, S. A.; Dias, W. B.; Thiruneelakantapillai, L.; Lane, M. D.; and Hart, G. W. Regulation of insulin receptor substrate 1 (IRS-1)/AKT kinase-mediated insulin signaling by O-Linked beta-N-acetylglucosamine in 3T3-L1 adipocytes. *J. Biol. Chem.* **285**, 5204–5211 (2010).

216. Park, S. Y., Ryu, J. & Lee, W. O-GlcNAc modification on IRS-1 and Akt2 by PUGNAc inhibits their phosphorylation and induces insulin resistance in rat primary adipocytes. *Exp. Mol. Med.* (2005). doi:10.1038/emm.2005.30

217. Vosseller, K., Wells, L., Lane, M. D. & Hart, G. W. Elevated nucleocytoplasmic glycosylation by O-GlcNAc results in insulin resistance associated with defects in Akt activation in 3T3-L1 adipocytes. *Proc. Natl. Acad. Sci. U. S. A.* (2002). doi:10.1073/pnas.072072399

218. Arias, E. B., Kim, J. & Cartee, G. D. Prolonged Incubation in PUGNAc

Results in Increased Protein O-Linked Glycosylation and Insulin Resistance in Rat Skeletal Muscle. *Diabetes* (2004). doi:10.2337/diabetes.53.4.921

219. Macauley, M. S.; He, Y.; Gloster, T. M.; Stubbs, K. A.; Davies, G. J.; and Vocadlo, D. J. Inhibition of O-GlcNAcase using a potent and cell-permeable inhibitor does not induce insulin resistance in 3T3-L1 adipocytes. *Chem. Biol.* **17**, 937–948 (2010).

220. Jahangir, Z.; Ahmad, W.; and Shabbiri, K. Alternate Phosphorylation/O-GlcNAc modification on human insulin IRSs: a road towards impaired insulin signaling in alzheimer and diabetes. *Adv. Bioinform.* (2014).

221. Liu, F., Iqbal, K., Grundke-Iqbal, I., Hart, G. W. & Gong, C. X. O-GlcNAcylation regulates phosphorylation of tau: a mechanism involved in Alzheimer's disease. *Proc Natl Acad Sci U S A* **101**, 10804–10809 (2004).

222. Park, J., Lai, M. K. P., Arumugam, T. V. & Jo, D. G. O-GlcNAcylation as a Therapeutic Target for Alzheimer's Disease. *NeuroMolecular Medicine* (2020). doi:10.1007/s12017-019-08584-0

223. Zhu, Y. *et al.* Pharmacological Inhibition of O-GlcNAcase Enhances Autophagy in Brain through an mTOR-Independent Pathway. *ACS Chem Neurosci* **9**, 1366–1379 (2018).

224. Reinholdt, L. G. *et al.* Molecular characterization of the translocation breakpoints in the Down syndrome mouse model Ts65Dn. *Mamm. Genome* **22**, 685–691 (2011).

225. Yuzwa, S. A. *et al.* A potent mechanism-inspired O-GlcNAcase inhibitor that blocks phosphorylation of tau in vivo. *Nat. Chem. Biol.* (2008). doi:10.1038/nchembio.96

226. Ghatak, A. & Combs, C. K. Iba1 immunoreactivity is enhanced following an antigen retrieval treatment with EDTA, pH 6.0. *MethodsX* **1**, 269–274 (2014).

227. Zachara, N. E., Vosseller, K. & Hart, G. W. Detection and analysis of proteins modified by O-linked N-acetylglucosamine. *Curr Protoc Mol Biol* **Chapter 17**, Unit 17 6 (2011).

228. Hebert Jr., L. F. *et al.* Overexpression of glutamine:fructose-6-phosphate amidotransferase in transgenic mice leads to insulin resistance. *J Clin Invest* **98**, 930–936 (1996).

229. Livak, K. J. & Schmittgen, T. D. Analysis of relative gene expression data using real-time quantitative PCR and the 2(-Delta Delta C(T)) Method. *Methods* **25**, 402–408 (2001).

230. Cassano, T. *et al.* Glutamatergic alterations and mitochondrial impairment in

a murine model of Alzheimer disease. *Neurobiol. Aging* (2012). doi:10.1016/j.neurobiolaging.2011.09.021

231. Bellanti, F. *et al.* Many faces of mitochondrial uncoupling during age: Damage or defense? *Journals Gerontol. - Ser. A Biol. Sci. Med. Sci.* (2013). doi:10.1093/gerona/gls332

232. Kuljis, R. O. & Salkovic-Petrisic, M. Dementia, diabetes, Alzheimer's disease, and insulin resistance in the brain: progress, dilemmas, new opportunities, and a hypothesis to tackle intersecting epidemics. *J Alzheimers Dis* **25**, 29–41 (2011).

233. Tramutola, A. *et al.* Proteomic identification of altered protein O-GlcNAcylation in a triple transgenic mouse model of Alzheimer's disease. *Biochim Biophys Acta Mol Basis Dis* **1864**, 3309–3321 (2018).

234. Comer, F. I. & Hart, G. W. O-Glycosylation of nuclear and cytosolic proteins. Dynamic interplay between O-GlcNAc and O-phosphate. *J Biol Chem* **275**, 29179–29182 (2000).

235. Slawson, C. & Hart, G. W. Dynamic interplay between O-GlcNAc and O-phosphate: the sweet side of protein regulation. *Curr Opin Struct Biol* **13**, 631–636 (2003).

236. Kamemura, K., Hayes, B. K., Comer, F. I. & Hart, G. W. Dynamic interplay between O-glycosylation and O-phosphorylation of nucleocytoplasmic proteins: alternative glycosylation/phosphorylation of THR-58, a known mutational hot spot of c-Myc in lymphomas, is regulated by mitogens. *J Biol Chem* **277**, 19229–19235 (2002).

237. Kamemura, K. & Hart, G. W. Dynamic interplay between O-glycosylation and O-phosphorylation of nucleocytoplasmic proteins: a new paradigm for metabolic control of signal transduction and transcription. *Prog Nucleic Acid Res Mol Biol* **73**, 107–136 (2003).

238. Ansari, S. A. & Emerald, B. S. The Role of Insulin Resistance and Protein O-GlcNAcylation in Neurodegeneration. *Front Neurosci* **13**, 473 (2019).

239. Gong, C. X., Liu, F., Grundke-Iqbal, I. & Iqbal, K. Impaired brain glucose metabolism leads to Alzheimer neurofibrillary degeneration through a decrease in tau O-GlcNAcylation. *J Alzheimers Dis* **9**, 1–12 (2006).

240. Kaasik, K. *et al.* Glucose sensor O-GlcNAcylation coordinates with phosphorylation to regulate circadian clock. *Cell Metab* **17**, 291–302 (2013).

241. Dias, W. B. & Hart, G. W. O-GlcNAc modification in diabetes and Alzheimer's disease. *Mol Biosyst* **3**, 766–772 (2007).

242. Liu, K. *et al.* Accumulation of protein O-GlcNAc modification inhibits proteasomes in the brain and coincides with neuronal apoptosis in brain areas with high O-GlcNAc metabolism. *J Neurochem* **89**, 1044–1055 (2004).

243. Tallent, M. K. *et al.* In vivo modulation of O-GlcNAc levels regulates hippocampal synaptic plasticity through interplay with phosphorylation. *J Biol Chem* **284**, 174–181 (2009).

244. Skorobogatko, Y. *et al.* O-linked beta-N-acetylglucosamine (O-GlcNAc) site thr-87 regulates synapsin I localization to synapses and size of the reserve pool of synaptic vesicles. *J Biol Chem* **289**, 3602–3612 (2014).

245. Bolte, S. & Cordelieres, F. P. A guided tour into subcellular colocalization analysis in light microscopy. *J Microsc* **224**, 213–232 (2006).

246. Butkinaree, C., Park, K. & Hart, G. W. O-linked beta-N-acetylglucosamine (O-GlcNAc): Extensive crosstalk with phosphorylation to regulate signaling and transcription in response to nutrients and stress. *Biochim Biophys Acta* **1800**, 96–106 (2010).

247. Seo, H. G. *et al.* Identification of the nuclear localisation signal of O-GlcNAc transferase and its nuclear import regulation. *Sci Rep* **6**, 34614 (2016).

248. Bourre, G. *et al.* Direct Crosstalk Between O-GlcNAcylation and Phosphorylation of Tau Protein Investigated by NMR Spectroscopy. *Front Endocrinol* **9**, 595 (2018).

249. Wang, A. C., Jensen, E. H., Rexach, J. E., Vinters, H. V & Hsieh-Wilson, L. C. Loss of O-GlcNAc glycosylation in forebrain excitatory neurons induces neurodegeneration. *Proc Natl Acad Sci U S A* **113**, 15120–15125 (2016).

250. Griffith, L. S., Mathes, M. & Schmitz, B. β-Amyloid precursor protein is modified with O-linked N-acetylglucosamine. *J. Neurosci. Res.* (1995). doi:10.1002/jnr.490410214

251. Gross, T. J. *et al.* Plasma metabolites related to cellular energy metabolism are altered in adults with Down syndrome and Alzheimer's disease. *Dev Neurobiol* **79**, 622–638 (2019).

252. Tramutola, A. *et al.* Intranasal rapamycin ameliorates Alzheimer-like cognitive decline in a mouse model of Down syndrome. *Transl Neurodegener* **7**, 28 (2018).

253. Yang, Y. R. *et al.* OGA heterozygosity suppresses intestinal tumorigenesis in Apc min/+ mice. *Oncogenesis* (2014). doi:10.1038/oncsis.2014.24

254. Yang, Y. R. *et al.* Elevated O-GlcNAcylation promotes colonic inflammation and tumorigenesis by modulating NF-kappaB signaling. *Oncotarget* **6**, 12529–

12542 (2015).

255. Zhang, Z., Tan, E. P., VandenHull, N. J., Peterson, K. R. & Slawson, C. O-GlcNAcase Expression is Sensitive to Changes in O-GlcNAc Homeostasis. *Front Endocrinol* **5**, 206 (2014).

256. Chang, K. A. *et al.* Phosphorylation of amyloid precursor protein (APP) at Thr668 regulates the nuclear translocation of the APP intracellular domain and induces neurodegeneration. *Mol Cell Biol* **26**, 4327–4338 (2006).

257. Lee, M. S. *et al.* APP processing is regulated by cytoplasmic phosphorylation. *J Cell Biol* **163**, 83–95 (2003).

258. Rebelo, S. *et al.* Tyr687 dependent APP endocytosis and Abeta production. *J Mol Neurosci* **32**, 1–8 (2007).

259. Yuzwa, S. A., Cheung, A. H., Okon, M., McIntosh, L. P. & Vocadlo, D. J. O-GlcNAc modification of tau directly inhibits its aggregation without perturbing the conformational properties of tau monomers. *J Mol Biol* **426**, 1736–1752 (2014).

260. D. Hamlett, E. *et al.* Cognitive Impairment, Neuroimaging, and Alzheimer Neuropathology in Mouse Models of Down Syndrome. *Curr. Alzheimer Res.* (2015). doi:10.2174/1567205012666150921095505

261. Sansevero, G., Begenisic, T., Mainardi, M. & Sale, A. Experience-dependent reduction of soluble β-amyloid oligomers and rescue of cognitive abilities in middle-age Ts65Dn mice, a model of Down syndrome. *Exp. Neurol.* (2016). doi:10.1016/j.expneurol.2016.06.006

262. Bimonte-Nelson, H. A., Hunter, C. L., Nelson, M. E. & Granholm, A. C. E. Frontal cortex BDNF levels correlate with working memory in an animal model of Down syndrome. *Behav. Brain Res.* (2003). doi:10.1016/S0166-4328(02)00082-7

263. Parrini, M. *et al.* Aerobic exercise and a BDNF-mimetic therapy rescue learning and memory in a mouse model of Down syndrome. *Sci. Rep.* (2017). doi:10.1038/s41598-017-17201-8

264. Mizushima, N., Yoshimori, T. & Levine, B. Methods in mammalian autophagy research. *Cell* **140**, 313–326 (2010).

265. Di Domenico, F. *et al.* Bach1 overexpression in Down syndrome correlates with the alteration of the HO-1/BVR-a system: insights for transition to Alzheimer's disease. *J Alzheimers Dis* **44**, 1107–1120 (2015).

266. Di Domenico, F. *et al.* Restoration of aberrant mTOR signaling by intranasal rapamycin reduces oxidative damage: Focus on HNE-modified proteins in a

mouse model of down syndrome. *Redox Biol* **23**, 101162 (2019).

267. Contreras, A. *et al.* Inhibition of hippocampal long-term potentiation by high-fat diets: Is it related to an effect of palmitic acid involving glycogen synthase kinase-3? *Neuroreport* (2017). doi:10.1097/WNR.0000000000000774

268. Hart, G. W. Nutrient regulation of signaling and transcription. *J Biol Chem* **294**, 2211–2231 (2019).

269. Wang, Z., Gucek, M. & Hart, G. W. Cross-talk between GlcNAcylation and phosphorylation: Site-specific phosphorylation dynamics in response to globally elevated O-GlcNAc. *Proc. Natl. Acad. Sci. U. S. A.* (2008). doi:10.1073/pnas.0806216105

270. Hawkins, M. *et al.* Role of the glucosamine pathway in fat-induced insulin resistance. *J. Clin. Invest.* (1997). doi:10.1172/JCI119390

271. Scott, J. W. & Oakhill, J. S. The sweet side of AMPK signaling: regulation of GFAT1. *Biochem J* **474**, 1289–1292 (2017).

272. Zibrova, D. *et al.* GFAT1 phosphorylation by AMPK promotes VEGF-induced angiogenesis. *Biochem J* **474**, 983–1001 (2017).

273. Albensi, B. C. Dysfunction of mitochondria: Implications for Alzheimer's disease. in *International Review of Neurobiology* (2019). doi:10.1016/bs.irn.2019.03.001

274. Chen, D., Li, X., Zhang, L. T., Zhu, M. & Gao, L. A high-fat diet impairs mitochondrial biogenesis, mitochondrial dynamics, and the respiratory chain complex in rat myocardial tissues. *J. Cell. Biochem.* (2018). doi:10.1002/jcb.27068

275. Wheatley, E. G. *et al.* Neuronal O-GlcNAcylation Improves Cognitive Function in the Aged Mouse Brain. *Curr Biol* **29**, 3359-3369 e4 (2019).

276. Gatta, E. *et al.* Evidence for an imbalance between tau O-GlcNAcylation and phosphorylation in the hippocampus of a mouse model of Alzheimer's disease. *Pharmacol Res* **105**, 186–197 (2016).

277. Ma, Z., Vocadlo, D. J. & Vosseller, K. Hyper-O-GlcNAcylation is anti-apoptotic and maintains constitutive NF-kappaB activity in pancreatic cancer cells. *J Biol Chem* **288**, 15121–15130 (2013).

278. Ferrer, C. M. *et al.* O-GlcNAcylation regulates cancer metabolism and survival stress signaling via regulation of the HIF-1 pathway. *Mol Cell* **54**, 820–831 (2014).

279. Tramutola, A. *et al.* Brain insulin resistance triggers early onset Alzheimer disease in Down syndrome. *Neurobiol Dis* **137**, 104772 (2020).

280. Copps, K. D. & White, M. F. Regulation of insulin sensitivity by serine/threonine phosphorylation of insulin receptor substrate proteins IRS1 and IRS2. *Diabetologia* **55**, 2565–2582 (2012).

281. Perluigi, M. *et al.* Neuropathological role of PI3K/Akt/mTOR axis in Down syndrome brain. *Biochim Biophys Acta.* **1842**, 1144–1153 (2014).

282. Dos Santos, J. P. A., Vizuete, A., Hansen, F., Biasibetti, R. & Goncalves, C. A. Early and Persistent O-GlcNAc Protein Modification in the Streptozotocin Model of Alzheimer's Disease. *J Alzheimers Dis* **61**, 237–249 (2018).

283. Yu, Y. *et al.* Differential effects of an O-GlcNAcase inhibitor on tau phosphorylation. *PLoS One* **7**, e35277 (2012).

284. Morino, K. & Maegawa, H. Role of O-GlcNAcylation in the Homeostasis of Metabolic Organs and its Potential Links with Diabetes and its Complications. *J Diabetes Investig* (2020). doi:10.1111/jdi.13359

285. Smet-Nocca, C. *et al.* Identification of O-GlcNAc sites within peptides of the Tau protein and their impact on phosphorylation. *Mol Biosyst* **7**, 1420–1429 (2011).

286. Lemere, C. A. *et al.* Sequence of deposition of heterogeneous amyloid beta-peptides and APO E in Down syndrome: implications for initial events in amyloid plaque formation. *Neurobiol Dis* **3**, 16–32 (1996).

287. Head, E., Helman, A. M., Powell, D. & Schmitt, F. A. Down syndrome, beta-amyloid and neuroimaging. *Free Radic Biol Med* **114**, 102–109 (2018).

288. Di Domenico, F. *et al.* Impairment of proteostasis network in Down syndrome prior to the development of Alzheimer's disease neuropathology: redox proteomics analysis of human brain. *Biochim Biophys Acta* **1832**, 1249–1259 (2013).

289. Tramutola, A. *et al.* Polyubiquitinylation Profile in Down Syndrome Brain Before and After the Development of Alzheimer Neuropathology. *Antioxid Redox Signal* **26**, 280–298 (2017).

290. Rahman, M. A., Hwang, H., Cho, Y. & Rhim, H. Modulation of O-GlcNAcylation Regulates Autophagy in Cortical Astrocytes. *Oxid Med Cell Longev* **2019**, 6279313 (2019).

291. Guo, B. *et al.* O-GlcNAc-modification of SNAP-29 regulates autophagosome maturation. *Nat Cell Biol* **16**, 1215–1226 (2014).

292. Jo, Y. K. *et al.* O-GlcNAcylation of ATG4B positively regulates autophagy by increasing its hydroxylase activity. *Oncotarget* **7**, 57186–57196 (2016).

293. Ozcelik, S. *et al.* Rapamycin attenuates the progression of tau pathology in

P301S tau transgenic mice. *PLoS One* **8**, e62459 (2013).

294. Schaeffer, V. *et al.* Stimulation of autophagy reduces neurodegeneration in a mouse model of human tauopathy. *Brain* **135**, 2169–2177 (2012).

295. Li, L. *et al.* Autophagy enhancer carbamazepine alleviates memory deficits and cerebral amyloid-beta pathology in a mouse model of Alzheimer's disease. *Curr Alzheimer Res* **10**, 433–441 (2013).

296. Ducheix, S., Magré, J., Cariou, B. & Prieur, X. Chronic O-GlcNAcylation and diabetic cardiomyopathy: The bitterness of glucose. *Frontiers in Endocrinology* (2018). doi:10.3389/fendo.2018.00642

297. Tan, E. P. *et al.* Sustained O-GlcNAcylation reprograms mitochondrial function to regulate energy metabolism. *J. Biol. Chem.* (2017). doi:10.1074/jbc.M117.797944

298. Pinho, T. S., Correia, S. C., Perry, G., Ambrósio, A. F. & Moreira, P. I. Diminished O-GlcNAcylation in Alzheimer's disease is strongly correlated with mitochondrial anomalies. *Biochim. Biophys. Acta - Mol. Basis Dis.* (2019). doi:10.1016/j.bbadis.2018.10.037

APPENDIX

Appendix A

Neurotherapeutics
https://doi.org/10.1007/s13311-020-00978-4

ORIGINAL ARTICLE

The Dysregulation of OGT/OGA Cycle Mediates Tau and APP Neuropathology in Down Syndrome

Ilaria Zuliani[1] · Chiara Lanzillotta[1] · Antonella Tramutola[1] · Antonio Francioso[1] · Sara Pagnotta[1] · Eugenio Barone[1] · Marzia Perluigi[1] · Fabio Di Domenico[1]

Accepted: 18 November 2020

Abstract
Protein O-GlcNAcylation is a nutrient-related post-translational modification that, since its discovery some 30 years ago, has been associated with the development of neurodegenerative diseases. As reported in Alzheimer's disease (AD), flaws in the cerebral glucose uptake translate into reduced hexosamine biosynthetic pathway flux and subsequently lead to aberrant protein O-GlcNAcylation. Notably, the reduction of O-GlcNAcylated proteins involves also tau and APP, thus promoting their aberrant phosphorylation in AD brain and the onset of AD pathological markers. Down syndrome (DS) individuals are characterized by the early development of AD by the age of 60 and, although the two conditions present the same pathological hallmarks and share the alteration of many molecular mechanisms driving brain degeneration, no evidence has been sought on the implication of O-GlcNAcylation in DS pathology. Our study aimed to unravel for the first time the role of protein O-GlcNacylation in DS brain alterations positing the attention of potential trisomy-related mechanisms triggering the aberrant regulation of OGT/OGA cycle. We demonstrate the disruption of O-GlcNAcylation homeostasis, as an effect of altered OGT and OGA regulatory mechanism, and confirm the relevance of O-GlcNAcylation in the appearance of AD hallmarks in the brain of a murine model of DS. Furthermore, we provide evidence for the neuroprotective effects of brain-targeted OGA inhibition. Indeed, the rescue of OGA activity was able to restore protein O-GlcNAcylation, and reduce AD-related hallmarks and decreased protein nitration, possibly as effect of induced autophagy.

Key Words O-GlcNAcylation · Down syndrome · OGT/OGA · APP · tau · autophagy

Introduction

Down syndrome (DS; Trisomy 21) is the most common chromosomal disorder and the most frequent genetic cause of intellectual disability affecting about 6 million people worldwide [1, 2]. Because of the advances in health care and management of co-occurring illnesses, the life expectancy of people with DS has largely improved [3, 4]. The triplication of genes on chromosome 21 and of their products can alter diverse pathways, including those involved with brain development, metabolism, and neuronal networks [5, 6]. Individuals with DS are also more likely to develop certain pathological conditions, including hypothyroidism, autoimmune diseases, epilepsy, hematological disorders, and Alzheimer-like dementia [7]. The clinical manifestation of Alzheimer-like dementia in DS resembles that occurring in the general population [8, 9], with slight differences in early presentation [10]. Nearly all individuals with full trisomy 21 aged 40 and older are found to have typical signs of Alzheimer's disease (AD) neuropathology, including extracellular amyloid plaques and intracellular neurofibrillary tangles [11]. The extra copy of amyloid precursor protein (APP) gene on chromosome 21 is associated with a 4- to 5-fold overexpression of APP that leads to an early onset and rapid accumulation of β-amyloid protein (Aβ) with age [9, 12]. Cortical deposits of Aβ 1-42 have even been discovered as early as at 12 years of age [13]. Triplication of specific kinases (e.g., DYRK-1) interacting with APP and tau represents a further link between gene imbalance and neuropathological features DS [14]. Furthermore, brain hypoglycemia and insulin resistance are emerging as common mechanisms of neurodegeneration in DS and AD [15–17]. Several

✉ Fabio Di Domenico
fabio.didomenico@uniroma1.it

[1] Department of Biochemical Sciences "A. Rossi Fanelli", Laboratory affiliated to Istituto Pasteur Italia-Fondazione Cenci Bolognetti, Sapienza University of Rome, P.le Aldo Moro 5, 00185 Rome, Italy

Published online: 30 November 2020

Appendix B

ARTICLE IN PRESS

Progress in Neurobiology xxx (xxxx) xxxx

Contents lists available at ScienceDirect

Progress in Neurobiology

journal homepage: www.elsevier.com/locate/pneurobio

Original Research Article

Chronic PERK induction promotes Alzheimer-like neuropathology in Down syndrome: Insights for therapeutic intervention

Chiara Lanzillotta[a], Ilaria Zuliani[a], Antonella Tramutola[a], Eugenio Barone[a], Carla Blarzino[a], Valentina Folgiero[b], Matteo Caforio[a,b], Diletta Valentini[c], Alberto Villani[c], Franco Locatelli[b,d], D. Allan Butterfield[e,f], Elizabeth Head[g], Marzia Perluigi[a], Jose F. Abisambra[h], Fabio Di Domenico[a,*]

[a] Department of Biochemical Sciences "A. Rossi Fanelli", Laboratory affiliated to Istituto Pasteur Italia-Fondazione Cenci Bolognetti, Sapienza University of Rome, Rome, Italy
[b] Department of Pediatric Hematology/Oncology and of Cell and Gene Therapy, Bambino Gesù Children's Hospital, Rome, Italy
[c] Pediatric and Infectious Disease Unit, Bambino Gesù Children's Hospital, Rome, Italy
[d] Department of Pediatrics, Sapienza University of Rome, Rome, Italy
[e] Department of Chemistry, University of Kentucky, Lexington, KY, USA
[f] Sanders-Brown Center on Aging, University of Kentucky, Lexington, KY, USA
[g] Department of Pathology & Laboratory Medicine, University of California, Irvine, CA, USA
[h] Department of Neuroscience and Center for Translational Research in Neurodegenerative Disease, University of Florida, Gainesville, FL, USA

ARTICLE INFO

Keywords:
Unfolded protein response
Down syndrome
PERK
Protein translation
Nrf2

ABSTRACT

A major challenge in neurobiology is the identification of the mechanisms by which protein misfolding leads to cellular toxicity. Many neurodegenerative disorders, in which aberrant protein conformers aggregate into pathological inclusions, present the chronic activation of the PERK branch of the unfolded protein response. The adaptive effects of the PERK pathway include reduction of translation by transient inhibition of eIF2α and antioxidant protein production via induction of Nrf2 transcription factor. In contrast, PERK prolonged activation leads to sustained reduction in protein synthesis and induction of cell death pathways. To further investigate the role of the PERK pathway in neurodegenerative disorders, we focused on Down syndrome (DS), in which aging confers a high risk of Alzheimer disease (AD). By investigating human DS frontal cortices, we found early and sustained PERK activation associated with the induction of eIF2α and ATF4 downstream signals. We also observed that the Nrf2 response is uncoupled from PERK and its antioxidant effects are repressed in a mechanism implicating the transcription repressor Bach1. The pharmacological inhibition of PERK in DS mice reduced eIF2α-related translational repression and promoted Nrf2 nuclear translocation, favoring the rescue of Nrf2/Bach1 imbalance. The further analysis of peripheral cells from living DS individuals provided strong support of the pathological link between PERK and trisomy 21. Our results suggest that failure to regulate the PERK pathway is a peculiar characteristic of DS pathology and it may represent an essential step to promote cellular dysfunction, which actively contributes in the brain to the early development of AD.

Abbreviations: PERK, protein kinase R (PKR)-like endoplasmic reticulum kinase; DS, Down syndrome; AD, Alzheimer disease; eIF2α, eukariotyc initation factor 2 alpha; UPR, Unfolded Protein Response; Nrf2, Nuclear factor erythroid 2-related factor 2; UPS, ubiquitin proteasome system; OS, Oxidative stress; AOR, antioxidant response; ER, endoplasmic reticulum; IRE1, Inositol-requiring enzyme 1; ATF6, activating transcription factor 6; BiP-GRP78, Binding immunoglobulin; PKR, protein kinase RNA; ISR, integrated stress response; ARE, antioxidant response element; DSy, Down syndrome young; DSo, Down Syndrome old; PBMC, Peripheral blood mononuclear cell; ACK, ammonium-chloride-potassium; LCLs, Lymphoblastoid cell lines; Thp, thapsigargin; GADD34, growth arrest and DNA damage-inducible protein; SDS, sodium dodecyl sulphate; ATF4, Activating Transcription Factor 4; mTORC1, mammalian target of rapamycin complex 1; rpS6, ribosomal protein S6; HO-1, Heme oxygenase 1; NQO1, NAD(P)H dehydrogenase [quinone] 1; HNE, 4-hydroxy-2-nonenal adducts; 3-NT, 3-nitrotyrosine; APP, amyloid precursor protein; Aβ, amyloid beta peptide; Chr21, chromosome 21; CNS, central nervous system; DDIT3, DNA-Damage-Inducible Transcript; GSK3β, glycogen synthase kinase 3B; AMPK, 5′ AMP-activated protein kinase; PI3K, Phosphoinositide 3-kinases

* Corresponding author at: Department of Biochemical Sciences, Sapienza University of Rome, P. le Aldo Moro 5, Rome, 00185, Italy.
E-mail address: fabio.didomenico@uniroma1.it (F. Di Domenico).

https://doi.org/10.1016/j.pneurobio.2020.101892
Received 18 March 2020; Received in revised form 30 June 2020; Accepted 2 August 2020

Please cite this article as: Chiara Lanzillotta, et al., Progress in Neurobiology, https://doi.org/10.1016/j.pneurobio.2020.101892

Appendix C

antioxidants

MDPI

Article

BVR-A Deficiency Leads to Autophagy Impairment through the Dysregulation of AMPK/mTOR Axis in the Brain—Implications for Neurodegeneration

Chiara Lanzillotta [1], Ilaria Zuliani [1], Chirag Vasavda [2], Solomon H. Snyder [2,3,4], Bindu D. Paul [2], Marzia Perluigi [1], Fabio Di Domenico [1,*] and Eugenio Barone [1,*]

[1] Department of Biochemical Sciences "A. Rossi-Fanelli", Sapienza University of Rome, 00185 Rome, Italy; chiara.lanzillotta@uniroma1.it (C.L.); ilaria.zuliani@uniroma1.it (I.Z.); marzia.perluigi@uniroma1.it (M.P.)

[2] The Solomon H. Snyder Department of Neuroscience, Johns Hopkins University School of Medicine, Baltimore, 21205 MD, USA; cvasavda@jhmi.edu (C.V.); ssnyder@jhmi.edu (S.H.S.); bpaul8@jhmi.edu (B.D.P.)

[3] Department of Psychiatry and Behavioral Sciences, Johns Hopkins University School of Medicine, Baltimore, 21205 MD, USA

[4] Department of Pharmacology and Molecular Sciences, Johns Hopkins University School of Medicine, Baltimore, 21205 MD, USA

* Correspondence: fabio.didomenico@uniroma1.it (F.D.D.); eugenio.barone@uniroma1.it (E.B.)

Received: 30 June 2020; Accepted: 23 July 2020; Published: 27 July 2020

Abstract: Biliverdin reductase-A (BVR-A) impairment is associated with increased accumulation of oxidatively-damaged proteins along with the impairment of autophagy in the brain during neurodegenerative disorders. Reduced autophagy inhibits the clearance of misfolded proteins, which then form neurotoxic aggregates promoting neuronal death. The aim of our study was to clarify the role for BVR-A in the regulation of the mTOR/autophagy axis by evaluating age-associated changes (2, 6 and 11 months) in cerebral cortex samples collected from BVR-A knock-out (BVR-A$^{-/-}$) and wild-type (WT) mice. Our results show that BVR-A deficiency leads to the accumulation of oxidatively-damaged proteins along with mTOR hyper-activation in the cortex. This process starts in juvenile mice and persists with aging. mTOR hyper-activation is associated with the impairment of autophagy as highlighted by reduced levels of Beclin-1, LC3β, LC3II/I ratio, Atg5–Atg12 complex and Atg7 in the cortex of BVR-A$^{-/-}$ mice. Furthermore, we have identified the dysregulation of AMP-activated protein kinase (AMPK) as a critical event driving mTOR hyper-activation in the absence of BVR-A. Overall, our results suggest that BVR-A is a new player in the regulation of autophagy, which may be targeted to arrive at novel therapeutics for diseases involving impaired autophagy.

Keywords: AMPK; autophagy; biliverdin reductase; mTOR; neurodegeneration; oxidative stress

1. Introduction

Biliverdin reductase (BVR) is an evolutionarily conserved and ubiquitously expressed enzyme involved in the heme degradation pathway. During its catabolism, heme is initially converted by heme oxygenase (HO) to biliverdin, which is then reduced to bilirubin through the action of BVR [1,2]. Two different isoforms of BVR were detected in humans and named BVR-A and BVR-B [3]. Although both isozymes catalyze the reduction of biliverdin, BVR-A selectively reduces biliverdin IXα to bilirubin IXα, one of the strongest endogenous antioxidants [3,4]. For that reason, BVR-A has

Appendix D

Journal of *Clinical Medicine*

MDPI

Article

The Anti-Diabetic Drug Metformin Rescues Aberrant Mitochondrial Activity and Restrains Oxidative Stress in a Female Mouse Model of Rett Syndrome

Ilaria Zuliani [1], Chiara Urbinati [2], Daniela Valenti [3], Maria Cristina Quattrini [4], Vanessa Medici [2], Livia Cosentino [2], Donatella Pietraforte [4], Fabio Di Domenico [1], Marzia Perluigi [1], Rosa Anna Vacca [3] and Bianca De Filippis [2,*]

1 Department of Biochemical Sciences, Sapienza University of Rome, 00185 Rome, Italy; ilaria.zuliani@uniroma1.it (I.Z.); fabio.didomenico@uniroma1.it (F.D.D.); marzia.perluigi@uniroma1.it (M.P.)
2 Center for Behavioral Sciences and Mental Health, Istituto Superiore di Sanità, 00161 Rome, Italy; chiara.urbinati@iss.it (C.U.); vanessamedici3@gmail.com (V.M.); livia.cosentino@iss.it (L.C.)
3 Institute of Biomembranes, Bioenergetics and Molecular Biotechnologies, National Council of Research, 70126 Bari, Italy; d.valenti@ibbe.cnr.it (D.V.); r.vacca@ibiom.cnr.it (R.A.V.)
4 Core Facilities, Istituto Superiore di Sanità, 00161 Rome, Italy; mariacristina.quattrini@iss.it (M.C.Q.); donatella.pietraforte@iss.it (D.P.)
* Correspondence: bianca.defilippis@iss.it

Received: 28 April 2020; Accepted: 28 May 2020; Published: 1 June 2020

check for updates

Abstract: Metformin is the first-line therapy for diabetes, even in children, and a promising attractive candidate for drug repurposing. Mitochondria are emerging as crucial targets of metformin action both in the periphery and in the brain. The present study evaluated whether treatment with metformin may rescue brain mitochondrial alterations and contrast the increased oxidative stress in a validated mouse model of Rett syndrome (RTT), a rare neurologic disorder of monogenic origin characterized by severe behavioral and physiological symptoms. No cure for RTT is available. In fully symptomatic RTT mice (12 months old MeCP2-308 heterozygous female mice), systemic treatment with metformin (100 mg/kg ip for 10 days) normalized the reduced mitochondrial ATP production and ATP levels in the whole-brain, reduced brain oxidative damage, and rescued the increased production of reactive oxidizing species in blood. A 10-day long treatment with metformin also boosted pathways related to mitochondrial biogenesis and antioxidant defense in the brain of metformin-treated RTT mice. This treatment regimen did not improve general health status and motor dysfunction in RTT mice at an advanced stage of the disease. Present results provide evidence that systemic treatment with metformin may represent a novel, repurposable therapeutic strategy for RTT.

Keywords: Rett syndrome; metformin; repurposing; PGC-1α; Nrf2

1. Introduction

Metformin is the most widely prescribed treatment for hyperglycemia and type 2 diabetes, even in pediatric patients [1,2]. It belongs to the class of biguanides and acts as a blood glucose-lowering agent by decreasing hepatic gluconeogenesis and improving insulin sensitivity. While metformin has been used to treat diabetes for over 60 years, recent evidences open up the possibility that this clinically approved drug may be repurposed for several other conditions, such as cancer, cardiovascular disorders, neurodegenerative diseases [3], and more recently, neurodevelopmental disorders characterized by intellectual disability [4,5]. Moreover, treatment with metformin was demonstrated to counteract the deleterious effects of aging and provide beneficial effects on mouse healthspan and lifespan [6].

Appendix E

EXPERT REVIEW OF PROTEOMICS
https://doi.org/10.1080/14789450.2019.1691919

Taylor & Francis
Taylor & Francis Group

REVIEW

Check for updates

Shining a light on defective autophagy by proteomics approaches: implications for neurodegenerative illnesses

Fabio Di Domenico, Ilaria Zuliani and Antonella Tramutola

Department of Biochemical Sciences "A. Rossi Fanelli", Sapienza University of Rome, Rome, Italy

ABSTRACT

Introduction: Autophagy is one of the most conserved clearance systems through which eukaryotes manage to handle dysfunctional and excess organelles and macromolecules. This catabolic process has not only a role in the maintenance of basal turnover of cellular components, but it is also essential in cells adaptation to stress conditions. In the last decades, defects in autophagic machinery have been identified as a feature in neurodegenerative diseases. In this context, mass spectrometry-based proteomics has become an important tool in the comprehensive analysis of proteins involved in the autophagic flux.

Area covered: In this review, we discuss recent contributions of proteomic techniques in the study of defective autophagy related to neurodegenerative illness. Particular emphasis is given to the identification of i) shared autophagic markers between different disorders, which support common pathological mechanisms; ii) unique autophagic signature, which could aid to discriminate among diseases.

Expert opinion: Proteomic approaches are valuable in the identification of alterations of components to the autophagic process at different steps of the process. The investigation of autophagic defects associated with neurological disorders is crucial in order to unravel all the potential mechanism leading to neurodegeneration and propose effective therapeutic strategies targeting autophagy.

ARTICLE HISTORY
Received 25 June 2019
Accepted 8 November 2019

KEYWORDS
Autophagy; proteomics; neurodegenerative diseases

1. Introduction

Neurodegenerative disorders such as Alzheimer disease (AD), Parkinson disease (PD), or Huntington disease (HD) are a heterogeneous group of pathologies affecting the nervous system with different etiologies. Some are hereditary, some are secondary to toxic or metabolic processes or both aspects are possible in each disorder. Neuropathologically, these neurodegenerative disorders are characterized by abnormalities of relatively specific regions of the brain and specific populations of neurons. During neurodegeneration, the brain undergoes both morphological and functional modifications affecting dendritic arborization, synapses, neurotransmission, circulation, and metabolism that are reflected in the alteration of motor and sensory systems, sleep, memory, and learning [1]. Mechanisms leading to neurodegenerations, shared by this group of diseases, comprise mitochondrial dysfunction, increased oxidative stress, increased endoplasmic reticulum (ER) stress, aggregation of specific proteins and increased neuroinflammations [2,3]. Intriguingly, the appearance of one or more detrimental aspects of the diseases, among those reported above, can trigger the others thus establishing a chain of reaction that culminate with neuronal damage and death. Mitochondria is the power station of the cell mainly involved in satisfying the request of adenosine triphosphate (ATP) by oxidative phosphorylation [4]. In addition, mitochondria also regulate other essential cellular functions including synthesis of pyrimidines and purines, synthesis of heme, nitrogen balance regulation through the urea cycle, ketone bodies production, sex hormone production, processing of xenobiotics, redox balancing, and regulation of the apoptotic machinery. The high demand for energy that drives ATP-mediated cellular functions, also generates a significant amount of reactive oxygen species (ROS), whose amounts become highly toxic in disease-related dysfunctional mitochondria [5]. Increased ROS can negatively affect specific components of the cell including nucleic acids, lipids, and proteins [6]. The oxidative modification of proteins might alter their conformation and function, thus inducing mechanisms involved in protein quality control, which may lead to protein repair (unfolded protein response) or to protein degradation (proteasome or autophagy) [7–9]. Such mechanisms are crucial in regulating protein synthesis, folding, and clearance of the neuron, thus maintaining the protein homeostasis (proteostasis). The unfolded protein response (UPR) consists of three independent signaling pathways that work in parallel and are activated upon the accumulation of unfolded proteins inside the ER [10]. The activation of the three arms of UPR lead to the reduction in global protein synthesis, the induction of antioxidant response and the promotion of cell survival and ER-associated degradation of proteins. In contrast, sustained ER stress and prolonged UPR activation can lead to the activation of the apoptotic machinery and ultimately to cell death [11,12]. The ubiquitin-proteasome system (UPS) and autophagy are two main pathways of protein and organelle

CONTACT Fabio Di Domenico fabio.didomenico@uniroma1.it Department of Biochemical Sciences 'A. Rossi Fanelli', Sapienza University of Rome, Rome 00185, Italy

Appendix F

Redox Biology 23 (2019) 101162

Contents lists available at ScienceDirect

Redox Biology

journal homepage: www.elsevier.com/locate/redox

Research Paper

Restoration of aberrant mTOR signaling by intranasal rapamycin reduces oxidative damage: Focus on HNE-modified proteins in a mouse model of down syndrome

Fabio Di Domenico[a], Antonella Tramutola[a], Eugenio Barone[a,b], Chiara Lanzillotta[a], Olivia Defever[a], Andrea Arena[a], Ilaria Zuliani[a], Cesira Foppoli[c], Federica Iavarone[d,e], Federica Vincenzoni[d,e], Massimo Castagnola[f], D. Allan Butterfield[g], Marzia Perluigi[a,*]

[a] Department of Biochemical Sciences, Sapienza University of Rome, Rome, Italy
[b] Universidad Autónoma de Chile, Instituto de Ciencias Biomédicas, Facultad de ciud, Providencia, Santiago, Chile
[c] CNR Institute of Molecular Biology and Pathology, Sapienza University of Rome, Rome, Italy
[d] Istituto di Biochimica e Biochimica Clinica, Università Cattolica del Sacro Cuore, Rome, Italy
[e] Fondazione Policlinico Universitario A. Gemelli, IRCCS, Rome, Italy
[f] Laboratorio di Proteomica e Metabonomica, IRCCS, Fondazione Santa Lucia - Rome and Istituto per la Chimica del Riconoscimento Molecolare, CNR, Rome, Italy
[g] Department of Chemistry and Sanders-Brown Center on Aging, University of Kentucky, Lexington, KY, USA 

ARTICLE INFO

Keywords:
Down syndrome
mTOR
Rapamycin
Oxidative stress
Protein-bound HNE

ABSTRACT

Increasing evidences support the notion that the impairment of intracellular degradative machinery is responsible for the accumulation of oxidized/misfolded proteins that ultimately results in the deposition of protein aggregates. These events are key pathological aspects of "protein misfolding diseases", including Alzheimer disease (AD). Interestingly, Down syndrome (DS) neuropathology shares many features with AD, such as the deposition of both amyloid plaques and neurofibrillary tangles. Studies from our group and others demonstrated, in DS brain, the dysfunction of both proteasome and autophagy degradative systems, coupled with increased oxidative damage. Further, we observed the aberrant increase of mTOR signaling and of its down-stream pathways in both DS brain and in Ts65Dn mice.

Based on these findings, we support the ability of intranasal rapamycin treatment (InRapa) to restore mTOR pathway but also to restrain oxidative stress resulting in the decreased accumulation of lipoxidized proteins. By proteomics approach, we were able to identify specific proteins that showed decreased levels of HNE-modification after InRapa treatment compared with vehicle group. Among MS-identified proteins, we found that reduced oxidation of arginase-1 (ARG-1) and protein phosphatase 2A (PP2A) might play a key role in reducing brain damage associated with synaptic transmission failure and tau hyperphosphorylation. InRapa treatment, by reducing ARG-1 protein-bound HNE levels, rescues its enzyme activity and conceivably contribute to the recovery of arginase-regulated functions. Further, it was shown that PP2A inhibition induces tau hyperphosphorylation and spatial memory deficits. Our data suggest that InRapa was able to rescue PP2A activity as suggested by reduced p-tau levels.

In summary, considering that mTOR pathway is a central hub of multiple intracellular signaling, we propose that InRapa treatment is able to lower the lipoxidation-mediated damage to proteins, thus representing a valuable therapeutic strategy to reduce the early development of AD pathology in DS population.

1. Introduction

An increasing number of studies highlight the involvement of aberrant mTOR signaling in the pathogenesis and progression of neurodegenerative disorders, including Alzheimer Disease (AD) [1,2]. Indeed, mTOR pathway has a prominent role in the central nervous system through the regulation of several intracellular processes, such as, protein synthesis, transcription, autophagy, metabolism, and organelle biogenesis [3,4]. These functions are central for the maintenance of brain homeostasis and to regulate the proliferation of neural stem

* Corresponding author. Department of Biochemical Sciences, Sapienza University of Rome, P.le Aldo Moro 5, Rome, 00185, Italy.
E-mail address: marzia.perluigi@uniroma1.it (M. Perluigi).

https://doi.org/10.1016/j.redox.2019.101162
Received 29 October 2018; Received in revised form 26 February 2019; Accepted 5 March 2019
Available online 09 March 2019

Appendix G

Tramutola et al. Translational Neurodegeneration (2018) 7:28
https://doi.org/10.1186/s40035-018-0133-9

Translational Neurodegeneration

RESEARCH Open Access

Intranasal rapamycin ameliorates Alzheimer-like cognitive decline in a mouse model of Down syndrome

Antonella Tramutola[1†], Chiara Lanzillotta[1†], Eugenio Barone[1,2], Andrea Arena[1], Ilaria Zuliani[1], Luciana Mosca[1], Carla Blarzino[1], D. Allan Butterfield[3], Marzia Perluigi[1*] and Fabio Di Domenico[1*]

Abstract

Background: Down syndrome (DS) individuals, by the age of 40s, are at increased risk to develop Alzheimer-like dementia, with deposition in brain of senile plaques and neurofibrillary tangles. Our laboratory recently demonstrated the disturbance of PI3K/AKT/mTOR axis in DS brain, prior and after the development of Alzheimer Disease (AD). The aberrant modulation of the mTOR signalling in DS and AD age-related cognitive decline affects crucial neuronal pathways, including insulin signaling and autophagy, involved in pathology onset and progression. Within this context, the therapeutic use of mTOR-inhibitors may prevent/attenuate the neurodegenerative phenomena. By our work we aimed to rescue mTOR signalling in DS mice by a novel rapamycin intranasal administration protocol (InRapa) that maximizes brain delivery and reduce systemic side effects.

Methods: Ts65Dn mice were administered with InRapa for 12 weeks, starting at 6 months of age demonstrating, at the end of the treatment by radial arms maze and novel object recognition testing, rescued cognition.

Results: The analysis of mTOR signalling, after InRapa, demonstrated in Ts65Dn mice hippocampus the inhibition of mTOR (reduced to physiological levels), which led, through the rescue of autophagy and insulin signalling, to reduced APP levels, APP processing and APP metabolites production, as well as, to reduced tau hyperphosphorylation. In addition, a reduction of oxidative stress markers was also observed.

Discussion: These findings demonstrate that chronic InRapa administration is able to exert a neuroprotective effect on Ts65Dn hippocampus by reducing AD pathological hallmarks and by restoring protein homeostasis, thus ultimately resulting in improved cognition. Results are discussed in term of a potential novel targeted therapeutic approach to reduce cognitive decline and AD-like neuropathology in DS individuals.

Keywords: mTOR, Autophagy, Rapamycin, Down syndrome, Alzheimer disease, APP, Tau, Oxidative stress

Background

Down syndrome (DS) is the most common genetic cause of intellectual disability due to total or partial triplication of chromosome 21 (trisomy 21) [1]. The increased risk to develop Alzheimer-like dementia in DS individuals is becoming a key issue to manage the extension of the lifespan of DS population. Indeed, if from one side the improved quality of life and the longer life expectancy are significant achievements of both social and medical care, the overall increase of mean age of DS individuals is associated with an elevated risk to develop age-associated disorders, among which Alzheimer disease (AD) [2]. The neuropathological conditions of DS subjects are complex and involve: deposition of senile plaques and neurofibrillary tangles, dysfunctional mitochondria, defective neurogenesis, increased oxidative stress and altered proteostasis [3]. Approximately two-thirds of individuals with DS develop dementia and brain pathological hallmarks in their 50s, but severity varies significantly among DS population [1]. The triplication of amyloid precursor protein (APP) is considered the major pathological event in both AD and

* Correspondence: marzia.perluigi@uniroma1.it; fabio.didomenico@uniroma1.it
†Antonella Tramutola and Chiara Lanzillotta contributed equally to this work.
[1]Department of Biochemical Sciences, Sapienza University of Rome, P.le Aldo Moro 5, 00185 Rome, Italy
Full list of author information is available at the end of the article